THE INFLUENCE OF DIFFERENT CHEMICAL TREATMENTS ON THE MECHANICAL PROPERTIES OF HEMP FIBRE-FILLED POLYMER COMPOSITES

by: **Evrard Mayembo**

Supervisor: **Dr. Christopher D. Woolard**

DECLARATION

1. "I know the meaning of plagiarism and declare that all the work in the document, save for that which is properly acknowledged, is my own.

2. This thesis/dissertation has been submitted to the Turnitin module (or equivalent similarity and originality checking software) and I confirm that my supervisor has seen my report and any concerns revealed by such have been resolved with my supervisor."

Signature: Signed by candidate Date: 2021/02/01

ACKNOWLEDGEMENTS

I would like to thank **Dr Christopher Dennis Woolard** for his guidance, financially supporting this project and the following people:

Penny Louw for her guidance support and for keeping the working environment safe.

Soraya Von-Willingh for her willingness to always help.

ABSTRACT

The fluctuation of engineering and general-purpose polymer prices, rapid exhaustion of fossil fuel world-wide reserves and heightened awareness about environment have led the research community to explore the use of natural biodegradable raw materials as substitutes for manmade resources.

Natural fibres are considered as substitutes for synthetic fibres in reinforced polymer matrix composites. Increased interest has been shown in natural fibres from plants such as cotton, jute, hemp as replacements for aramid, glass, and carbon fibres. This is due to their biodegradability, low cost, low density, and satisfactory strength to weight ratio. However, they present certain disadvantages compared to synthetic fibres which include high moisture sorption rates, low durability, and weak fibre/matrix bonding strength. The poor adhesion between natural fibres and polymer matrices leads to poor mechanical properties for natural fibre reinforced composites. Improvement of the fibre/matrix interface is required to increase the mechanical properties of the natural fibre filled polymer composite

In this study, the influence of selected chemical treatments on the mechanical properties of hemp-filled epoxy composites was investigated. The aim of this study was to enhance fibre/matrix interface and hence the mechanical properties of hemp yarn-reinforced epoxy composites by modifying the chemical nature of a high crystallinity hemp yarn through chemical treatments such as alkalization, silanization (3-aminopropyltriethoxysilane) and a maleic anhydride treatment. The effectiveness of the chemical treatments was assessed by means of XRD, FTIR and TGA. Density measurements of as-received yarns (1.42-1.45 g cm^{-3}) were within the range reported in the literature. Crystallinity measurements revealed the as-treated yarns as having high crystallinity indices (87% weft and 84.7 warp yarns). The surface treatments used increased the crystallinity index only slightly. A decision was taken to use warp yarns (UTS = 799 MPa) rather than warp yarns (UTS = 503 MPa). Silane treatment reduced the tensile strength of yarns slightly (753 MPa) while the treatment of the fibres with maleic anhydride (562 MPa) and alkali treatment (518 MPa) had a much more significant effect on ultimate tensile strength. By contrast the modulus of the treated yarns all increased compared to the as-received yarns. Silanization was confirmed by energy dispersive X-ray spectroscopy while maleation was confirmed by the presence of characteristic absorbances

in FTIR spectra. TGA revealed that silanization improved fibre thermal stability while maleic anhydride treatment did the opposite, possibly due to decarboxylation reactions.

Four type of fibre/matrix interfaces, based on the treated and non-treated fibres, were generated through the production of the hemp reinforced epoxy composite plates. The results showed insignificant variations in the mechanical and thermal properties compare with the as-received hemp-filled epoxy composites which showed the high mechanical properties and thermal stability. The silanization and alkalization slightly decreased the properties of their respective properties although this was deemed statistically insignificant. The maleic anhydride treatment worsened the mechanical properties significantly. Scanning electron microscopy revealed appreciable fibre-matrix debonding which is indicative of a weak fibre/matrix interface. This was postulated as a reason for the lack of any significant reinforcement of the epoxy composites by maleic anhydride treated fibres. The tensile properties were also predicted and no statistically significant differences were observed although the experimental strengths values appeared to be lower than the predicted strengths.

In general, the lack of appreciable improvement in mechanical properties of as-received fibres was concluded to be due to the initially high crystallinity of the as-received fibres. This provided little scope for further alkalization to change the surface significantly as little further removal of hemicellulose and lignin could occur.

Table of Contents

LIST OF FIGURES

LIST OF TABLES

1 Introduction

1.1 Subject of thesis

The subject of the thesis is an investigation of the effect of different chemical treatments on the mechanical properties of hemp fibre-filled polymer composites, specifically epoxy matrix composites. Three surface treatments were used to modify the surface properties of hemp fibre/yarns. This study is aimed to enhance the fibre/matrix interface and hence the mechanical properties of hemp yarn-reinforced epoxy composites.

1.2 Background to thesis

The fluctuation of engineering and general purpose polymer prices, rapid exhaustion of fossil fuel world-wide reserves and heightened awareness about the environment have led the research community to explore the use of biodegradable raw materials as substitutes for manmade resources (Manaia, Manaia and Rodriges, 2019)(Karim *et al.*, 2020). Natural fibres, especially cellulosic materials, are considered to be potential replacements for synthetic fibres in reinforced polymer matrix composites (Puglia, Biagiotti and Kenny, 2005) (Mohammed *et al.*, 2015) (Karim *et al.*, 2020). Figure 1 presents one such plant resource, hemp, and fibres extracted from that plant.

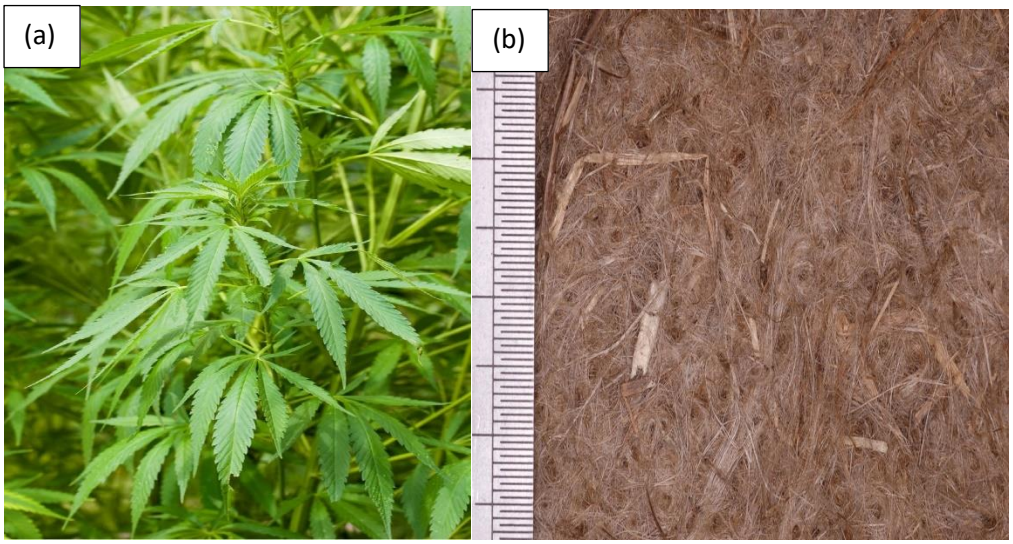

Figure 1: (a)hemp plant and (b) hemp fibres (Shahzad, 2013).

Plant fibres used in natural fibre reinforced polymer composites present certain advantages such as low density, high specific strength and stiffness, ease of availability, renewability, low

energy processing inputs, low cost of production and non-toxicity during processing. However, plant fibres also present some disadvantages caused by their internal structure variations (del Borrello *et al.*, 2020). These variations are responsible for fibre swelling due to moisture absorption, low impact strength, limited maximum service temperatures, low durability, and weak fibre/matrix bonding strength, make them less competitive compared to synthetic fibres (Fuqua, Huo and Ulven, 2012)(Mohammed *et al.*, 2015) (Manaia, Manaia and Rodriges, 2019).

The weak fibre/matrix interface is responsible for poor adhesion between natural fibres and the polymer matrix. This leads to natural fibre reinforced-composites with poor mechanical properties. Hence, improvement of the fibre/matrix interface is required to increase the mechanical properties of natural fibre filled polymer composite(Pickering, Efendy and Le, 2016)(Gurunathan, Mohanty and Nayak, 2015) (Manaia, Manaia and Rodriges, 2019) (Karim *et al.*, 2020).

1.3 Objectives

The key question underpinning this study was to assess whether the properties of epoxy composites, reinforced with already mercerized or alkalized hemp yarns, could have their properties enhanced by the treatment of the surface of these yarns.

It has to be noted that the mercerization is also known as alkalization and consists in the alkali treatment of cellulosic fibres based on the nature and concentration of the solution, its temperature, time of treatment (Fa, 2013).

The objectives of this study were to:

- characterize the as-received hemp yarns.
- measure the tensile properties of the already pre-treated, hemp fibres and select the hemp yarns that exhibited better tensile properties.
- perform different chemical treatments on as-received hemp fibres. These treatments were designed to modify the surface properties of the hemp fibres.
- investigate the effectiveness of different surface treatments on the interfaces formed between the coupling agents, hemp fibres and epoxy resin.
- measure the mechanical properties of the received/treated hemp fibre filled epoxy composites.

- model the mechanical properties of the composites produced in this study.

1.4 Scope of thesis

Several constraints were placed on the completion of this project, not least the strictures imposed by CoViD-19. This meant that the scope of the project was adjusted accordingly.

The composite component materials used in this study were restricted to one hemp supply (pre-treated hemp fabric yarns from Hemporium) and one epoxy system, SD8100/SR8224. As received and treated hemp yarns were used to produce composites and their testing specimens.

The chemical treatments were limited to:

- an alkali treatment,
- treatment with one silane coupling agent system, 3-aminopropyltriethoxysilane, and
- one acid anhydride treatment, viz. with maleic anhydride.

Composite characterization was restricted to the following techniques:

- thermal decomposition studies using thermogravimetry,
- Fourier transform infrared studies,
- mechanical testing using uniaxial tensile and 3-point bending flexural testing, and
- failure surface characterization by scanning electron microscopy.

The modelling of mechanical properties was limited to the general rule of mixtures due to the lack of experimental factors.

1.5 Development

Chapter 2 begins with a review of natural fibres with an emphasis on hemp fibres and their properties. This is followed by a brief explanation of the passage of plant fibres to composite materials. Thereafter comes a detailed discussion of the need for surface treatments as well as an explanation of selected surface treatments and their effect on the mechanical properties of hemp fibres reinforced polymer composites. The experimental design, methods and the testing equipment used are described in chapter 3. Results and a discussion, presented in chapter 4, lead to conclusions in chapter 5 and recommendations for future study in chapter 6.

2 Literature review

2.1 Natural fibres

Natural fibres can be defined as fibres derived from natural sources such as animals, minerals and plants (Nishino, 2004). Animal fibres include wool and silk (Nishino, 2004). Mineral fibres are derived from asbestos, inorganic whiskers, basalt etc. (Nishino, 2004). Plant fibres are derived from plants such as sisal, flax, hemp, jute, bamboo, kenaf, and wood fibres (Bhattacharyya, Subasinghe and Kim, 2015) (Mohammed *et al.*, 2015). This research focuses on natural plant fibres, specifically fibres derived from hemp.

2.1.1 Plant fibres

2.1.1.1 Classification of natural plant fibres

Plant fibres, also known as cellulosic or lignocellulosic fibres due to their high cellulose and lignin content, have been classified according to several criteria. One of these is the variation in fibre type associated with variations in fibre geometry and constituent makeup. Depending on their fibre aspect ratio, vegetal fibres can be considered true fibres when their aspect ratio is 20:1 or greater. Otherwise, they are considered fillers (Fuqua, Huo and Ulven, 2012). True fibres find their sources from wood fibres and crop fibres such as fruit, bast, leaf, seed, and grasses. However, fillers can be obtained from seed hulls and husks, and agricultural crop harvesting by-products such as residues from corn and sugar processing (Fuqua, Huo and Ulven, 2012). Figure 2 presents the classification of natural plant fibres. The chemical composition of natural plant fibres is known to make the surfaces of the fibres hydrophilic (Haghdan and Smith, 2015). This is because of hydroxyl groups at these surfaces.

Hemp plant

Also known as *Cannabis sativa* L., (Figure 1 (a)), hemp is classified in the angiosperm phylum. It is a plant with vessel elements in the xylem (woody core) as shown in Figure 1 (a). The plant has bushes, herbs, and two cotyledons, seed and leaves and hence is classified under the sub-group of euticotyledons. In hemp plants, fibres are located on the surface of the stem, which is found in the cortex of the plant.

2.2 From plant to fibre/yarns

Fibre production is a three-phase process that starts with fibre extraction, then proceeds to fibre separation followed by spinning, weaving and the finishing (Puglia, Biagiotti and Kenny, 2005).

2.2.1 Fibre extraction

The extraction phase, planting and growing, can take approximately 12 months, depending on the variety of the plant and the final desired quality. After planting and growing, the plants are harvested so that fibres may be extracted. During this phase, better aspect ratios, length/diameter, of the fibre, are desired because they positively influence the mechanical properties of composites produced (Puglia, Biagiotti and Kenny, 2005).

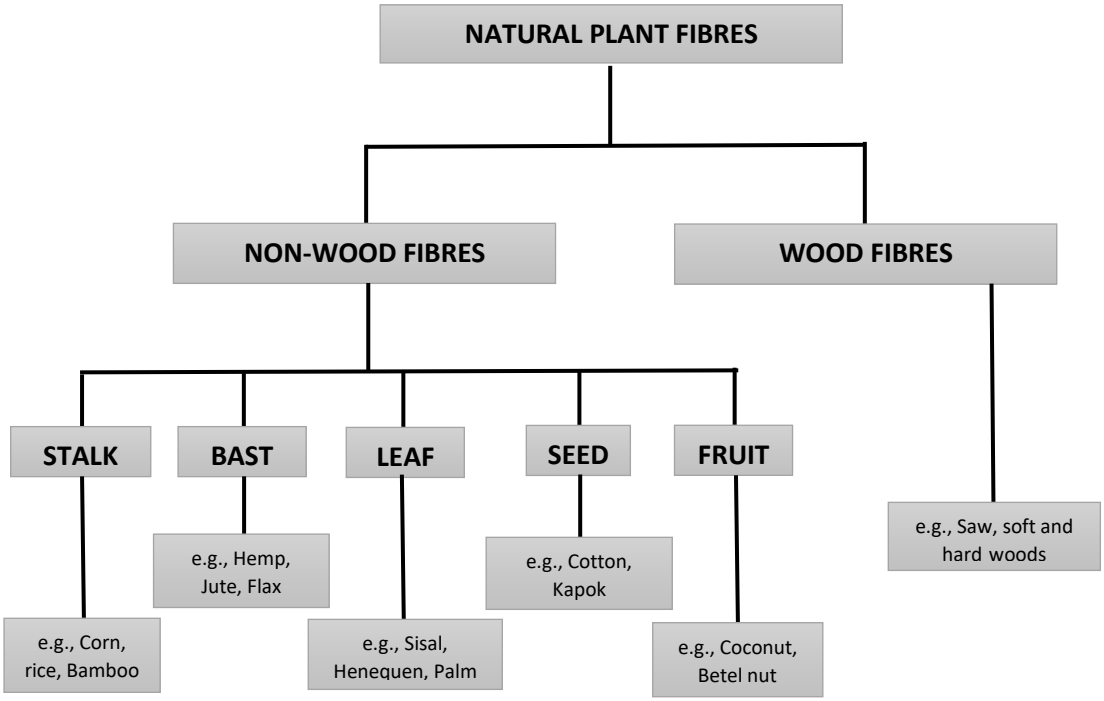

Figure 2: Classification of natural fibres (Puglia, Biagiotti and Kenny, 2005) (Karim et al., 2020).

According to the general family of the fibres (stalk, leaf, bast, seed and fruit fibres), the fibre extraction may vary (Puglia, Biagiotti and Kenny, 2005). In this research, focus was placed only on bast fibres. Bast fibres are obtained from phloem tissue.

Located in the stem of a plant as shown in Figure 3 (a), bast fibres are extracted by a process known as retting, defined as an extraction process generated by microbes that separate the

bast fibres from the surrounding tissue by breaking linkages that hold the stem together. Retting can be either a field retting or water retting (Puglia, Biagiotti and Kenny, 2005). Field retting can be performed in the presence of moisture, in a fungi and yeasts environment. This allows the microbial breakdown to happen and plant stems are cut or pulled up and left in the field to rot, afterwards. The same procedure can be followed by using water, with the plant stems being placed in tanks for 4 days. At the end of these process, fibre bundles are mostly produced as shown Figure 2 (b) (Puglia, Biagiotti and Kenny, 2005).

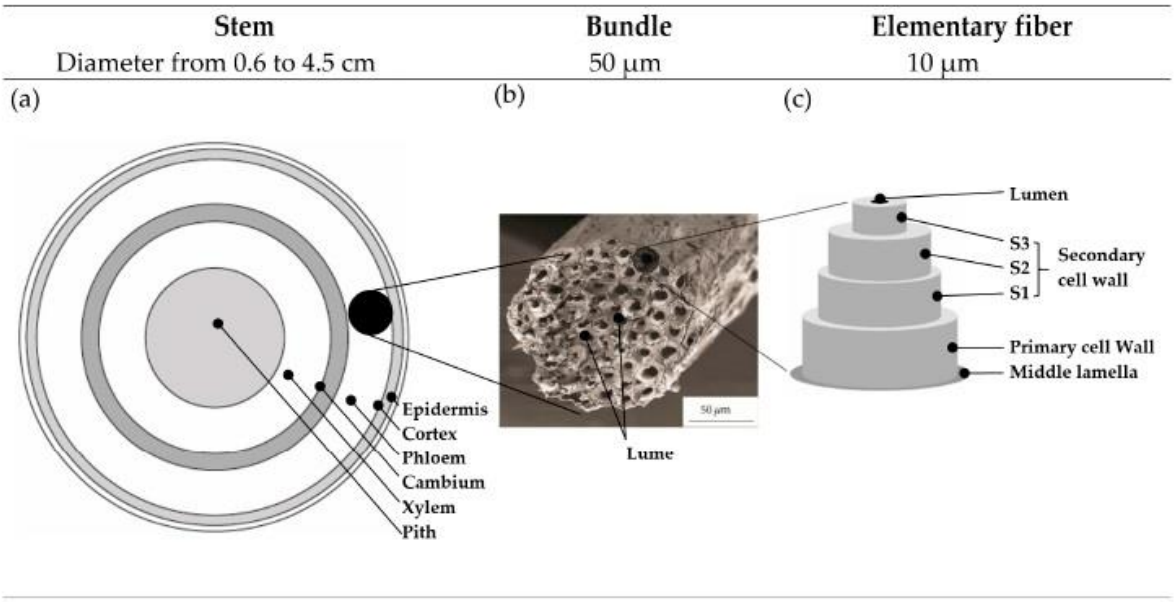

Figure 3: Structure of hemp fibre: (a) transverse hemp stem, (b) cross-section morphology of the hemp fibre bundle, and (c) schematic depiction of hemp elementary fibre (Manaia, Manaia and Rodriges, 2019).

2.2.2 Spinning

After the retting, fibres are dried and baled. They then go through scutching whereby they are mechanically processed. This occurs by crushing divided into 2 stages, breaking and swingling. In the breaking step, the woody core is broken into fibres of less than 1 cm named shives. The shives are then removed by tangential scraping of the broken stems. This is called swingling. Afterwards, the fine fibres undergo a twisting process, spinning, to obtain a yarn.

2.3 Physical structure and surface morphology of a hemp fibre

2.3.1 Physical structure of a hemp fibre

A plant fibre is set of long, thin, pointed cells formed by cell walls on the outside and the inside. It can refer to a single elementary fibre or bundles of these elementary units. It is made up of cellulose, hemicellulose, lignin, pectin and waxes (Chang Hong, 2004) (Fuqua, Huo and Ulven, 2012). Single plant fibres are made up several layers: the centre lumen, secondary wall (S3, S2 and S1), and primary wall from inside to outside, as shown in Figure 3(c) and 4(a). It has been found that the amount of biomass constituents differs slightly in each cell wall layer. The hemicellulose content is about the same in each layer while the amount of cellulose in each layer increases from the outer primary layer to the innermost secondary layer (Chang Hong, 2004).

2.3.2 Surface morphology of a hemp fibre

The morphology of hemp fibres investigated using scanning electron microscopy by Wang, Sain and Oksman, 2007, revealed a rough surface of a hemp fibre bundle , which was reported to be covered by non-lignocellulosic components, as shown in Figure 4 (b). Ouajai and Shanks, 2005, studied the morphology of hemp fibres and reported the same surface characteristics as Wang, Sain and Oksman, 2007, (Figure 4.c). These components, pectin and waxes, protect the fibres against environmental stress(Lan, 2018).

2.3.3 Surface structure of a hemp

Depending on the spinning process of individual fibres or fibre bundles, yarns can be classified as ring spun, rotor spun, air-jet spun, friction spun and warp spun yarns. Ring spun yarns are the most encountered yarns (Tyagi, 2010). The surface morphology of ring spun yarns, generated by the number of twists per unit length defined known as the twist level, can be as either S-twist or Z-twist according to the direction of the twist as shown in Figure 5 (Chattopadhyay, 2010).

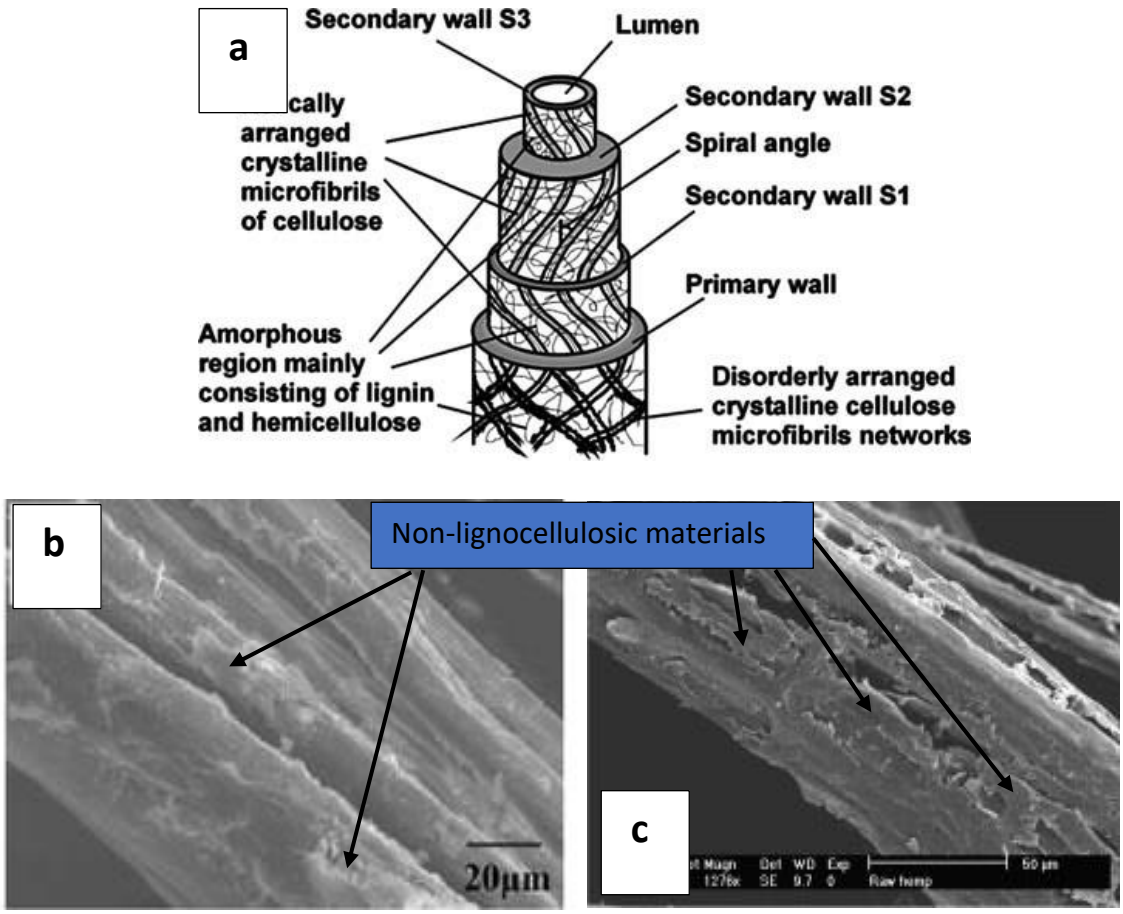

Figure 4: (a)The structure of a single microfibril (Fuqua, Huo and Ulven, 2012); (b) & (c) Scanning Electron Microscopy of surface morphology of natural hemp fibre (Sirisart Ouajai and Shanks, 2005)(Wang, Sain and Oksman, 2007).

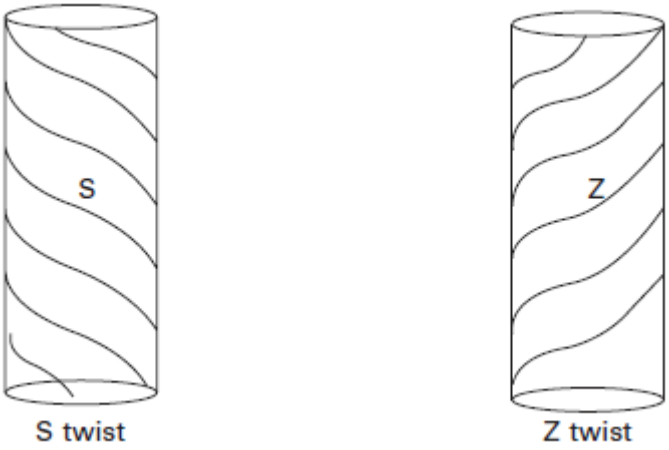

Figure 5: S and Z twist direction of natural fibres spun yarns.

2.4 Chemical composition of a plant

Plant or lignocellulosic fibres are made up of three main constituents which are cellulose, hemicellulose and lignin. They also contain pectin and waxes. Table 1 presents the chemical composition of the most common vegetable fibres.

Fibre	Latin name	Cellulose (wt.%)	Hemicellulose (wt.%)	Lignin (wt.%)	Pectin (wt.%)
Flax	*Linum usitatissimum*	60-81	14-18.6	2.0-3.0	1.8-2.3
Jute	*Corchorus capsularis, C. olitorius*	51-72	12-20.4	5.0-13	0.2
Abaca	*Musa textilis*	60.8-64	21	12	0.8
Sisal	*Agave sisalana Perrine*	43-88	13-Oct	4.0-12	0.8-2.0
Kenaf	*Hibiscus cannabinus*	36	21	18	2
Ramie	*Boehmeria nivea Gaud, variety tenacissima*	68.6-76	13.1-15.0	0.6-1.0	1.9-2.0
Hemp	*Cannabis sativa L.*	70-78	17.9-22	3.7-5.0	0.9
Cotton	*Gossypium spp. (commonest G. hirsutum)*	82.7-92	2-5.7	0.5-1.0	5.7
Coir	*Cocos nucifera L.*	43	0.3	45	4
Banana	*Nusa acuminata L.*	60-65	6.0-19	5.0-10	3.0-5.0
Henequen	*Agava fourcroydes Lemaire*	60-78	4.0-28	8.0-13	3.0-4.0
Bagasse	*Saccharum officinarum L.*	40	30		10
Pineaple	*Acanas comosus*	80-81	16-19	12	2.0-2.5
Wood	-	45-50	23	27	-
Corn Stover	-	31-39	34-41	2.0-14	3.0-7.0

Table 1: Chemical composition of lignocellulosic fibres (Chang Hong, 2004).

2.4.1 Cellulose

Cellulose is a natural polymer composed of D-glucose units linked together by β-(1→4)-glycosidic linkages to form long aligned-chains (Figure 6.b), which in turn are connected together to generate bundles called microfibrils (Medina and Dzalto, 2018) (Usmani *et al.*, 2017). Cellulosic chains present three hydroxyl (-OH) groups that form inter- and intramolecular hydrogen (H) bonds with other functional groups and moisture. The presence of an H-bonding network is therefore responsible for the hydrophilic nature of natural plant fibres. In addition, the hydrogen bonds and van der Waals forces cause the cellulose molecules to have a highly ordered arrangement which results in crystalline regions. The cellulose content is primarily responsible for the tensile properties of lignocellulosic fibres (Trache *et al.*, 2016).

According to the processing of the polymer, cellulose can exist in various allomorphic forms (I, II, III_a, III_b, IV_a, and IV_b). In nature, cellulose I exists as cellulose I_α (triclinic structure) and cellulose I_β (monoclinic structure). It has been shown that cellulose I_α only exists in some algae, whereas cellulose I_β can be found in all plants. By using different chemical or thermal treatment, cellulose I can be transformed into cellulose II, cellulose II, or cellulose IV (Trache *et al.*, 2016) (Fuqua, Huo and Ulven, 2012).

2.4.2 Hemicellulose

Hemicellulose is a randomly organized and slightly cross-linked biopolymer composed of polysaccharides such as xylose, mannose, glucose, galactose, and arabinose (Trache *et al.*, 2016). Hemicellulose acts as a filler between cellulose and lignin. Mechanically, it contributes little to the stiffness and strength of natural fibres, as shown in Figure 6 (c).

2.4.3 Lignin

Lignin is a high molecular weight, disordered and cross-linked polymer. It acts as a biological barrier and binder that glues hemicelluloses and celluloses present in the plants to form cell walls (Fuqua, Huo and Ulven, 2012). Its structure presents a very complex, three-dimensional randomized network making up an amorphous phenolic polymer with aliphatic and aromatic constituents (De Carvalho Mendes *et al.*, 2015). The polymerization of lignin monomers is initiated by oxidases or peroxidases. The primary structure of lignin is generated by radical coupling between lignin monomers leading to the formation of β–O–4 , α–O–4, 4 –O –5, β–β, β–5, β–1 and more complex structures involving 3 sub-units (dibenzodioxocin) , as shown in Figure 6, d & e (Duval and Lawoko, 2014).

2.4.4 Pectin

Pectin is a collective name for heteropolysaccharides, which are a major matrix component of the cell walls in long non-wood fibres, particularly the important bast fibres. Pectin gives flexibility to plants. It is soluble in water only after a partial neutralization with alkali or ammonium hydroxide (Fuqua, Huo and Ulven, 2012).

2.4.5 Waxes

Plant waxes are mixtures of substituted long chains of aliphatic hydrocarbons and as well as alkaline and lipids, fatty acids, primary and secondary alcohols, ketones, aldehydes, and other ingredients (Lan, 2018).

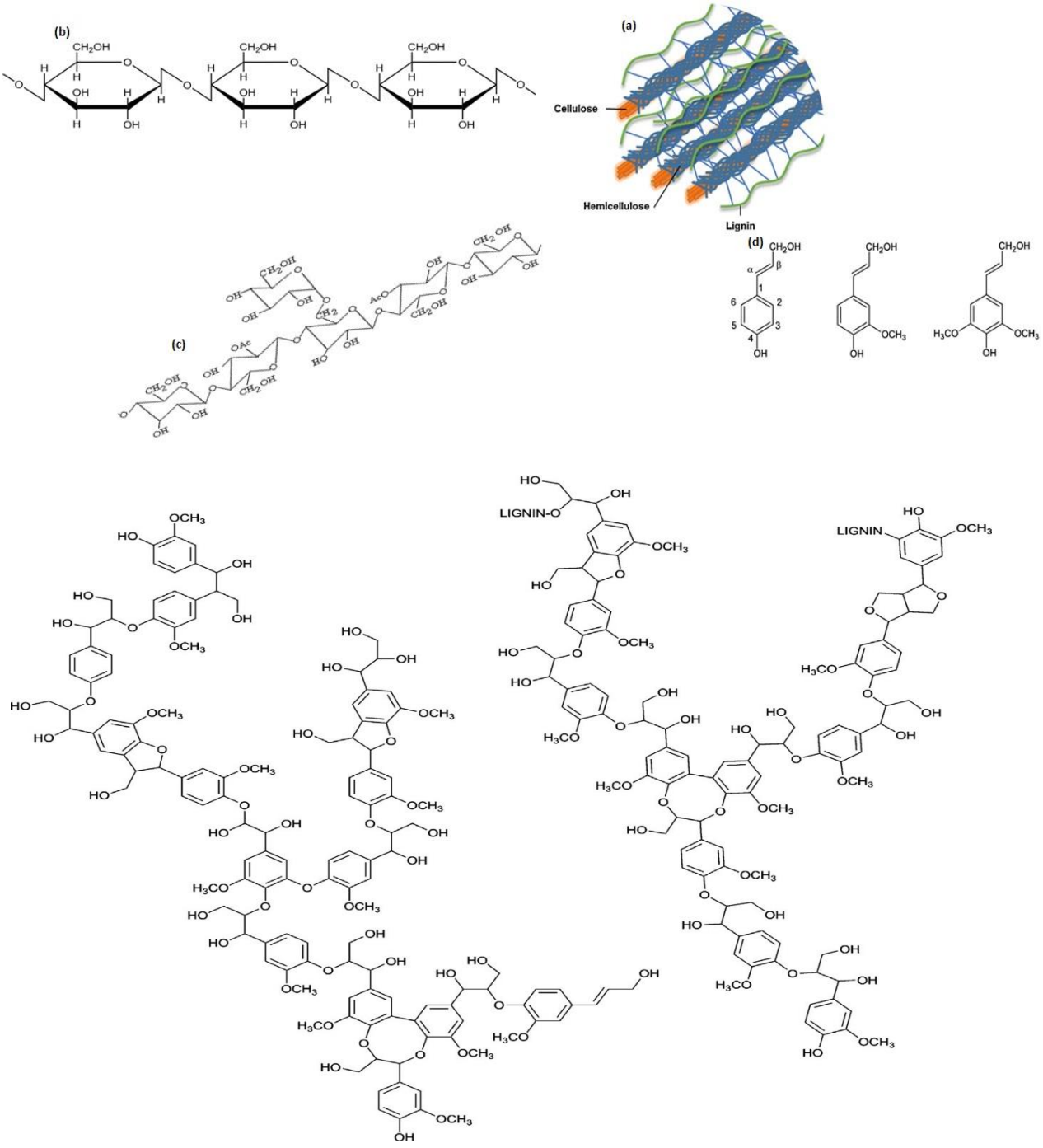

Figure 6: (a) Representation of a macrofibril fibre; (b) Chemical structure of Cellulose; (c) Chemical structure of hemicellulose and (d) lignin (Fuqua, Huo and Ulven, 2012)(Duval and Lawoko, 2014)(Trache et al., 2016).

2.5 Chemical interaction between lignocellulosic components

Cellulose is a long linear chain of glucose polymers linked by hydrogen and ether (glucosidic) bonds (a) and (b), respectively, as shown in Figure 7. However, lignin is dominantly built with molecules such as p-coumaryl- , coniferyl- and sinapyl alcohol connected by ether and carbon to carbon bonds. Hemicellulose, a term used to identify a family of polysaccharides different from the ones found in cellulose and lignin, contains individual molecules linked by ether and ester bonds.

The linkages connecting the building molecules of the three main components of lignocellulosic biomass can be classified as interpolymer linkages and intrapolymer linkages. Interpolymer linkages are bonds that connect the individual components, whereas the intrapolymer linkages provide linkages between the different components of lignocellulosic biomass (Huijgen, Bermudez and Bakker, 2010).

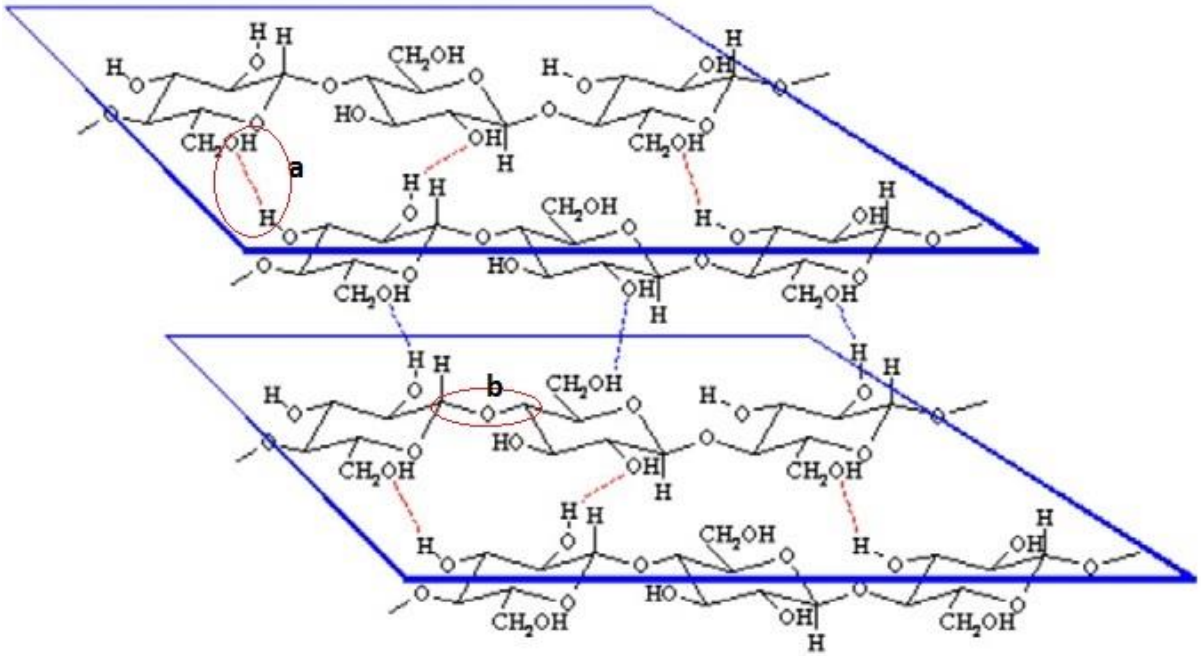

Figure 7: (a)Hydrogen and (b) ether linkages present in cellulose Linkages between and within lignocellulosic components (Huijgen, Bermudez and Bakker, 2010).

2.5.1 Intrapolymer linkages

These types of bonds are found in all the three main lignocellulosic biomass components and can be summarized as in table 2.

Bonds	lignocellulosic components
Hydrogen bond	Cellulose
Carbon to carbon bond	Lignin
Ether bond	Lignin, cellulose and hemicellulose
Ester bond	Hemicellulose

Table 2: Linkages between and within lignocellulosic components (Huijgen, Bermudez and Bakker, 2010).

2.5.2 Interpolymer linkages

Researchers discovered that lignin is connected to cellulose and to hemicellulose by hydrogen bonds. Moreover, the presence of covalent bonds connecting lignin with hemicellulose via ester bonds was also revealed. The existence of ether bonds between lignin and polysaccharides was also reported, although there is still not any specification about the nature of the polysaccharides (Huijgen, Bermudez and Bakker, 2010).

The above description of the chemical interaction of lignocellulose components is responsible for the complex rigidity of the lignocellulosic biomass structure. Indeed, the processing of lignocellulosic reinforced polymer composites requires accessibility of cellulose present in the plant fibres. Nonetheless, the complexity of the lignocellulosic biomass structure impedes the accessibility of chemicals to the cellulose polymer. This is governed by the following factors: high lignin content; protection of cellulose by lignin and hemicellulose; cellulose sheathing by hemicellulose; high crystallinity and degree of polymerization of cellulose; low accessible surface area of cellulose and strong fibre strength. Hence, the extraction of lignin and hemicellulose is necessary to avail the cellulose polymer encompassed in the lignin and hemicellulose polymeric matrix (Baxter *et al.*, 2008)

One must first understand the functional groups of lignocellulose components and the extractive reaction related to them in order to process an effective extraction of hemicellulose and lignin.

2.5.3 Functional groups of lignocellulose components

Depending on the nature of the utilization of the end-products produced from lignocellulosic biomass, the functional groups can be divided as follows:

- Functional groups that are involved in the hydrolysis of the polysaccharides to their monomers and the possible subsequent degradation reactions of these monomers.

- Functional groups that are involved in the (partial) depolymerisation of lignin (into fragment or phenolic compounds so that cellulose fraction becomes more accessible for enzymes (Huijgen, Bermudez and Bakker, 2010).

For this research, focus was only placed on the first functional groups.

Functional Groups	Type of reactions	Components	Conditions	Descriptions
Aromatic ring	Chlorination and nitration	Lignin		formation of mono- and dicarboxylic acids by oxidizing the aromatic group with chlorine, chlorine dioxide or oxygen
Ether bond	Solvolytic reaction	Lignin	Acidic	Conversion of ether bond into hydroxyl → into carbonyl or carboxyl → finally into C_2 or C_3
			Alkaline	Separation of the aromatic rings
		Cellulose	Acidic	Protonation of the oxygen atom replaced by hydroxyl group of water
			Alkaline	Formation of an intermediate epoxide
Ester bond	Hydrolyse	Hemicellulose	Acidic	Irreversible hydrolysis of the acetyl group that forms the ester bond
			Alkaline	The same hydrolysis is performed in alkaline conditions through a reaction named saponification
Hydroxyl group	Substitution	Lignin		Transformation of the hydroxyl group to an aryl or allylic ether
Hydrogen bond*	Substitution	Cellulose and hemicellulose		Alteration of the cellulose structure to obtain a lower energy hydrogen bond than the hydrogen bond formed by the molecules of water; Forming higher energy hydrogen bonds than the ones formed in cellulose.

Table 3: Overview of functional groups in lignocellulosic components and their breaking reactions (Huijgen, Bermudez and Bakker, 2010)(Huijgen, Bermudez and Bakker, 2010).

2.6 Properties of hemp fibres/yarns

Hemp fibres are valued for their superior strength and fibre length (Mehta *et al.*, 2006)(Moyeenuddin A. Sawpan, Pickering and Fernyhough, 2011)(Fuqua, Huo and Ulven, 2012). The overall properties of fibres from these plants are regulated by the combined effect of cellulose, hemicellulose, lignin, and waxes (Fuqua, Huo and Ulven, 2012). Of all the properties focus was placed on certain physical, mechanical and thermal properties.

2.6.1 Physical properties

The physical properties of vegetal fibres depend on their internal structure and composition (Fuqua, Huo and Ulven, 2012) (Komuraiah, Kumar and Prasad, 2014) (Fortea-Verdejo *et al.*, 2017).

2.6.1.1 Fibre density and linear density

Mostly determined by the pycnometer method using liquid water as displacement medium, the density of hemp fibres is one of the properties that gives them advantages specific mechanical properties compared to other fibres (Rohen *et al.*, 2017). The linear density, also known as the fineness of fibres, is a key parameter that influences the mechanical properties of yarns. It can be measured by either the direct or the indirect system. The direct system consists of measuring the mass of a known length of yarn, while in the indirect system the length of a known mass of yarn is measured (Hari, 2012). In the literature the density of hemp fibres is reported as being in the range 1.4-1.6 g cm^{-3} (Liu *et al.*, 2017).

2.6.2 Mechanical properties

As is the case for the physical properties, mechanical properties of natural plant fibres from the same soil vary due to fibre processing conditions. It was demonstrated that the variance in properties was the result of a dissimilarity of the fibre origin, which influences the fibre structure and hence the crystallinity, composition, and microfibrillar angle. Additionally, the microfibril angle, the angle formed by the cellulose microfibrils and the longitudinal cell axis, is a crucial factor in determining the mechanical properties of the macroscopic fibre. Experiments run on macroscopic fibres with regards to the mechanical properties showed an increase in mechanical properties with a decrease in the microfibril angle, as shown in Figure 8 (Nishino, 2013)(Shahzad, 2013).

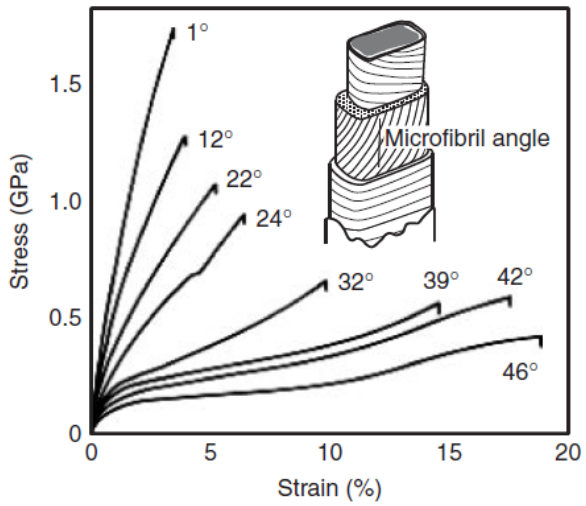

Figure 8: Variation of the stress of hemp fibres with twist angle.

For hemp, tensile strengths and Modulus have been reported to be in the range of 200 and 1000 MPa and 18 and 66 GPa for the tensile strengths and Modulus, respectively (Thygesen *et al.*, 2011)(Liu *et al.*, 2017). These values are lower than synthetic glass and carbon fibres. The lower density of hemp fibres than glass fibres means that the specific (per unit mass) strength and modulus of hemp fibres are equivalent to those of glass fibres, making hemp fibres an attractive replacement (Liu *et al.*, 2017).

2.6.2.1 Tensile properties of cellulose based fibres

The tensile properties of lignocellulosic fibres are mainly governed by their cellulose content. The higher the cellulose content, the higher the tensiile strength (Fuqua, Huo and Ulven, 2012)(Komuraiah, Kumar and Prasad, 2014)(Manaia, Manaia and Rodriges, 2019). Additionally, the presence of dislocations, in natural hemp fibres influence their tensile properties. Dislocations are defined as kinks or microcompressions. They appear under polarized light as light bands crossing the fibres (Figure 9) (Thygesen and Eder, 2007; Hughes, 2012). The relationship between dislocations in natural fibres and the tensile properties has also been investigated. Although research did not reveal a direct effect on the tensile strength, it revealed that dislocations served as crack initiators and caused shear failure between the microfibrils. The lower the number of dislocations, the higher the load the fibre could bear during testing, hence the higher the tensile strength (Thygesen and Eder, 2007).

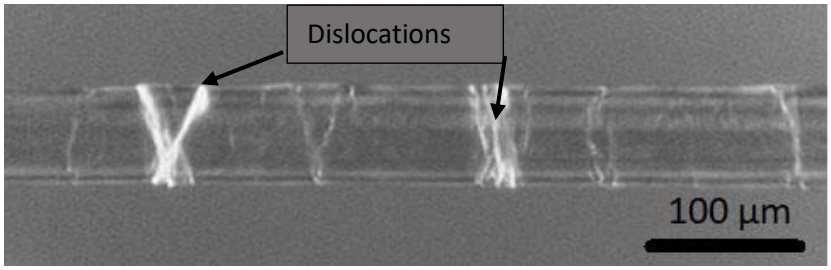

Figure 9: Polarized light microscope image of dislocations (Hughes, 2012).

2.6.2.2 Tensile properties of natural fibre yarns

Yarn textiles are made up of fibres, whose tenacity and elongation affect the strength and elongation of yarns. The tensile properties of vegetal fibre yarns are affected by fibre factors such as fibre length, fineness and hairiness. When pulled in tension, the resistance to fibre slippage, between fibres, increases. The longer the fibres, the longer overlapping of fibres, hence, the greater resistance to fibre slippage. This increases the resistance to breakage and, therefore, the strength of the yarn (Tyagi, 2010). Finer fibres have also been reported to increase the frictional resistance to slippage, which increases the yarn strength (Tyagi, 2010). Furthermore, the yarn hairiness is influenced by the fibre length and fibre fineness. The torsional stiffness of the fibre is increased by the fibre fineness and fibre length, which will probably make the fibres bend together with twists, therefore, increasing hairiness. The increase in hairiness will then increase the resistance to slippage and, hence, the yarn strength

Elastic Modulus

The Young's Modulus (E) of a polymer crystal reveals significant information about the spatial arrangments adopted by the atoms in the polymer crystal lattice. Measurements of the elastic modulus of the crystalline regions along the chain axis of different polymers by X-ray diffraction helped researchers to examine the extensibility of a polymer crystal. This was attributed to the molecular conformation as well as the mechanism of deformation in the crystal lattice. During the application of a load on a natural fibre, the microfibrils start to align with the fibre axis. Furthermore, the hydrogen bonding, which is responsible for the ordered arrangement of the polymer chains, breaks. This generates more amorphous regions in the fibres and therefore reduces the overall ability of the fibre to resist changes. It was also reported that the higher the cellulose content, the higher the crystalline regions. As a result, the higher the elastic modulus.

2.6.3 Thermal properties of natural fibres

The measurement of changes in physical properties of stalk, leaf or bast fibres, thermal expansion, and thermal degradation, as a function of temperature can be determined by thermal analysis. The variation of physical properties associated with the chemicals present in biomass such as cellulose, hemicellulose and lignin are the trigger for this analysis (Chang Hong, 2004). As an example, S. Ouajai and Shanks, 2005, investigated the thermal stability of hemp fibres by thermogravimetric analysis (TGA), mass loss and derivative thermogravimetric curves as shown in Figure 10. The results showed a peak representive of a familiar phenomenon of lignocellulosic fibres, which is the vaporization and elimination of bound water in the samples between 50 and 160^{o}C. The degradation of small molecules (sugar, wax, etc.) and depolymerisation of hemicellulose was associated with the shoulder peak at about 250–320^{o}C. The major decomposition peak was observed at about 390–400^{o}C and was associated with the degradation of cellulose. After switching gases from nitrogen to air, a last peak, occurred from the residue loss and was reported to have occurred in the nitrogen environment.

Additionally, the chemical composition of biomass can be determined by using kinetics of reactions in the solid-state. The kinetic parameters are determined from the weight loss of decomposed samples and data from the derivative thermogravimetric (DTG) curves (Carrier *et al.*, 2011)(Maschio *et al.*, 1997).

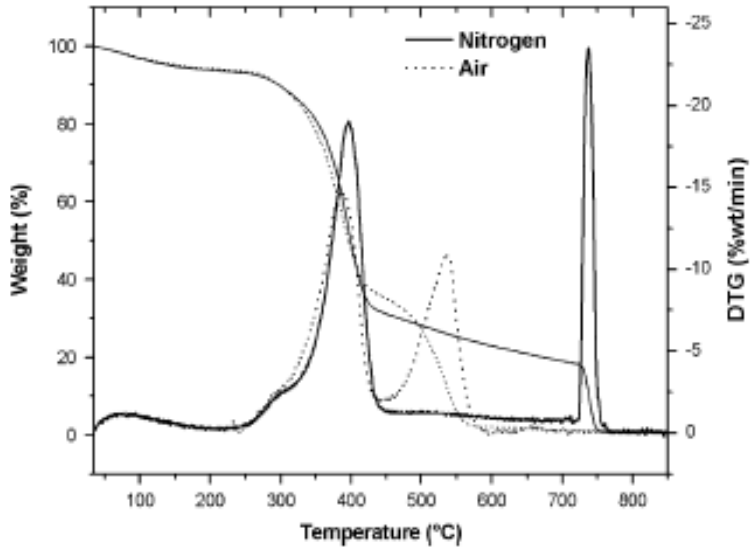

Figure 10: Thermal gravimetric curves and derivative thermogravimetric curves of hemp fibres in Air and Nitrogen.

The kinetics parameters, A, E and n can be determined using the linearized form of the Arrhenius equation (y = B + Cx + Dz) by applying the least squares technique as described below (Mansaray and Ghaly, 1999) (Slopiecka, Bartocci and Fantozzi, 2011) (Kalita *et al.*, 2009).

Procedure to determine parameters of reaction kinetics

The decomposition of coal may be represented by the rate equation

$$\frac{dC}{dt} = k\cdot(1-C)^{n} \qquad (1)$$

With $C := 1 - \frac{m - mf}{mi - mf}$ (2) the conversion factor, k the specific rate constant and n the reaction order.

Assuming that the specific rate constant, k, varies with temperature according to the Arrhenius equation, viz.

$$k := A\cdot\exp\left(\frac{-E}{RT}\right) \qquad (3)$$

and combining equations (1), (2) and (3), we obtain

$$\frac{\frac{-dm}{dt}}{mi - mf} = A\cdot\exp\left(\frac{-E}{RT}\right)\cdot\left(\frac{m - mf}{mi - mf}\right)^{n} \qquad (4)$$

the combined equation can also be written in the linear form as

$$\ln\left(\frac{-1}{mi - mf}\cdot\frac{dm}{dt}\right) = \ln(A) - \frac{E}{R\cdot T} + n\cdot\ln\left(\frac{m - mf}{mi - mf}\right) \qquad (5)$$

the equation (5) is of the form

$$y = B + Cx + Dz$$

where

$$y = \ln\left(\frac{-1}{mi - mf}\cdot\frac{dm}{dt}\right) \qquad x = \frac{1}{T} \qquad z = \ln\left(\frac{m - mf}{mi - mf}\right) \qquad B = \ln(A) \qquad C = \frac{-E}{R} \qquad D = n$$

2.6.4 Crystallinity

The crystallinity index of lignocellulosic fibres, which is one of the parameters that influences the processing of polymers, depends on the polymorphic state of cellulose. The correlation of this parameter to polymer properties such as the viscosity, density and tensile modulus, make it indispensable to understand a fibrous material's behaviour before and after the treatment of the natural fibres (Beckermann and Pickering, 2008).Wang, Sain and Oksman, 2007, determined the crystallinity of hemp fibres at every stages of the chemical treatment they performed. X-ray powder diffraction of untreated, acid and alkali treated samples were performed and the intensities of crystalline and amorphous cellulose as a function of the scanning angle 2θ were recorded as shown in Figure 11. The results showed that treated hemp fibres depicted higher peak intensities, at 2θ angle between 21.6 and 23 (corresponding to the absorbed crystalline cellulose peak), than untreated hemp fibres. As a result, the crystallinity index of the hemp fibres (number in brackets) showed higher values for the treated hemp fibres as shown in Figure 11. This was reported to be caused by the removal of more amorphous material in the lignocellulosic fibres.

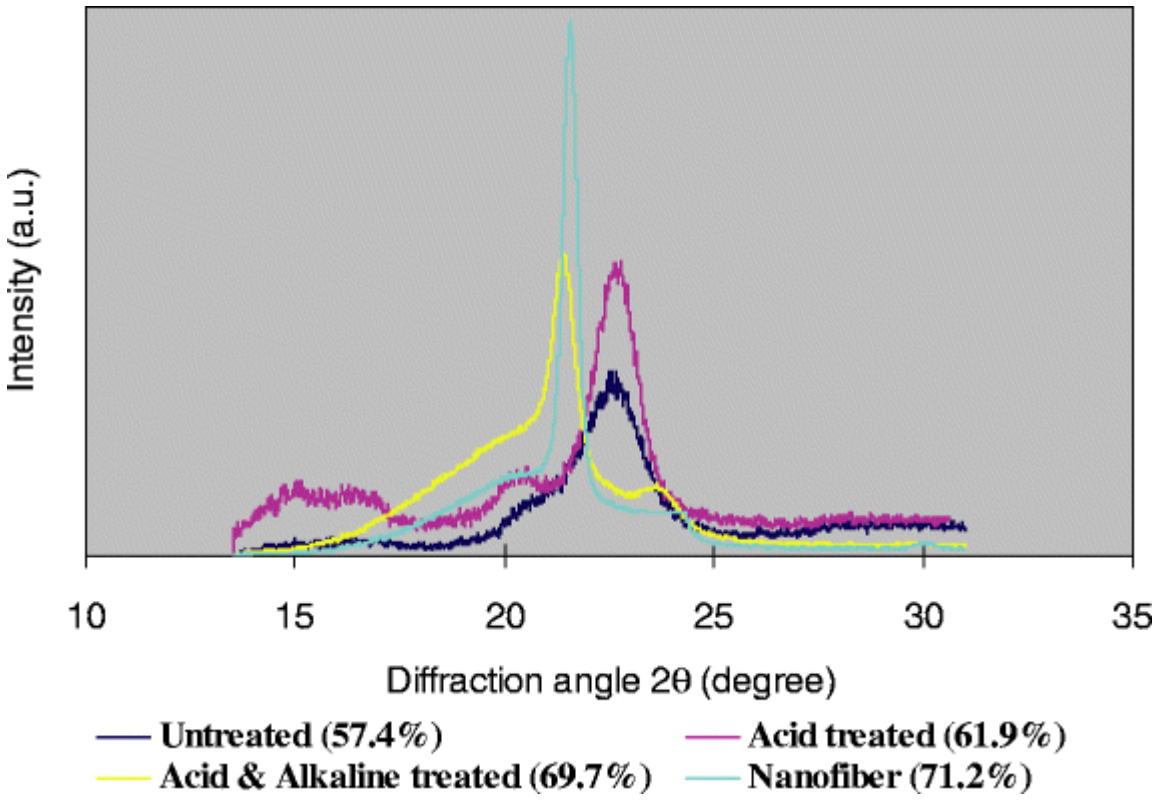

Figure 11: X-ray diffractogram and crystallinity indexes after every stage of chemical and mechanical treatment (Wang, Sain and Oksman, 2007).

2.7 From hemp fibres/yarns to composites

Natural fibre reinforced polymer composites are mainly manufactured using methods such as pultrusion, filament winding, hand lay-up, resin transfer moulding, vacuum bagging, compression moulding and injection moulding (Salit *et al.*, 2015). For this study, attention will only be given to moulding processes and especially compression moulding of bast fibres reinforced polymer composites.

Compression moulding is a process during which a mixture of materials, which occupies 30–70 % of the female mould cavity, is placed in a lower mould cavity and compressed into the desired-shape by an upper mould. After curing, the mould is opened, and the formed part ejected. This process can be performed at elevated or room temperature (Ho *et al.*, 2012).

Extensive work has been carried out for the last two decades on the evaluation of mechanical properties of natural fibres reinforced thermoset polymer composites. The studies were mostly focused on bast fibres and bast/hybrid polymer composites such as woven jute and jute fabric reinforced polyester, kenaf and kenaf/glass fibre reinforced polyurethane composite. Bakar *et al.*, 2015, reported some of these studies where composites were produced by compression moulding and the reported results showed better mechanical properties of the produced composites. This was attributed to the moulding parameters such as pressure and temperature, and the non-alteration of the fibre orientation that limited a reduction not only in physical properties but also the isotropic properties of the composites (Bakar *et al.*, 2015).

2.7.1 Interface

During the production of composites, reinforcements connect to the matrix at their interface, which influences the overall properties of the produced composite according to their composition. The composition of natural fibres and the complexity of their structural hierarchy is responsible for the presence of different types of interfaces in lignocellulosic fibres. These interfaces govern the fragmentation and dispersion of cellulose fibres when mixed with polymer matrices (Jain, Mukherjee and Kwatra, 2014) (Moigne *et al.*, 2018).

An optical microscopy analysis regarding the fibre size and shape distributions of certain natural fibres as flax, sisal and wheat straw fibres after being compression moulded in a polypropylene (PP) matrix revealed the presence of three major entities (Figure 12) (Moigne *et al.*, 2018):

- Elementary or individualized fibres;
- Fibre bundles made of individualized fibres maintained together by the middle lamella rich in lignin;
- Low aspect ratio particles (Jain, Mukherjee and Kwatra, 2014) (Moigne *et al.*, 2018).

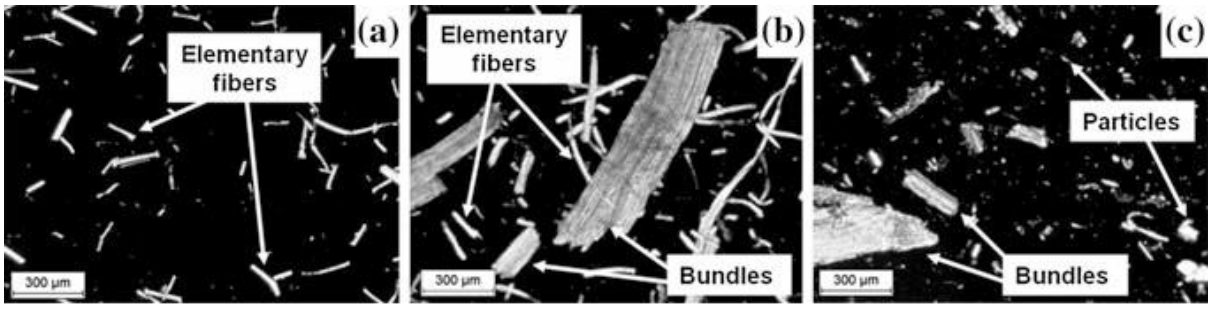

Figure 12: Optical microscopy images of the three entities obtained in light transmission mode between crossed polarizers of composites diluted with Decalin (Moigne et al., 2018).

2.7.1.1 Fibre distribution

Additionally, a study of the dispersion state of untreated and treated flax yarns in flax tow fabrics reinforced epoxy composites manufactured by thermo-compression was reported. The study showed that the dispersion of the fibre was related to the composition and structural hierarchy of the lignocellulosic fibres and was responsible for the creation of new interfaces as shown in Figure 13. These interfaces differ from each other in terms of physico-chemical interactions and strength of cohesion. The same study, mentioned above (Moigne *et al.*, 2018), also revealed that the fibre dispersion observed caused a reduction of the fibre treated surfaces exposed to the matrix after the manufacturing process, leading to a decrease in the properties of the treated fibre surface. Generally, the mixture of natural fibres with a polymer matrix results in the creation of the following interfaces in the resulting composite:

- the interface between the polymer matrix and the elementary fibres and/or the bundles;
- the interface in between the layers within the fibre bundles; and

- the interface between the layers within the cell walls (Wang, Sain and Cooper, 2006)

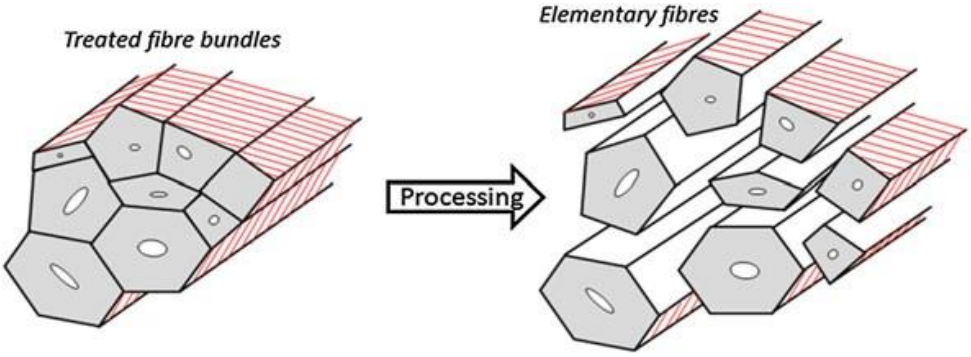

Figure 13: Representation of treated surfaces (dashed zones) before processing and the ones exposed to the matrix after processing (Wang, Sain and Cooper, 2006).

Also known as transitional phases named interphases, interfaces are three-dimensional zones composed of a two-dimensional zone of contact between the reinforcement and the matrix and a finite thickness zone extending on both sides of the interface within the reinforcement and especially within the matrix (Figure 14) (Moigne *et al.*, 2018).

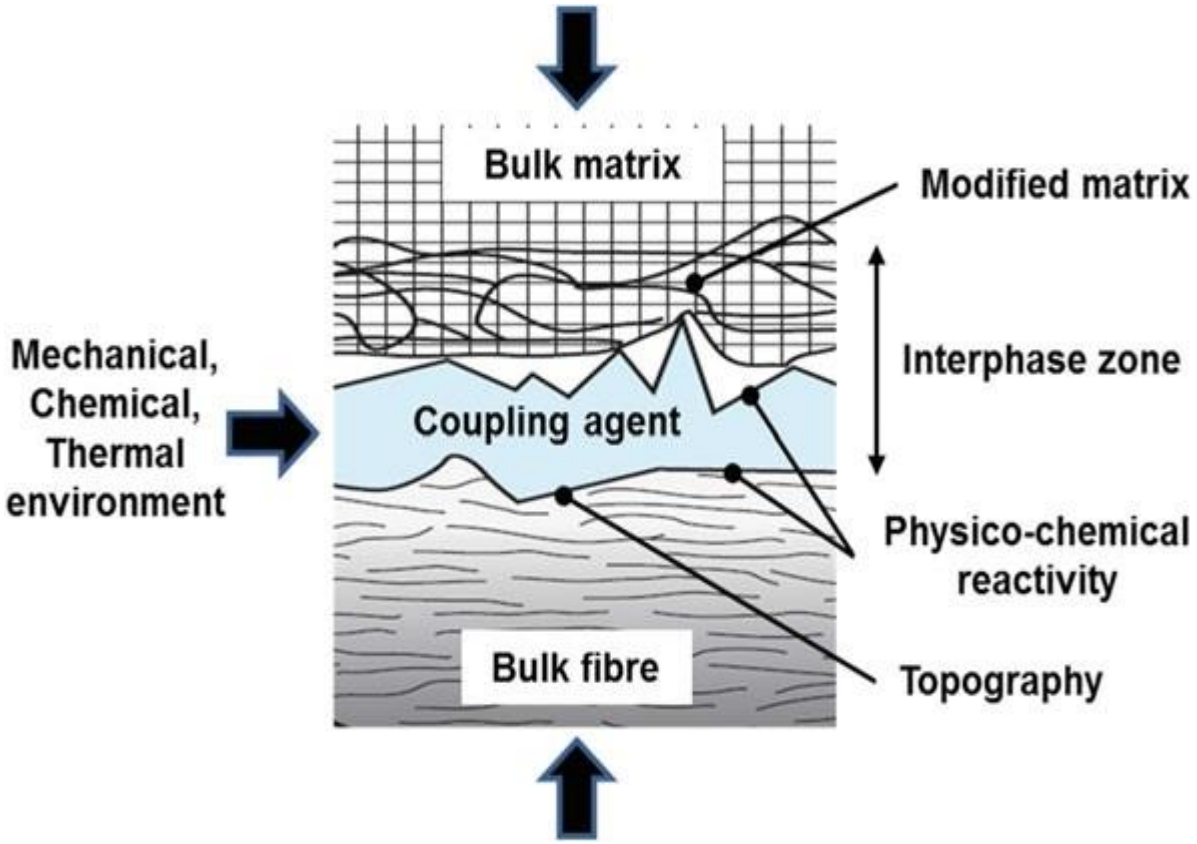

Figure 14: Fibre/matrix interface in a composite material (Moigne et al., 2018).

2.7.2 The concept of wetting and intermolecular interaction

Defined as the ability of a liquid to make a sustainable contact with a solid surface, the wetting that generates the fibre/matrix adhesion, occurs when intermolecular interactions between two components of different phases are brought together. Fibre wetting, influenced by surface roughness and surface polarity, is a prior step to any interactions or bonding between fibres and matrix in the adhesion process (Van De Velde and Kiekens, 1999) (Karaduman *et al.*, 2018).

In the adhesion process, several interactions such as ion-ion, ion-dipole, dipole-dipole, van der Waals interactions, and hydrogen bonding can occur (Karaduman *et al.*, 2018).

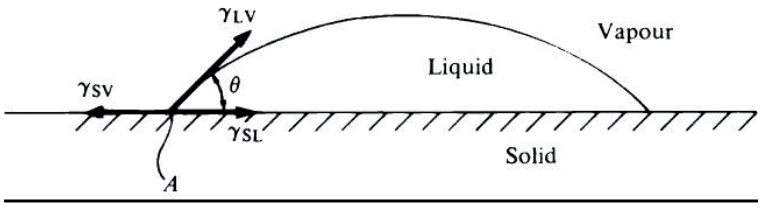

Figure 15: Theory of the contact angle (Karaduman et al., 2018).

The contact angle, θ, is defined as the angle between the normal to the solid and liquid surface at the point of interest along the three-phase interline. The contact angle may be related to the surface energies, i.e.,γ's, of the three interfaces by Young's equation:

$$\gamma_{SV} = \gamma_{SL} + \gamma_{LV}\cos\theta$$

γ_{SV}: effective boundary tension of the solid-vapour interface (or solid/vapour interfacial energy);

γ_{SL}: effective boundary tension of the solid-liquid interface (or solid/liquid interface energy); and

γ_{LV}: liquid surface tension.

Perfect wetting means that the resin spreads over the greatest possible surface area of the fibres i.e., the contact angle, $\theta = 0^{o}$. The solid is also said to be wet out by the liquid. In principle the liquid can then, if there is sufficient room, spread out to form a monomolecular film. In relation to the Young's equation, this is favoured by high γ_{SV}, i.e., high solid-vapour surface energy, low γ_{SL}, and low liquid surface tension.

The second case is for $0^o < \theta < 90^o$. The liquid is said to wet the solid, but not completely. The solid prefers, to some extent, to be covered by the liquid as opposed to the gas.

In the third case, $90^o < \theta < 180^o$, the liquid is said not to wet the solid. This situation is favoured by high surface tension liquids on low surface energy solids.

2.8 Surface treatments

2.8.1 Chemical pulping

The main goal of chemical pre-treatments is to produce a cellulose fibre, a shapeless form of material named pulp, by disrupting the structure of biomass through the fractionation of lignin as well as hemicellulose and cellulose polymers (Huijgen, Bermudez and Bakker, 2010) (Lee, Hamid and Zain, 2014) (Hintz and Lawal, 2018).

The lignocellulose pre-treatment has four objectives: firstly, to hydrolyse lignocellulosic complex (break down covalent bonds between and within lignin, hemicellulose and cellulose) and secondly to solubilize the non-cellulose contents (lignin, hemicellulose and extractives). The solubilization of the non-cellulose contents occurs after a partial degradation of the components to fractions with lower molecular weights. Additionally, the pre-treatment is also aimed at reducing cellulose crystallinity and increasing the porosity of the materials for subsequent depolymerisation process. The common chemical pre-treatments for biomass depolymerisation are: acid hydrolysis, alkaline hydrolysis, oxidative delignification, organosolv and ionic liquids (Huijgen, Bermudez and Bakker, 2010) (Lee, Hamid and Zain, 2014).

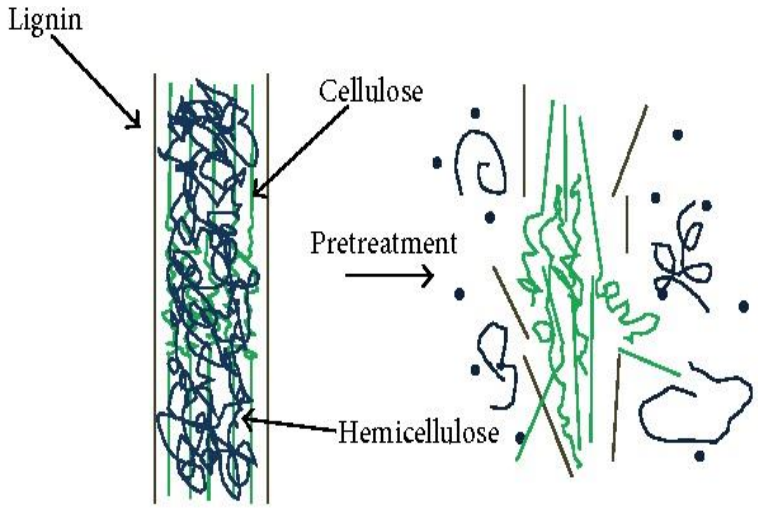

Figure 16: Schematic illustration of effects of pretreatment on lignocellulose components (Lee, Hamid and Zain, 2014).

2.8.1.1 Acid hydrolysis

During this process, the rigid structure of lignocellulose biomass is broken down (Figure 16) by hydronium ions from acids such as HCl, H_2SO_4, H_3PO_4, and HNO_3 which then fragment the biomass components by breaking intermolecular and intramolecular linkages among the cellulose, hemicellulose and lignin. The acid hydrolysis can be performed with either strong or diluted acid. Strong or concentrated acids involve the use of higher concentrated acids (30 – 70%), whereas, weak or diluted acids use lower concentrated acids with 5 – 10% or 10 – 30% concentrations for high temperature and continuous flow or low temperature and batch processes, respectively (Huijgen, Bermudez and Bakker, 2010) (Agbor *et al.*, 2011) (Anwar, Gulfraz and Irshad, 2014) (Lee, Hamid and Zain, 2014).

The solubilisation of hemicellulose occurs after holding the mixture of the acid solution and the biomass at a specific temperature for specific period. This causes the fragmentation of hemicellulose into monomeric sugars and hydrolysed oligomers; hence increasing the porosity of the cellulose fibre by removing hemicellulose (Huijgen, Bermudez and Bakker, 2010).

In comparison to concentrated acids that present drawbacks such as acid recovery, toxicity and corrosion, diluted acid does not cause any of these drawbacks. As a result, they are the most used acid hydrolysers (Huijgen, Bermudez and Bakker, 2010) (Agbor *et al.*, 2011) (Anwar, Gulfraz and Irshad, 2014) (Lee, Hamid and Zain, 2014).

2.8.1.2 Alkaline hydrolysis

This is one of the most widely use fibre treatment processes (Akil *et al.*, 2011). The alkaline pre-treatment involves the use of NaOH, KOH, $Ca(OH)_2$, hydrazine and aqueous ammonia. These components provide hydroxide ions, which react with the intermolecular ester bond crosslinking hemicellulose and lignin. This reaction is known as a saponification reaction. The cleavage of the ester bonds causes a degradation of the lignin polymer, which results in an increase of the availability of cellulose and hemicellulose for further treatments. The benefits of this pre-treatment can be summarized in the following points:

- swelling of cellulose that renders a partial depolymerisation of cellulose, reduction of the crystallinity of cellulose and an increase of internal surface area,
- increasing the porosity of the material by removing crosslinks, and
- partial solvation of hemicellulose by breaking its intramolecular glycosidic ether bonds. Depolymerisation of lignin by breaking its intramolecular ether bonds also occurs(Huijgen, Bermudez and Bakker, 2010) (Agbor *et al.*, 2011) (Anwar, Gulfraz and Irshad, 2014).

Break down of fibres bundles of the untreated fibres into smaller fibres is called fibrillation. The surface modification has been observed to cause surface roughness in fibres, exposing more of the cellulose fibre component (Dhandapani, Nayak and Mohanty, 2016).

It has been reported that an alkali pre-treatment should be preceded by a dilute acid pre-treatment to facilitate the removal of the hemicellulose component from the lignocellulosic complex (Lee, Hamid and Zain, 2014).

2.8.1.3 Bleaching pulping

After the chemical pulping, the lignin compounds are not fully removed from the pulps and their presence is responsible for the dark brown colour of the pulp. The bleaching process is then performed to remove the remaining lignin. Additionally, this process is also aimed to free the pulp from all the dirt and undesirable by-products that could not be separated from the lignocellulose biomass (Douglas, 1987).

The pulp bleaching can be carried out by either oxidizing agents such as chlorine gas, sodium hypochlorite, chlorine dioxide, oxygen gas, and hydrogen peroxide or a reducing agent such as sodium hydrosulphite. Each bleaching agent presents specific functions, advantages and disadvantages (Douglas, 1987).

The bleaching process is always performed as a process of combining bleaching and extraction treatments. Commonly called bleaching sequences, they are governed by the nature of different bleaching agents and their successions. Generally, bleaching sequences start with the removal of the lignin compounds (delignification segments), which is followed by an increase in brightening of the pulp (brightening segments) (Douglas, 1987).

2.8.2 Chemical treatments

Despite their advantages compared to synthetic fibres, hydrophilic lignocellulosic fibres present certain drawbacks such as instability at high temperature and high levels of moisture sorption, which is the most crucial disadvantage. The difference in chemical structure of the fibres and the matrix, which is hydrophobic, causes a problem when coupling the fibres and matrix components. This results in a surface incompatibility between polar cellulose plant fibres and the non-polar polymer matrix, leading to weak bond strength at the natural fibre and polymer matrix interface, and, hence providing a natural fibre reinforced polymer composite with poor mechanical properties (Li, Tabil and Panigrahi, 2007a) (Shih *et al.*, 2012) (Sood and Dwivedi, 2018).

A fibre treatment that can be performed by means of a chemical treatment is then required to enhance the mechanical properties of the composite by improving the surface bonding strength between the fibres and the matrix materials through a reduction of the polar behaviour of lignocellulose fibres (Li, Tabil and Panigrahi, 2007a) (Shih *et al.*, 2012) (Sood and Dwivedi, 2018). The fibre treatment of natural fibres can be performed by chemical methods such as silane treatment, benzoylation, peroxide treatment, acetylation or the use of maleated coupling agents (Li, Tabil and Panigrahi, 2007a) (Kabir *et al.*, 2012).

2.8.2.1 Acetylation

Although it was primarily used to stabilize microfibril cell walls against moisture, over the years, acetylation has been used to alter the nature of cellulosic fibres from hydrophilic to hydrophobic (Li, Tabil and Panigrahi, 2007b). This is achieved by removing the hydroxyl groups responsible for the moisture content. The surface treatment method is basically an esterification reaction which occurs in the presence or not of an acid catalyst such as H_2SO_4 (Figure 17). Under heating conditions, acetyl groups (CH_3CO-) from acetic anhydride substitutes the hydroxyl groups (-OH) in the cell wall of natural fibres (Kabir, 2012).

Due to the lower accessibility of acetic anhydride to cellulose in the microfibrils, a boosting of the esterification reaction is required. Natural fibres are then immersed in an acetic acid and acetic anhydride solution afterwards. Moreover, it has been recommended to alkali treat lignocellulosic fibres prior to the acetylation treatment to promote the esterification reaction (Bledzki *et al.*, 2008).

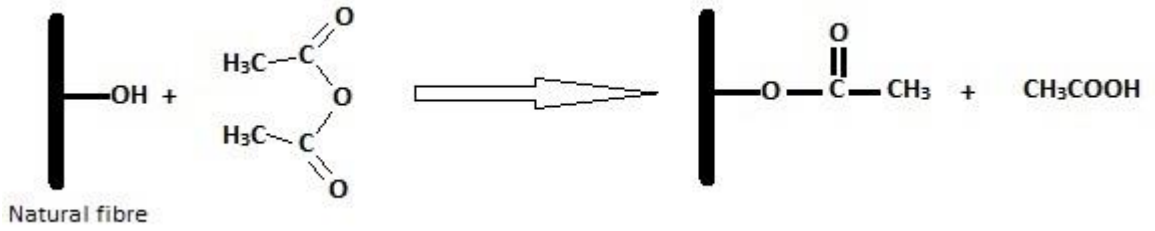

Figure 17: Illustration of an acetylation reaction of a natural fibre and anhydride acid Linkages between and within lignocellulosic components (Huijgen, Bermudez and Bakker, 2010).

A 3-hour acetylation treatment was performed on pre-alkali treated hemp fibres by immersing them in a glacial acidic solution. Afterwards, the fibres were washed and dried. Microstructural analysis revealed a rougher surface caused by the treatment, and the chemical composition showed an increase in the cellulose content. This resulted in an enhancement of the chemical and mechanical bonding in the hemp fibres, hence in an increase of the strength properties of the hemp fibres (Wang, Kabir and Kong, 2013).

Work was performed on popular bast fibres such as jute, flax, kenaf and hemp to study the influence of acetic anhydride treatment on the moisture content, thermal stability. Researchers reported that all the bast fibres showed an increase in moisture resistance and thermal stability accordingly to the concentration of the acetic anhydride solution (Kabir, 2012).

2.8.2.2 Benzoylation

Benzoylation treatment is also an effective method to change the nature of chemical fibres from hydrophilic to hydrophobic. Generally, natural fibres are first mercerized in NaOH aqueous solution in order to create more reactive sites on the surface of natural fibres for benzoylation, as shown in Figure 18. This is achieved by partially removing hydrogen bonding on the surface of the alkali treated natural fibre (Cho, Kim and Drzal, 2013).

Figure 18: Illustration of a benzoylation reaction Linkages between and within lignocellulosic components (Huijgen, Bermudez and Bakker, 2010).

Work was done on jute fibres whereby they were first alkali pre-treated by being immersed in a 1% NaOH solution at 30°C for 4h. The NaOH solution was then removed from the fibre surface by washing them sequentially with water, dilute acetic acid and distilled water. The fibres were finally dried at room temperature for 24 h and in an oven at 80°C for 6 h. The grafting of pre-treated fibres was realized by mixing the fibres with benzoyl chloride and agitating for 15 min. The mixture was then filtered, washed with distilled water and dried. The resulting fibres were placed in an ethanol solution for 1 h to remove excess benzoyl chloride from the jute fibres and were finally water washed and oven dried at 80°C for 6 h (Swain and Biswas, 2017).

The treated jute fibre filled composites were subjected to an abrasive study using the ASTM-G65 standard and their response was compared to those of untreated and alkali-treated jute fibre filled composites. The results revealed that improper interfacial adhesion between fibre and matrix led to fibre pull out and possible fracture, resulting in a reduction of wear properties of the composites. The benzoyl chloride treated fibre filled epoxy composites presented better wear properties than the untreated and alkali treated fibre-based composites. This is due to the reduction in porosity and an improvement in interfacial adhesive properties between the jute fibres and epoxy matrix (Swain and Biswas, 2017).

2.8.2.3 Maleic anhydride treatment

Maleic anhydride molecules are also used to improve the interfacial adhesion between the fibres and the matrix. During the treatment, the coupling agent through an esterification reaction reacts with the free hydroxyl groups present on the fibres (Figure 19) and with the matrix on the other end, creating an interphase which enables the formation of better fibre/matrix interfaces. The reagent not only reacts with free hydroxyl groups mostly present in the amorphous cellulose but also removes some. This reduces the hydrophilic behaviour of lignocellulosic fibres and fibre swelling. As a results, the capacity of load transfer within the composite is increased and, hence, the mechanical properties of the natural fibres reinforced polymer composite are improved (Mishra and Naik, 1998, 2005; Tanasă *et al.*, 2020).

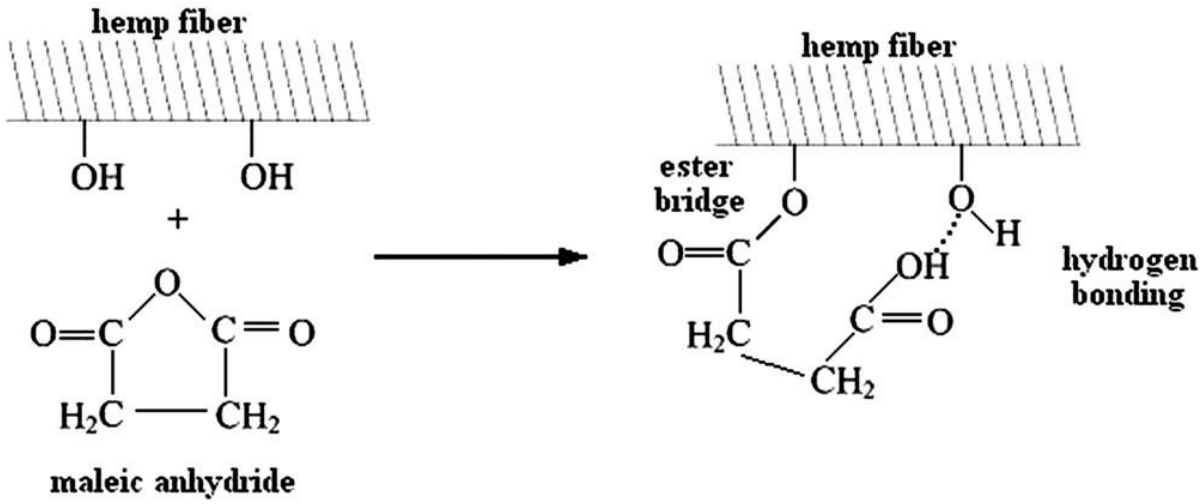

Figure 19: Esterification reaction of the fibre surface by the maleic anhydride (Tanasă et al., 2020).

The effect of maleic anhydride treatment on the mechanical properties of hemp fibres reinforced high density polyethylene (HDPE) composites was investigated by Roumeli *et al.*, 2015. The hemp fibres were treated for 18 h at 65 ± 2°C, with 1:20 (w/v) fibre/solvent ratio, in a mixture of 2% maleic anhydride dissolved in xylene. Afterwards, fibres were first washed with xylene to remove the unreacted maleic anhydride before they were dried at 60°C. Untreated and treated hemp fibres reinforced HDPE were then produced and the effect of the maleic anhydride was investigated. The results revealed an increase in tensile properties from 25.5 ± 0.5 MPa to 28.3 ± 0.7 MPa for the untreated and treated hemp fibres reinforced HDPE. It was reported that the increase in tensile properties were caused by the esterification of the hemp fibres by the maleic anhydride that was responsible for a better adhesion between the hemp fibres and the matrix and therefore improving the tensile properties.

2.8.2.4 MAPP treatment

Also known as maleated PP, MAPP is used as a coupling agent not only to change the hydrophobic behaviour of natural fibres but also to modify the surface of the polymer matrix to enhance the quality of interfacial interactions in the fibre reinforced polymer composite (Faruk *et al.*, 2012) (Cho, Kim and Drzal, 2013).

Acacia mangium wood fibres were grafted with MAPP, i.e., Epolene E-43 and Epolene G-3003 by Taib *et al.*, 2004. Firstly, different mixtures of dried fibres and MAPP, at different concentrations (1, 3, and 5 wt.%) with 1.5 L of toluene in a glass reaction flask, were exposed to high temperature under reflux for 1 hour for the complete dissolution of MAPP. Secondly,

200g of Acacia mangium wood fibres were added to the mixture, the resulting mixture were taken to room temperature after 5 minutes of reaction and filtered to separate fibres from the solution. Thirdly, the non-covalently bonded components to the fibre were extracted using soxhlet in the presence of toluene for 24 hours. The fibres were finally dried at 70°C. They finally tested the tensile properties of the fibres and the results revealed an increase compared to the non-treated fibres.

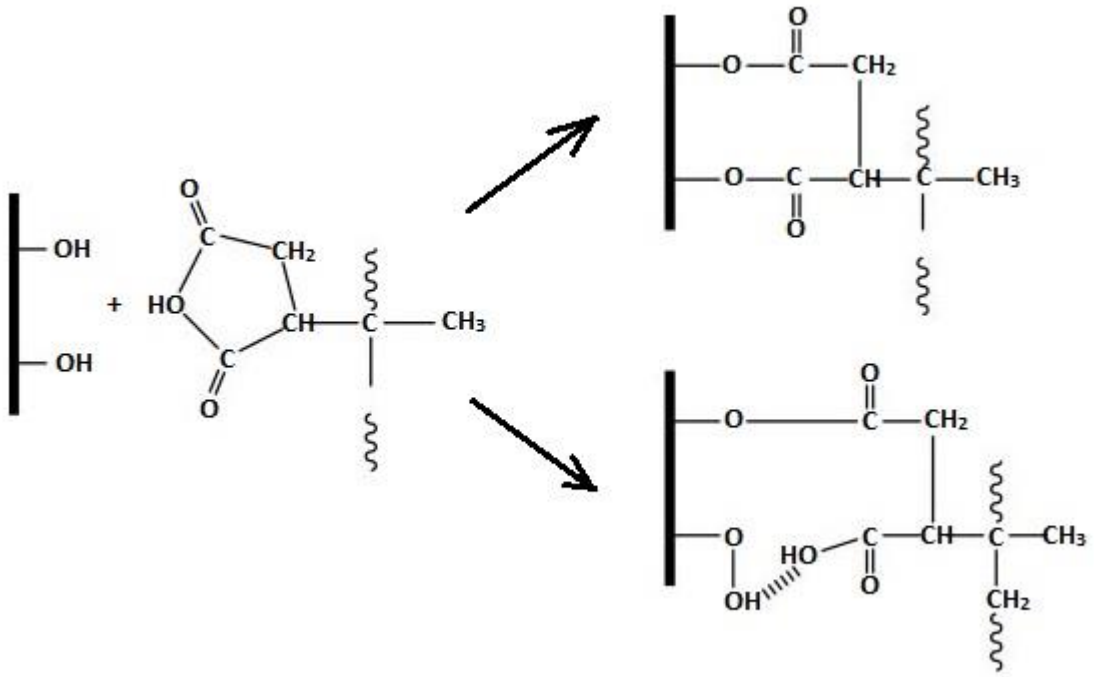

Figure 20: Illustration of a MAPP reaction (Cho, Kim and Drzal, 2013).

2.8.2.5 Peroxide treatment

Mostly used because of its ease, the peroxide treatment is also utilized to alter the polarity of natural fibres. The mechanism of the treatment involves the reaction of $RO^{\bullet}$ radicals from chemical agents ,such as dicumyl peroxide or benzoyl peroxide, with hydrogen atoms present at free hydroxyl groups of the microfibrils (Cho, Kim and Drzal, 2013) (Ali *et al.*, 2018).

$RO^{\bullet}$ + Cellulose–OH ⟶ R-OH + Cellulose

Figure 21: Illustration of a peroxide treatment reaction (Cho, Kim and Drzal, 2013).

The effect of dicumyl peroxide (DCP) surface treatment on the tensile properties of short sisal fibre-reinforced polyethylene composites was examined. Alkali-treated sisal fibres were immersed in a 6% solution of DCP in the presence of acetone for 30 min. The fibres were removed after decanting and air dried afterwards. It was reported that the tensile strength and modulus of the DCP treated fibre-based PE composites increased by approximately 50% compared to the untreated sisal filled PE composites. A similar increase was also observed for the modulus. This improvement in the mechanical properties was attributed to the enhanced adhesion between the treated fibres and PE matrix (Kuruvila, Sabu and Pavithran, 1996).

2.8.2.6 Silane treatment

Silanes are organofunctional molecules that react with the surface of cellulose-based natural fibres at one end and the polymer matrix resin at the other end. Their general formula is $X_3Si\text{-}R/\ R_{(4-n)}\text{-}Si\text{-}(R'X)_n$ (n=1,2) where R represents a chemical group that can react with the functional group in the polymer matrix; and X a functional group able to allow reactions to take place between the silane and the hydroxyl groups located on the natural fibres (Xie *et al.*, 2010).

2.8.2.6.1 Hydrolysis processes of silanes

It has been reported that alkoxysilanes can directly react with –Si–OH groups of silica to form –Si–O–Si– bonds without undergoing any pre-hydrolysis. However, the lower acidity of hydroxyl groups present on natural fibres inhibits this reaction. Therefore, silanes need to undergo hydrolysis to react with the hydroxyl groups of cellulosic fibres. Furthermore, cellulose rarely reacts with other chemicals and the OH groups on the fibres are not easily accessible. To overcome this, an activation of the alkoxysilane by hydrolysing the alkoxy groups off is then required. This results in the formation of more reactive silanol groups. Consequently, the silanol can react with the hydroxyl groups of fibres or condense themselves on the surface of fibres and/or in the cell walls forming a macromolecular network. The resultant –Si–O–C– are not only less susceptible to hydrolysis but also prevent a reversible hydrolysis reaction by blocking hydroxyl groups (Xie *et al.*, 2010). Although the –Si–O–C– bonds formed are eventually not stable towards hydrolysis, blocking the hydroxyl groups and the formation of macromolecules may facilitate an improvement of interfacial adhesion of treated fibres and polymer matrices. Hence, the nature of the microfibril is changed from the hydrophilic to the hydrophobic nature reducing the fibre's water adsorption behaviour and

improving fibres resistance to the applied load and therefore enhancing the mechanical properties of the fibres (Xie *et al.*, 2010)(Faruk *et al.*, 2012).

2.8.2.6.2 Fibre surface coating and cell wall modification

Among all the different methods used to apply silane solutions to natural fibres, the spraying method is one option. A solution is first prepared by mixing the silanes with organic solvents or solvents/water mixtures. Then the prepared solution is sprayed onto the fibre surface. When dealing with water-free solutions, the water from fibres and air can partially hydrolyse the sprayed silanes. However, the fibre cell walls are not affected during this treatment. The fast evaporation of solvent in air and the fact that the nano-pores cannot open up will make it difficult for the chemical to penetrate into the fibre cell walls. As a result this surface treatment method only modifies the natural fibre surface (Xie *et al.*, 2010).

Researchers manufactured a natural fibre filled composite using the extrusion process. During the extrusion of the composites, they directly introduced a silane solution and an activator into the extruder. To finalize the hydrolysis and condensation of the extruded composite, they placed it in an environment with high humidity and temperature. The silanes introduced in the extruder did not only react with the interface of fibre and matrices but also with the matrices. Thus, this process technique is also considered as a surface treatment (Xie *et al.*, 2010).

However, during a bulking treatment, which is the modification of fibre surfaces and cell walls by silanes during the natural fibre treatment with pre-hydrolysed silanes, the diffusion of silanes into cell walls depends on the molecular size of silane. This is influenced by the aging of the hydrolysed silane solution. When the hydrolysis processes of silanes are not well performed, a possible fast condensation of silanols can lead to an increase of the molecular size of the silane. Also known as the impregnation process, the bulking treatment of fibre cell walls can modify the properties of cell walls, thus, enhancing the properties of the resulting composites. It must be noted that the impregnation process presents some disadvantages. For instance, fine short fibres can gather together thus preventing themselves from dispersing in the solution; the drying process may require a lot of energy (Xie *et al.*, 2010)

2.8.2.6.3 Interaction mechanisms between silanes and natural fibres

2.8.2.6.3.1 Adsorption between silanols and hydroxyl groups of fibres

The monitoring of the isothermal adsorption of silanols groups onto cellulose fibre surfaces using FTIR and UV spectroscopy has been reported (Xie *et al.*, 2010). When hydrolysed silane solutions are mixed with natural fibres, news –Si-O-Si- bonds are formed due to the affinity of silanol groups among themselves. The silanol ɣ-aminopropyltriethoxysilane (APS), methacrylpropyltriethoxysilane (MPS) and ɣ-diethylenetriaminopropyltriethoxysilane (TAS) are primarily adsorbed by the fibre surface such that they form a monolayer. Secondly, due to the condensation reaction, more is absorbed and a rigid polysiloxane layer is formed. As a result, a concentration gradient may be present in the cell walls because of the obstruction of any diffusion by the polysiloxane layer. Hence, the hydrolysis parameters such as pH of solution have to be controlled to reduce the condensation rate in order to promote diffusion. APS and TAS showed a higher adsorption towards the surfaces of cellulose fibres than MPS. This may be attributed to the presence of strong hydrogen bonds between the amino groups and the fibre hydroxyl groups (Xie *et al.*, 2010).

2.8.2.6.3.2 Bonding of silanols and the hydroxyl groups of fibres

Although the –Si-O-C bonds and the -Si-O-Si- formed bonds are not susceptible to any hydrolysis, the free silanol groups can react to generate new -Si-O-Si- network linkages on/in the fibres during solvent evaporation. This has been displayed by ^{29}Si-NMR studies. At room temperature, the hydrogen bonds formed at the fibre surface during the adsorption mechanism do not turn to –Si-O-C- linkages. Heat is then required for the removal of water/solvent in the fibres and at the adsorption sites between silanols and fibre hydroxyl groups. As a result, -Si-O-C- bonds are formed.

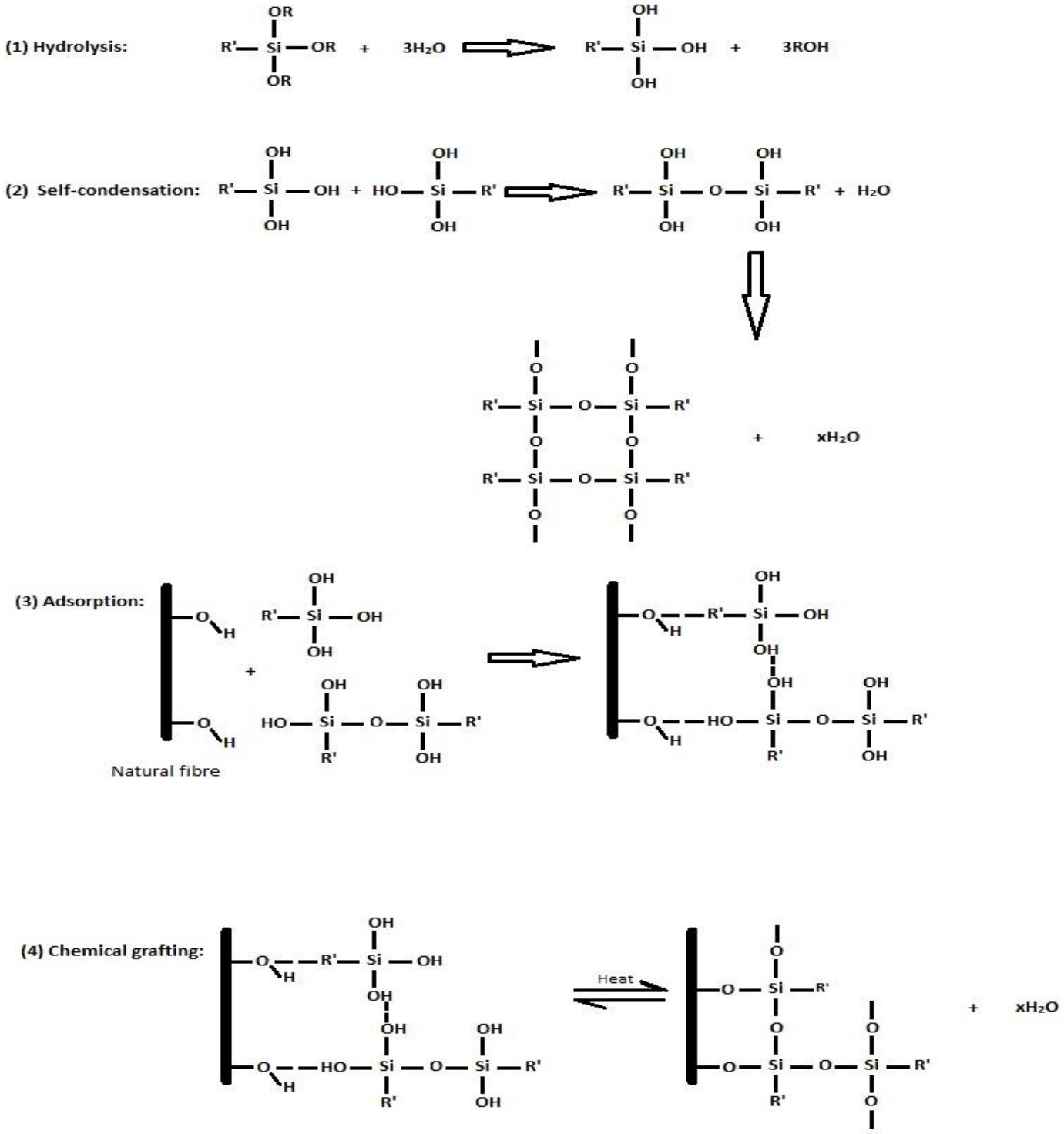

Figure 22: Illustration of all the silane treatment stages (Cho, Kim and Drzal, 2013).

The thermal stability of silane treated flax fibres was studied by means of thermogravimetric analysis (TGA). The fibres were soaked in a vinyl-trimethoxy silane (VTS) aqueous solution for 1 h and exposed to a temperature range of 30-800°C. The results revealed an increase in

thermal stability of hemicellulose and pectin (Xie *et al.*, 2010). It has been reported that silane treatments do not have a tremendous influence on the fibre tensile strength. This was attributed to the presence of fibre-damaging elements such as acid catalysts or high temperature (Xie *et al.*, 2010).

2.9 Effect of chemical treatments on the mechanical properties of natural fibres reinforced polymer composites

Depending on the applied chemical treatment, bast fibres, in general, and hemp fibres, in particular, can display different mechanical and thermal properties in composites produced from them. Some surface treatments have been reported to enhance the mechanical and thermal properties of composites filled with plant fibres, whereas others have been reported to degrade their properties. Below is a review of selected surface treatments on the mechanical properties of bast fibres reinforced polymer composites.

A study was performed to investigate the influence of different alkali and silane treatments on the mechanical properties of hemp reinforced epoxy composites (Sepe *et al.*, 2016). Different concentration of sodium hydroxide (NaOH) and (3–glycidyloxypropyl) trimethoxysilane solutions were used to alter the surface chemistry of the hemp fibres. Hemp fibres were first treated in different solution of NaOH, 1 wt% and 5 wt%, for 30 minutes before they were washed with distilled water until they reach a neutral pH. Afterwards, the fibres were dried in an oven at 70°C for 24h.

Silane treatments using 1 wt%, 5 wt% and 20 wt% of (3–glycidyloxypropyl) trimethoxysilane solution in ethanol and water, with an 80/20 vol %, were also performed on hemp fibres. After a pre-hydrolysis of silane in ethanol/water for 1 h at room temperature, fibres were soaked in the hydrolyzed silane solution for 1 h before they were oven dried at 70°C for 24 h.

Six laminates were produced by reinforcing epoxy with untreated, alkali- and silane-treated hemp fibres using a Vacuum Infusion Process in a mould at room temperature. Tensile and flexural specimens were cut off from the composite laminates and tensile and flexural tests were performed according to ASTM D 790 and ASTM D 3039, respectively.

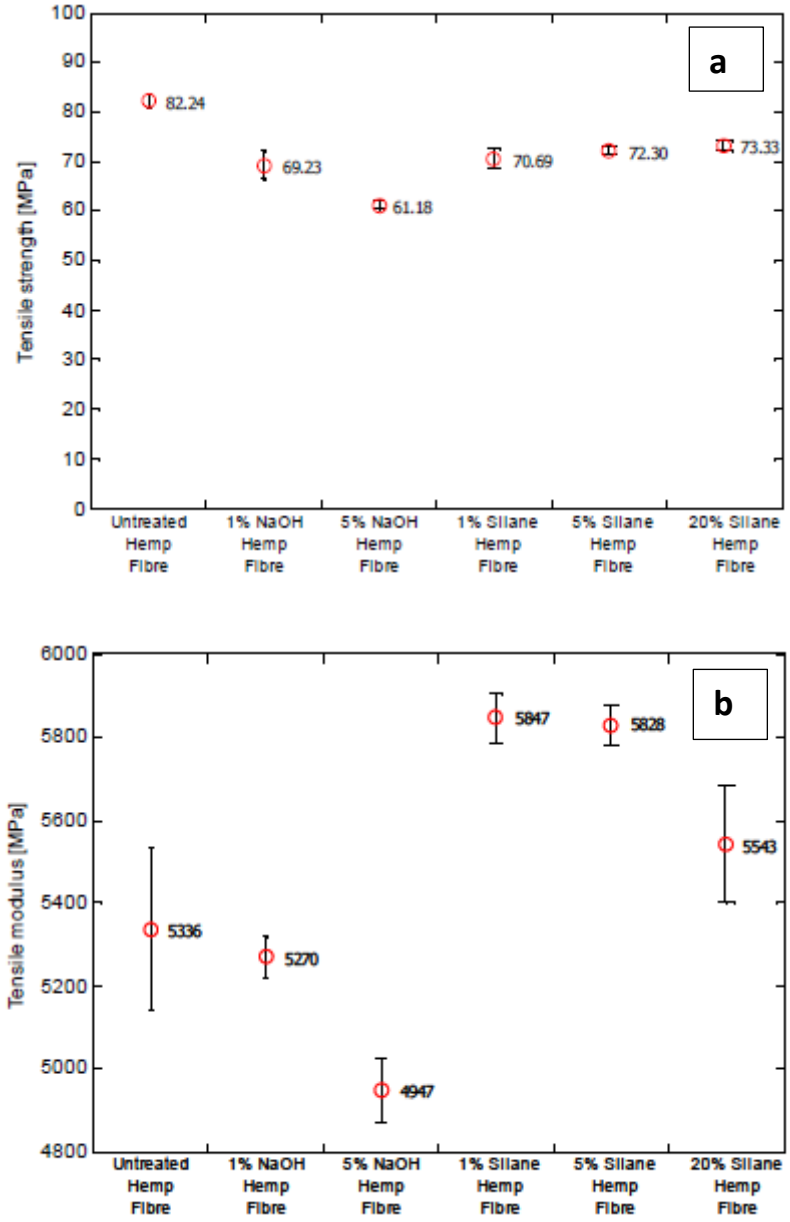

Figure 23: Tensile properties of treated hemp fibres reinforced polyester composites (Sepe et al., 2016).

Figure 23 (a) and (b) presents the results of the tensile and flexural tests performed on untreated, alkali- and silane-treated hemp fibres reinforced epoxy composites performed by Sepe *et al.*, 2016.

Their study revealed a reduction in the tensile strength of the alkali- and silane-treated hemp fibres reinforced epoxy composites compared to the untreated hemp fibres reinforced epoxy composites. For the alkali-treated reinforced hemp fibres epoxy composites, this was attributed to the removal of hemicellulose and lignin from the hemp fibres by the alkali-

treated causing the microfibril to be pulled apart easily. For the silane treatment, they argued that the improvement in the bonding between the hemp fibres and the matrix caused a slight increase in the tensile strength compare to the alkali-treated hemp fibres reinforced epoxy composites (Sepe *et al.*, 2016). Additionally, the tensile moduli showed the same variation as the variation of the tensile strength except for the 20 wt% silane-treated hemp fibres reinforced epoxy composites. Generally, silane-treated hemp fibres epoxy composites displayed higher tensile moduli due to better bonding between the hemp fibres and the epoxy resin compared to untreated and alkali-treated hemp fibres reinforced epoxy composites (Sepe *et al.*, 2016).

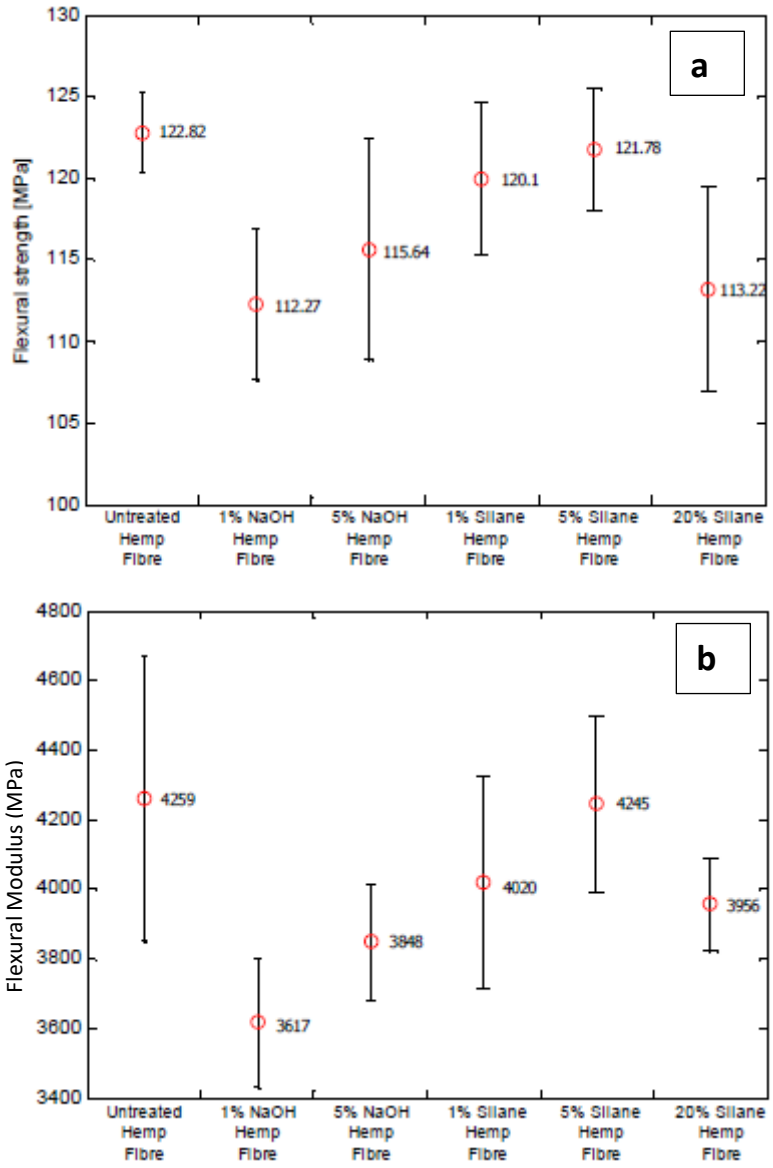

Figure 24: Flexural properties of treated hemp fibres reinforced polyester composites (Sepe et al., 2016).

The flexural strengths and modulus of the untreated, alkali- and silane-treated hemp fibres reinforced epoxy composites showed the same pattern as shown in Figure 24 (a) and (b). The 5 wt% silane-treated and the untreated hemp fibres reinforced epoxy composites displayed the highest flexural strengths and modulus. Additionally, the tensile strength of the 1 wt% silane-treated hemp fibres reinforced epoxy composites was close to the one of the untreated hemp fibres reinforced epoxy composites. This showed that the silane treatment did not influence the flexural properties of the tested laminates. Moreover, the 1 wt% alkali-treated hemp fibres reinforced epoxy composites showed the lowest tensile strength. This showed how negative the impact of the alkali treatment, at this concentration, was on the hemp fibres (Sepe *et al.*, 2016).

Sepe *et al.*, 2016, concluded that the alkali treatment by removing hemicellulose and lignin caused the microfibril to easily be pulled out whereas the silane treatment improved the hemp fibre and epoxy matrix interface. Therefore, the overall properties of the silane-treated hemp fibres reinforced epoxy composites were higher than the overall properties of the alkali-treated hemp fibres reinforced epoxy composites.

Aziz and Ansell, 2004, also investigated the effect of a 6 wt% NaOH solution on the flexural properties of hemp fibres reinforced polyester composites. The hemp fibres were treated in the NaOH solution for 48 h before they were washed with distilled water and dried for 5 h in an oven at 110°C. Composite laminates were then produced by compression moulding. Afterwards, 3-point bend specimens were cut off from the laminate plates and tested. Their results showed an increase in tensile strength from 77 MPa to 101 MPa for the untreated hemp reinforced polyester composites and the alkali-treated hemp fibres reinforced polyester composites. This was attributed to the better mechanical interlocking and chemical bonding between the hemp fibres and the resin which led to an increase in the mechanical properties. These results were in contrast to Sepe *et al.*, 2016.

The effect of alkalization, alkalization + acetylation and alkalization + silanization treatments on the mechanical properties of hemp fibres reinforced polyester composites was also investigated by Kabir, 2012. Hemp fibres were first alkali-treated with different concentrations of NaOH solutions, 0 wt%, 4 wt%, 6 wt%, 8 wt% and 10 wt%. After, the hemp fibres were washed for 8 h at room temperature before they were dried at 100°C for 6 h in an oven.

The alkali-treated hemp fibres were immersed in a mixture of acetic anhydride and acetic acid (glacial) at room temperature for 3 h. Fibres were then washed with distilled water to remove the unreacted acetic anhydride before they were dried at 100°C for 6 h in an oven.

Other pre-treated hemp fibres were also treated with a 3 wt% oligomeric siloxane solution dissolved in a mixture of methanol/water (60/40, v/v) for 3 h at room temperature. Afterwards, the fibres were dried in an oven at 110°C for 5 h. The composites were made by making use of Vacuum Assisted Resin Transfer Moulding and hand layup processes.

Tensile and flexural specimen tests were cut off from the composite plates and the tensile and flexural properties were tested according to ASTM D 790 and ASTM D 3039, respectively.

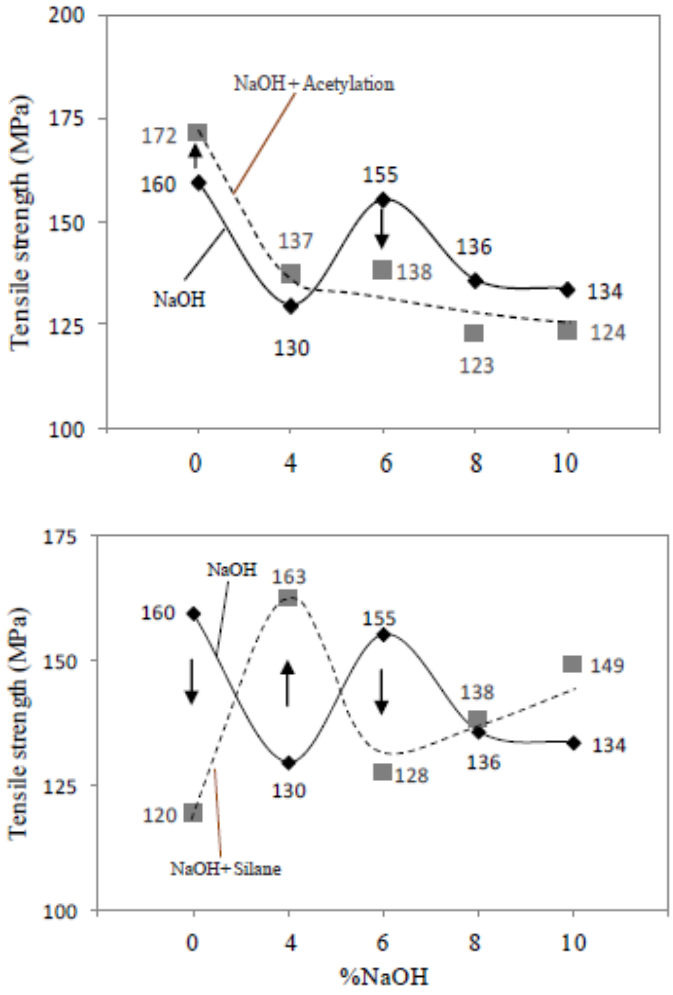

Figure 25: Tensile properties of alkali, alkali + silane and alkali + acetylation (Kabir, 2012).

Kabir, 2012, reported a decrease in the tensile strength of the 4 wt% alkali-treated hemp fibres reinforced polyester composites compared to the untreated hemp fibres reinforced

polyester composites. An increase was then observed at 6 wt% whereas the tensile properties decreased between 8 – 10 wt% of alkali-treated hemp fibres reinforced polyester composites. The decrease at 4 wt% NaOH was associated with the lack of enough materials from the alkaline solution to remove hemicellulose and lignin that prohibited a good bonding between the matrix and the cellulose. This lead to a weak interface and, hence, reduced the tensile strength of the composites (Kabir, 2012). At 6 wt% NaOH, the tensile strength of the alkali-treated hemp fibres reinforced polyester composites increased due to the removal of hemicellulose and lignin, which allowed a better bonding between the fibre and matrix, hence, increased the tensile properties of the alkali-treated hemp fibres reinforced polyester composites (Kabir, 2012). At 8 and 10 wt% NaOH, the excessive action of the alkaline solution on the hemp fibres removed an important quantity of hemicellulose and lignin, which made the cellulose microfibrils weaker and, hence decrease the tensile strength of the alkali-treated hemp fibres reinforced polyester composites at these NaOH concentrations (Kabir, 2012).

Figure 25 presents an increase in tensile strength at 0 wt% NaOH for the acetyl-treated hemp fibres reinforced polyester composites. Kabir, 2012, argued that during this treatment, the reaction occurred in two stages. Initially, the acetyl groups removed the hemicellulose and lignin that finally allowed the elimination of hydroxyl groups from the fibres by their esterification by acetyl groups. This enabled a better adhesion between the hemp fibres and the matrix, which then increased the tensile properties (Kabir, 2012). The acetyl treatment on the 4 wt% NaOH pre-treated hemp fibres showed higher tensile strength (Figure 25) compared to the alkali-treated hemp fibres reinforced polyester composites at the same NaOH concentration. This was the result of the better exposure of hydroxyl groups from the hemp fibres from the action of the 4 wt% NaOH treatment, which facilitated the esterification of the hydroxyl groups on the alkali-treated hemp fibres. The removal of further amounts of hemicellulose and lignin during the acetylation also allowed the formation of a better interface between the hemp fibres and matrix. This improved the overall capacity of the material to bear load and, hence, increased the tensile strength (Kabir, 2012). At 6 and 10 wt% NaOH, a considerable amount of hemicellulose and lignin had already been removed. A further acetylation of the alkali pre-treated hemp fibres caused removal of some of the remaining hemicellulose and lignin form the hemp fibres and weakened the hemp fibres structure. This resulted in a lack of hydroxyl groups for the esterification with the acetyl

groups and, hence, led to the formation of a weak interface between the hemp fibres and the matrix. As a result, this caused a decrease in the tensile properties of the alkali + acetylated-treated hemp fibres reinforced polyester composite at this concentration (Kabir, 2012).

For the silane treatment, the silanization of the untreated fibres showed a huge reduction in the tensile strength as shown in Figure 25. Kabir, 2012, attributed this reduction to the presence of moisture on the untreated hemp fibres that negatively affected the presence of the formed silanol molecules. Additionally, the coupling agent reacted with hydroxyl groups from the fibres on one end and the matrix on the other end. Although, the strong interface formed between the fibres and the matrix, the presence of the non-removed hemicellulose and lignin covering the hemp fibres did not allowed the chemical agents to access enough free hydroxyl groups from the fibres. This created a new layer of silane molecules covering the hemp fibres, which then resulted in an overall poor bonding in the composite material. During the pulling of the composite, the silanol molecules layer responsible for shear deformation at the interface, made it easy for the fibres to be pulled out from the matrix, hence, decreasing the tensile strength. For the 4 wt% alkali pre-treated hemp fibres, the silanized-treated hemp fibres reinforced polyester composites revealed a higher tensile strength compare to the alkali-treated reinforced polyester composite. This was caused by the removal action of the alkali treatment, which removed some hemicellulose and lignin to allow the silanol molecules to be formed on the hemp fibres by reacting with existing free hydroxyl groups. As a result, better bonding at the interface was achieved, introducing higher resistance against tensile loading thus improving composite strength (Kabir, 2012). With the 6 wt% alkali pre-treated hemp fibres, the silanized hemp fibres reinforced polyester composite showed a reduction in tensile strength compared to the 6 wt% NaOH treated hemp fibres reinforce polyester composites. The effect of a higher concentration of 6 wt% was responsible for the removal of more hemicellulose and lignin compared to the 4 wt% NaOH treatment. This did not allow the silane treatment to form more silanol molecules that would help the interface of the composite to be strong enough to resist higher loading. As a result, a decrease in tensile properties was observed (Kabir, 2012). The silane treatment performed on the 6 wt% NaOH pre-treated hemp fibres cause a reduction in strength in the resulting treated hemp fibres reinforced polyester composite compared to the 6 wt% NaOH hemp fibres reinforced polyester composite. This was attributed to the action of the pre-treatment

applied on the hemp fibres that removed hemicellulose and lignin constituents and their associated hydroxyl groups from the fibres. The silane treatment could then not facilitate enough hydroxyl groups to form silanol molecules within the fibres. The lack of silanol formation reduced the coupling efficiency between the fibres and matrix, and this results in weak interfaces that reduced the overall composite strength (Kabir, 2012). The 8 and 10 wt% NaOH treated hemp fibres polyester composites exhibited lower tensile strength than the 8 and 10 wt% NaOH pre-treated silanized hemp fibres polyester composites. Kabir, 2012, argued that higher NaOH concentrations cause the depolymerization of the crystallized cellulose which exposed hydroxyl groups to react with other molecules. Moreover, the silane treatments effectively allowed the formation of sufficient silanol molecules responsible for a strong fibre/matrix interface. This enhanced the load transfer capacity of the composites which increased their tensile properties.

Mishra and Naik, 2005, study the effect of maleic anhydride treatment on the mechanical properties of hemp fibres reinforced polystyrene composites. Hemp fibres were treated in a solution of maleic anhydride dissolved in xylene at 65 ± 2°C for 18 h. Afterwards, the fibres were filtered and washed with fresh xylene to remove unreacted maleic anhydride and dried in an oven at 60°C. Composites were then produced by compression moulding and the testing specimens were then cut from the laminates. The tensile properties of the untreated hemp fibres reinforced polystyrene composite were lower than the tensile properties of the maleic anhydride-treated hemp fibres reinforced polystyrene composites. These were 4.90 MPa vs 5.84 MPa and 512 MPa vs 840.60 MPa for the tensile strength and the Young's modulus, respectively. The flexural properties were also measured and showed an increase from the untreated hemp fibres reinforced polystyrene composite to the maleic anhydride-treated hemp fibres reinforced polystyrene composites from 18.83 MPa to 32.72 MPa and 2889 MPa to 4174 MPa, respectively. This increase in mechanical properties was ascribed to the action of the maleic anhydride that esterified free hydroxyl groups from the hemp fibres and caused better bonding between the treated fibres and the matrix compared to the untreated hemp fibres. This improved the load transfer capacity of the overall composite and as a result, an increase in mechanical properties was observed.

Bodur, Bakkal and Sonmez, 2016, compared the separate influence of NaOH and maleic anhydride-treated textile fibre reinforced epoxy composites to the combined effect of the

alkali-maleic anhydride treatment on the tensile properties of textile fibre reinforced polymer composites at different concentration varying from 1 wt% to 7 wt% of NaOH, maleic anhydride and NaOH-Maleic anhydride, respectively. Although the contrary was expected, at every concentration, the tensile properties, the tensile strength (TS) and Young's modulus (YM), of the NaOH-Maleic anhydride treated textile fibre reinforced polymer composites drastically dropped compared to the tensile properties of alkali- and maleic anhydride-treated textile fibre reinforced polymer composites as shown in Figure 26.

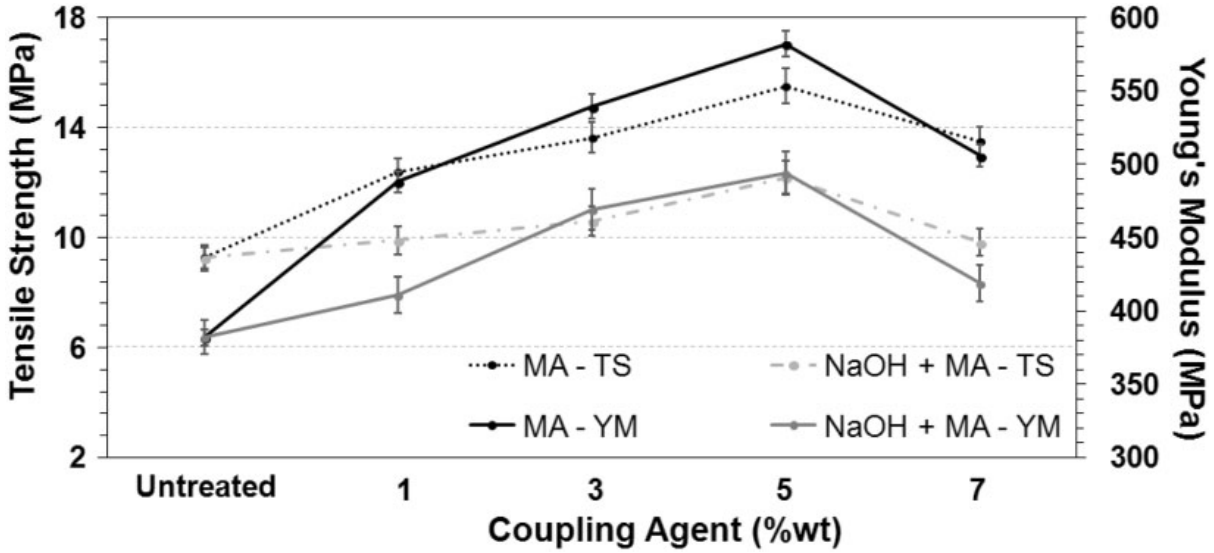

Figure 26: Influence on alkali (NaOH) + maleic anhydride (MA) treatment on the tensile strength (TS) and young modulus (YM) on the textile fibre reinforced polymer composites (Bodur, Bakkal and Sonmez, 2016).

The differences in the mechanical properties reported above were caused by the different effects the chemical treatments and coupling agents have the natural fibres and therefore their composites. The alkalization is known to remove lignin and hemicellulose from the lignocellulosic fibres. This enables the matrix to connect with the free hydroxyl groups present on the microfibril by creating a direct fibre/matrix interface. However, the silane and maleic anhydride coupling agents react on one side with the free hydroxyl groups of the fibres and with the matrix on the other side to create an interphase, which connects the fibres to the matrix. The differences in chemical compositions of the coupling agents are responsible for the different fibre/matrix formed and therefore the differences in mechanical properties of the produced composites.

It has to be noted that based on previous studies on chemical modification of natural fibre yarns/based composites, this study aims to address the critical gaps found in literature and provide solutions for these problems.

2.10 Mechanical properties modelling

The properties of plant fibre reinforced polymer composites used to be determined mainly by experimental techniques such as mechanical testing and surface experimental methods. For a deep understanding of the mechanical properties of natural plant reinforced polymer composites, researchers have been using mechanical properties prediction models such the general rule of mixtures (ROM), the modified rule of mixtures (mROM), the Halpin-Tsai model and the Cox model, etc (Madsen and Lilholt, 2003; Cao, Wang and Wang, 2014)(Benkhelladi, Laouici and Bouchoucha, 2020). Cao, Wang and Wang, 2014, used the rule of mixtures (ROM), the inverse rule of mixtures (IROM) and the Hirsch model to compare the effectiveness of the model in predicting the impact strength. Their results show that their experimental data were generally closer to the predicted values from the inverse rule of mixtures (IROM) as shown in Figure 27. And, it was concluded to be the best model compared to the other mechanical properties' prediction used in their study.

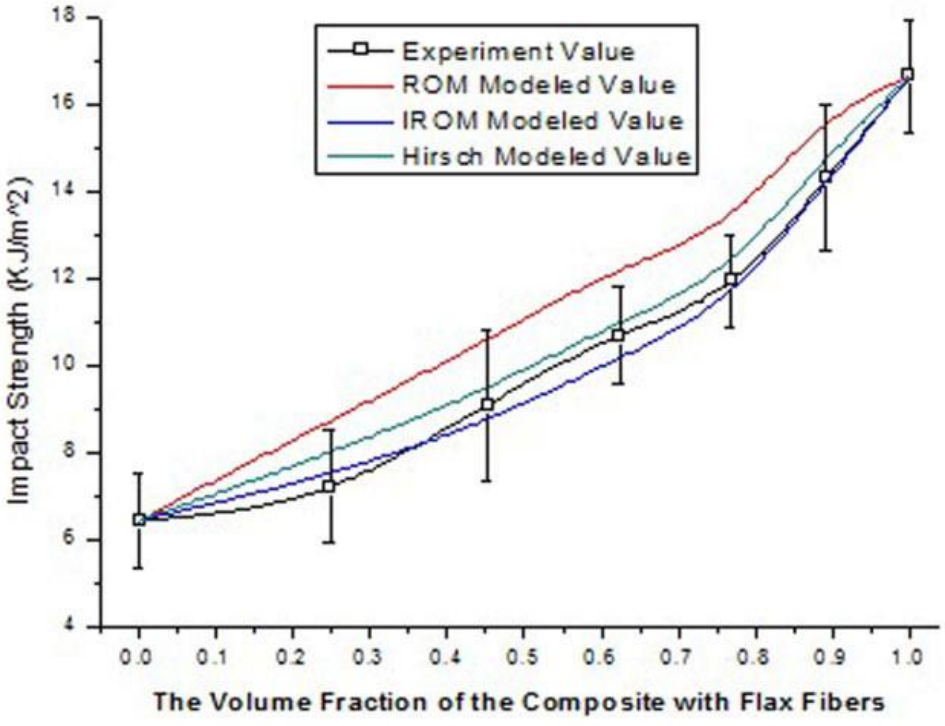

Figure 27: Predicted impact strength values vs the experimental values (Cao, Wang and Wang, 2014).

3 Experimental procedure

3.1 Material preparation and selection

Pre-treated hemp fabric, labelled 100% natural, was supplied by Hemporium SA (Cape Town). Specific details of the treatment this hemp fabric had undergone, before testing in this study, were not available. To prevent the procured woven fabric from not impregnating the resin due to the proximity of the different yarns, decision was taken to use the hemp yarns as reinforcement. A characterization of the warp and weft hemp yarns was then necessary before one type of yarn was chosen. Samples of 5cm×5cm were cut off from 5 different places of the hemp fabrics as shown in Figure 28 (a & b) with warp and weft directions depicted on. The cut fabrics were then separated into warp and weft yarns and finally isolated as either single fibres or fibre bundles as shown in Figure 28 (c & d).

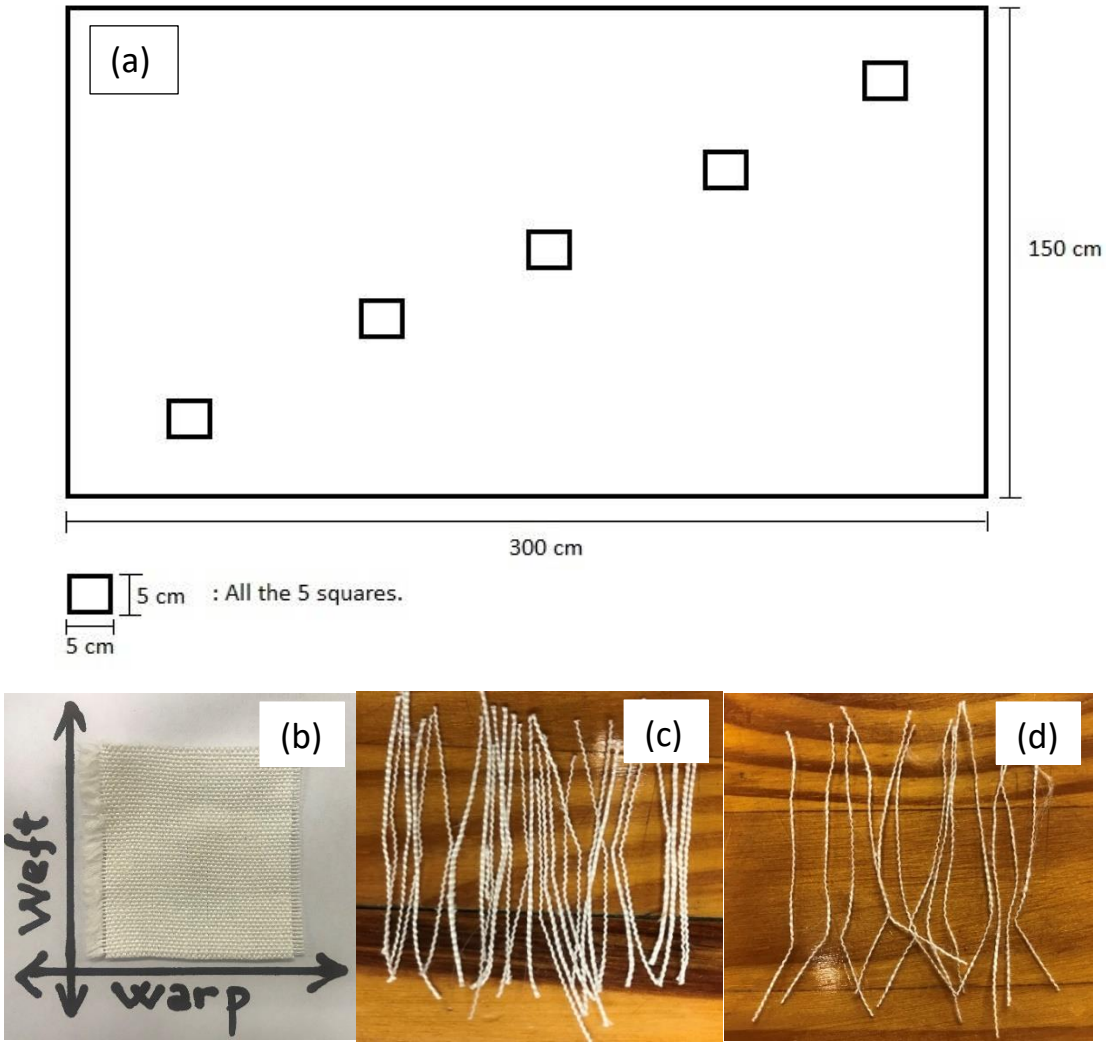

Figure 28: (a) Mercerized hemp fabric dimensions and sampling zones (5x5 cm2 squares); (b) 5x5 cm^2 sample; (c) weft hemp yarns and (d) warp hemp yarns.

Epoxies are linear or 3D cross-linked thermosetting polymers, formed from reactions between epoxy resins and hardeners. Studies have been performed on the relation between the cross-linking density and mechanical properties of epoxy polymers. Results reveal that the higher the cross-linking density, the better the mechanical properties. Among all the parameters influencing the polymer structure, the functionality of monomers indicates whether the final structure of the cured polymer will be linear or cross-linked. According to their functionality, reactants are classified in three groups: mono-functional, bi-functional and multi-functional. Bi-functional and multi-functional monomers are respectively responsible for the formation of linear and cross-linked structure, whereas mono-functional reactants form short chains (Batzer and Lohse, 1976)(Lascano *et al.*, 2019).

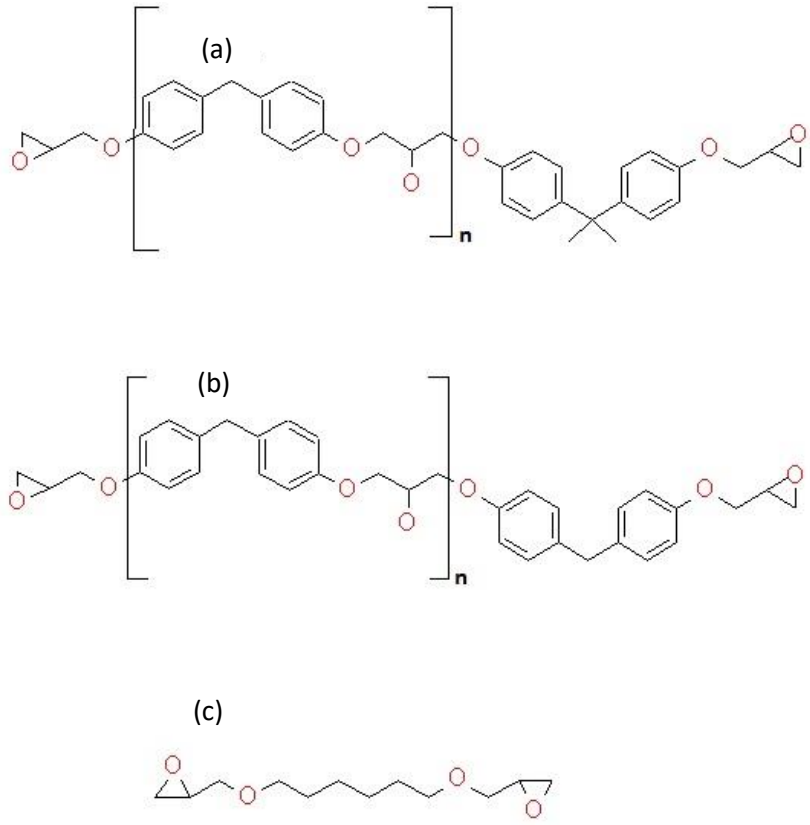

Figure 29:Resin mixtures present in the Sicomin system : (a) diglycidyl ether of bisphenol-A; (b) diglycidyl ether of bisphenol-F and (c) hexanediol diglycidyl ether (Avantor, 2012).

The choice of the epoxy system, Sd 8100/Sr 8224 (Sicomin Epoxy systems), was based on the desired high level of cross-linking in the epoxy composite after curing, which is achieved by a

resin/hardener functional ratio of 2:1 responsible for the cross-linking during the curing of the epoxy resin (Batzer and Lohse, 1976) (Lascano *et al.*, 2019). For this research, the functional ratio of the resin/hardener system was 2:1. Additionally, other factors such as viscosity, curing cycle were taken into consideration. As presented in table 4 below, the viscosity of the epoxy system was found to be low enough that the resin and hardener could be mixed manually. The working time appeared to be enough to mix the aligned yarns with the resin in the mould cavity before it could be placed under pressure. Figure 29 and 30, respectively, presents resin and hardeners present in the Sicomin Epoxy system.

Properties	Resin	Hardener
Viscosity (mPa.s) @ 25°C	765±155	5±2
Curing cycle	24h @ AT + 8h @80°C	
Working hour (min)	46	

Table 4:Properties extracted from the SD8100/SR822X (Sicomin Epoxy Systems) with AT = Ambient Temperature; full data sheet (Sicomin, 2019).

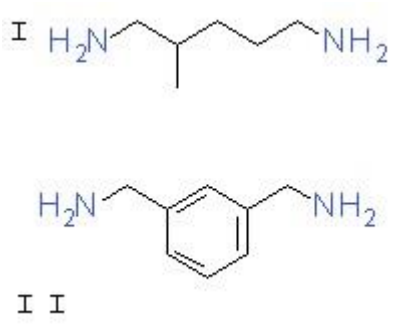

Figure 30: Hardeners: I: 2-methylpentane-1,5-diamine; II: 1,3-bis(aminomethyl)Benzene (Safety, Sheet and Classification, 2001).

3.2 Characterization of the hemp fibres and yarns

Among all the key properties of fibres and yarns, the characterisation centred on the yarn structure, yarn/plant inter-structures, twist per cm, surface characteristics, cross-sectional shape, and linear density.

3.2.1 Optical microscopic observation of hemp fibres and yarns

The examination of yarn/plant inter-structures of hemp fibres were first performed using an optical microscope. The microscope used was a Nikon Inverted Metallurgical microscope: ECLIPSE MA200 equipped with 10×, 20×, 50×, 100× objectives, a Nikon DS-L3 (DS Camera Head DS-Fi1 – DS Cooled Camera Head DS-Fi1c) camera control unit and a 100W Halogen lamp for episcopic or diascopic illumination. 12 single fibres/fibre bundles, a mixture of weft and warp yarns, from different areas on the hemp fabric were positioned on 12 microscopic slides with their ends glued by a cyanoacrylate glue. Afterwards, the slides were placed on the microscopic stage one after another for examination of their surface texture and yarn/plant inter-structures using a polarized light (single wavelength).

To observe the cross-sectional shape of the yarns, hemp yarns were cold mounted using a Specifix epoxy resin system (Struers), prior to microscopy analysis. After curing for 24h, the sample was ground with 1200 and 2000 grit sizes SiC papers, supplied by Struers, washed with distilled water and dried, then water polished with 3µm grit size diamond disc (Struers), and finally dried.

3.2.2 Fibre density and linear density

The pycnometer method was used to determine the density of hemp yarns as described by Rohen *et al.*, 2017 using distilled water as a solvent. The hemp yarns were dried for 12h at 60°C prior to the test whereafter they were weighed. The pycnometer was cleaned, dried and weighed. The pycnometer was filled with distilled before it was put in the desiccator for 2h to remove air bubbles and was weighed, afterwards. The pycnometer was emptied, dried before the dry hemp yarns were put in it. The pycnometer was then filled with distilled water. After 2h in the desiccator to remove the air bubbles, the pycnometer was weighed and the temperature of water was measured. The relative density of the hemp yarns was finally determined using the equation below:

$$\rho_{fibre} = \rho_{water}(m_3)/[(m_2-m_1) - (m_4-m_1-m_3)]$$

with m_1: mass of the clean and dried pycnometer in grams

m_2 = mass of the pycnometer filled with distilled water in grams

m_3 = mass of the dry hemp yarns in grams

m_4 = mass of the pycnometer with distilled water and the dry specimen in grams

ρ_{water} = density of water in g/cm^3 at the measurement temperature.

The linear density of hemp yarns was also determined using the direct system whereby the hemp yarn linear density was expressed by measuring the mass of a known length of yarn. The linear density of the hemp yarn was expressed in Tex and determined using the following equation:

$$\text{Tex (Denier)} = \frac{W \times 1\ Km}{\text{L} \times 1\ \text{g}}$$

where W = mass of the yarn in grams
L = length of the yarn in kilometres

3.3 Surface treatment of hemp yarns

The as-supplied fabric warp and weft yarns were subjected to several surface treatments. This was done to determine whether further treatment of an already mercerized yarn would impact the properties of the final epoxy composite, reinforced with such a yarn.

3.3.1 Alkali treatment

Hemp yarns, weft and warp, pulled out from the hemp fabrics were alkali-treated by soaking them in a 6wt% sodium hydroxide (NaOH) at room temperature, supplied by Kimix Chemicals, solution for 5h, with a fibre to solution ratio of 1:10 by mass. Afterwards, the alkali-treated hemp fibres were washed with distilled water and dried at 100°C for 12h.

3.3.2 Silane treatment

3-aminopropyltriethoxysilane was chosen for silane treatment because it contains an amine group (similar to the hardeners) making it likely it would react with the epoxide groups of the epoxy resin being investigated.

A 5wt% silane solution was prepared by mixing 3-aminopropyltriethoxysilane (ɣ-APS) solution with 50v/50v ethanol/distilled-water solution, with the ɣ-APS and ethanol supplied by Sigma-Aldrich and Kimix Chemicals, respectively. Drops of acetic acid glacial, 99.8% purity (Kimix Chemicals) were added to the mixture to adjust the pH to 3.5 and the silane solution was stirred for 3h to allow hydrolysis to occur. The fibres were then immersed in the solution for 6h at room temperature and removed afterwards. Fibres were finally washed thoroughly with water to get rid of all unnecessary chemicals until a pH of 7 was reached before they were dried at 80°C for 12h.

3.3.3 Maleic anhydride treatment

As received hemp yarns, weft and warp, were immersed in a 2% (v/v) solution of maleic anhydride dissolved in xylene with a fibre to solution ratio of 1:20 at 65±2°C for 18h; both chemicals were manufactured by Sigma-Aldrich. Afterwards, the yarns were filtered out; then washed with xylene to remove unreacted maleic anhydride and water afterwards to get rid of all the unreacted maleic anhydride. Finally, fibre yarns were oven dried at 80°C for 12h.

3.4 Tensile properties of untreated and treated yarns

The tensile properties of untreated and treated yarns were determined according to the ASTM D2256 Standard using a Zwick (1484) machine with a 10 kN load cell and cross-head speed of 2 mm/min. To minimize the effect of the humidity that the yarns may have absorbed during sample preparation, samples were placed in a desiccator overnight prior to testing and were only removed once they had to be subjected to testing.

3.5 Investigation of the surface treatment effectiveness on hemp yarns

To monitor the influence of the chemical treatments on the treated hemp yarns, X-ray Diffraction (XRD), Fourier Transform Infrared (FTIR) spectroscopy) and Scanning Electron Microscopy (SEM) analysis were performed.

3.5.1 X-ray diffraction analysis

To prepare the samples for the XRD analysis, 5 g of each type of hemp yarns were condensed, both untreated and treated, by placing them in a mortar and pressing at 20 Tons using a 30 TON L–330 press. The XRD experiment was performed with a MeasSrv (2ZC2VB2) instrument using a cobalt source and a wavelength of 1.79026 Å.

The crystalline cellulose content was quantified by determining the Crystallinity Index (CI) using the peak height method for natural cellulose as described below by the Segal equation (French, 2014) (Sunny, Pickering and Lim, 2020):

$$CI = \frac{\mathrm{I200} - \mathrm{Iam}}{\mathrm{I200}} \times 100$$

where I_{200} represents the intensity of the (200) peak at 2θ = 22.7°, which is due to the diffraction of both the crystalline and amorphous cellulose; and I_{am} is the diffraction of amorphous cellulose between 200 and 110 peaks at 2θ = 18.3°, as shown in Figure 31.

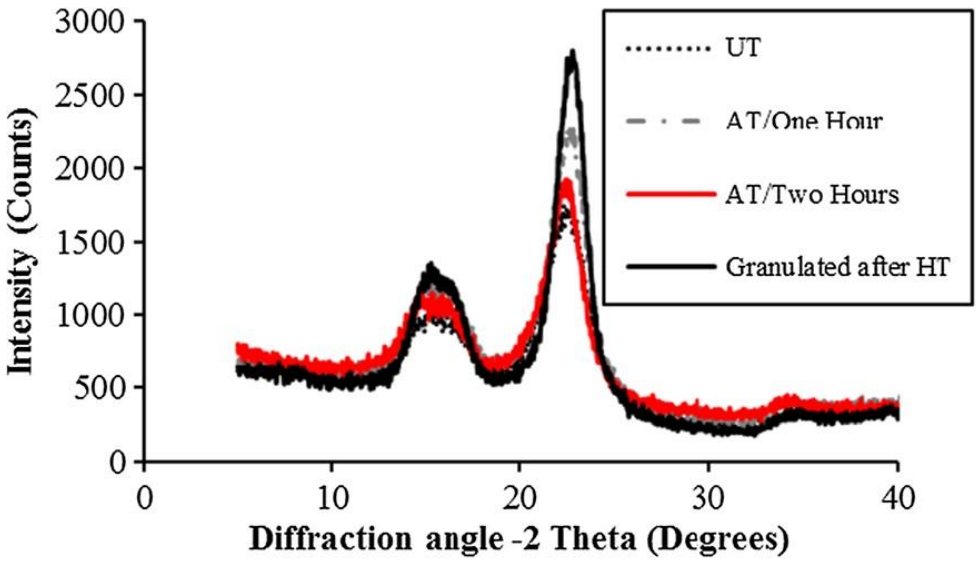

Figure 31: X-ray diffraction curves for untreated (UT), atmospheric treated (AT) and high temperature treated (HT) hemp fibres (Sunny, Pickering and Lim, 2020).

3.5.2 FTIR spectroscopy

Fourier Transform Infrared (FTIR) spectroscopy was utilized to monitor the changes in the molecular structure of hemp yarns. FTIR measurements were performed on a Perkin-Elmer FTIR 100 Spectrometer Spectrum system with a universal diamond attenuated total reflectance (ATR) probe. In the range of 4000-400 cm^{-1}, with a resolution of 16 cm^{-1}, 16 scans were obtained from the samples and averaged.

3.5.3 Scanning electron microscopy

Surface morphology and cross section observation of yarns were investigated by scanning electron microscopy (SEM). This was performed on as-received and treated yarn samples to investigate any changes effected on the surface and in the cross section of yarns. Energy dispersive X-ray spectroscopy (EDS) was also performed on silane-treated hemp warp yarns to investigate the presence of silicon. SEM was performed using a FEI Nova NanoSEM (230) equipped with a high resolution in-lens secondary electron (SE) detector, beam deceleration mode, low vacuum mode, low voltage backscatter detector and an EDS detector. The settings for this experiment were as follows: a voltage of 5.0 kV, In-lens SE detector and resolution at optimum working distance (low vacuum).

3.6 Composite processing

3.6.1 Minimum and maximum achievable

To produce a composite part, a minimum and maximum achievable fibre content has to be determined. The minimum fibre volume fraction for plant fibre reinforced thermoset was reported to be approximately 10% (Shah *et al.*, 2012).

The theoretical maximum achievable fibre volume fraction of a fibre reinforced composite depends on the fibre packing geometry. The maximum volume fractions for quadratic and hexagonal arrangement of synthetic fibres are well known to be 78.5% and 90.7%, respectively, (Shah *et al.*, 2012). However, plant fibres present lower packing ability assemblies compared to man-made fibre assemblies. This is explained by the fact that the theoretical maximum fibre content of staple yarns depends on both the linear combination of the yarn packing geometry within the composite and fibre packing within the yarn. The maximum volume fraction of a plant reinforced composite is then (Shah *et al.*, 2012):

$$V_{f.max} = V_{f.max.FRP} \times \phi;$$

where ϕ = the packing fraction;

$v_{f.max}$ = volume fraction maximum;

$v_{f.max.FRP}$ = volume fraction maximum of fibre reinforced polymer.

The packing fraction ϕ exponentially depends on the twist level (T, turns per meter or tpm) of the twisted yarn and is expressed as follows:

$$\phi = 0.7\times(1 - 0.78e^{-0.0195T})$$

By substituting equation X into equation Y, we obtain a mathematical model for determining the maximum achievable fibre volume fraction in staple twisted yarn reinforced composites (Shah *et al.*, 2012).

$$v_{f.max} = \frac{\pi}{4}\times 0.7\times(1 - 0.78e^{-0.0195T})$$

3.6.1.1 Determination of the twist level (T)

Related to the twist angle of a yarn, the twist level expressed in turns per meter was calculated using equation (X) after measuring the twist angle by scanning electron microscopy. The experiment was carried out on 10 different hemp yarn samples having the same length. The samples were placed on the sample holder without any coating prior to the analysis. The twist angle was determined by measuring the angle between individual fibres and the primary axis of the yarn. Then the level of twist (T) was calculated using the equation below:

$$\tan\alpha = 2\pi RT \quad \text{(Chattopadyay, 2010)}$$

where α = twist angle

R = radius of the yarn

T = level of twist.

After calculating the level of twist and by assuming the quadratic arrangement of twisted yarns within the composite (Shah *et al.*, 2012), the theoretical fibre content was found to be approximately 58.9%, calculated using equation X. However, experimentally filling the mould cavity with hemp yarns with a fibre content of 45%, was found to be unachievable with the equipment available. The maximum achievable was found to be approximately 30%, as shown in Figure 32 (a) and (b). For this research, the minimum and maximum fibre loading for the

produced composite was chosen to be 10 and 20%, respectively. A third loading of 15% was also investigated as shown in Figure 32 (c).

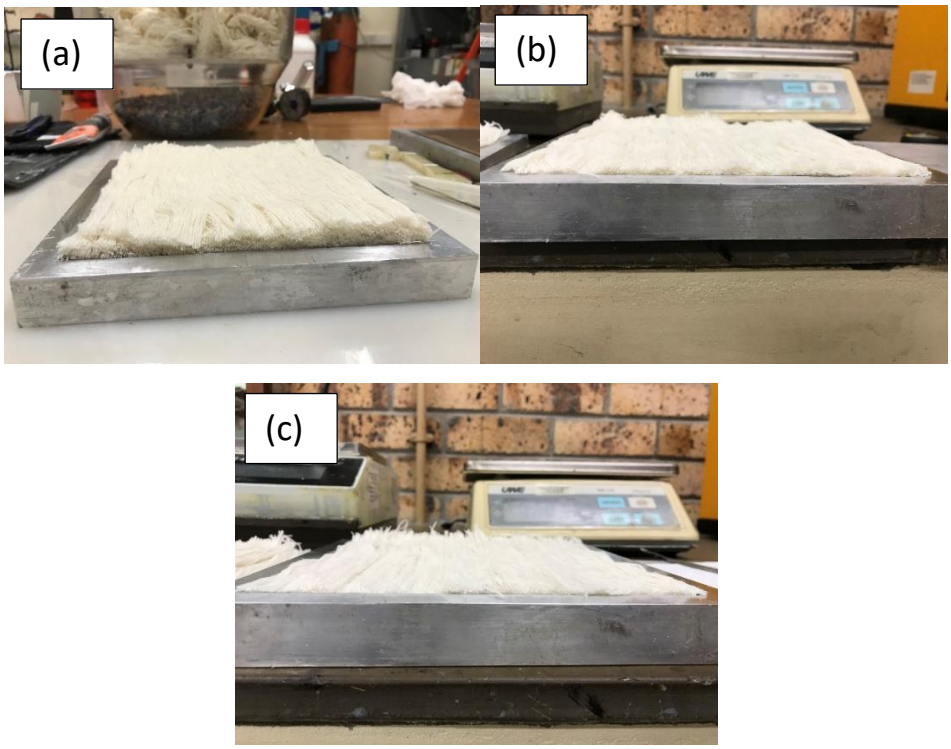

Figure 32: (a)Fibre content of 45%; (b) fibre content of 30% and (c) fibre content of 20%.

3.7 Composite parts

For this work, a neat epoxy, used as reference, and 12 composite parts of 175×170×4 mm^3 (119g) were produced. As received and treated hemp reinforced epoxy parts were then produced by compression moulding different mixtures of the epoxy matrix with three different fibre contents of 10%, 15% and 20%, as shown in table 5. For each fibre content, 4 composite parts were produced and labelled from A to L, as described in table 6. The matrix used for this work was the Sicomin SD 8100/ SR 8224 epoxy system, with a resin/hardener mixing ratio of 100/22 by weight.

Fibre Contents		Epoxy System Contents (100:22 ratio)		
Percentage (%)	Weight (g)	Percentage (%)	Weight (g)	
10	11.9	90	107.1	
			Resin	**Hardener**
			87.78	19.32
15	17.85	85	101.15	
			Resin	**Hardener**
			82.91	18.24
20	23.8	80	95.2	
			Resin	**Hardener**
			78.03	17.17

Table 5: Fibre contents, reinforcement and resin weight, and resin:hardener ratios.

Sample Labels (Fibre content, %)	Sample Labels (Fibre content, %)	Sample Labels (Fibre content, %)	Description
A (10)	E (15)	I (20)	As-received hemp yarns reinforced epoxy composite
B (10)	F (15)	J (20)	Alkali-treated hemp yarns reinforced epoxy composite
C (10)	G (15)	K (20)	Silane-treated hemp yarns reinforced epoxy composite
D (10)	H (15)	L (20)	Maleic anhydride-treated hemp yarns reinforced epoxy composite

Table 6: Sample labels and their descriptions.

3.7.1 Composite manufacturing

Of all the manufacturing processes of natural fibre reinforced polymer composites, the compression moulding manufacturing process was selected because of available equipment.

Figure 33 (a & b) presents the two-part mould that was designed using the computer aided design and drawing software, Solidworks. The mould had dimensions 205x200x22 mm^3 with a cavity, in the base part mould, of 170x165x4 mm^3 with a 8 mm deep groove and 2.5 mm holes in the top part of the mould for excess resin and air flow, respectively.

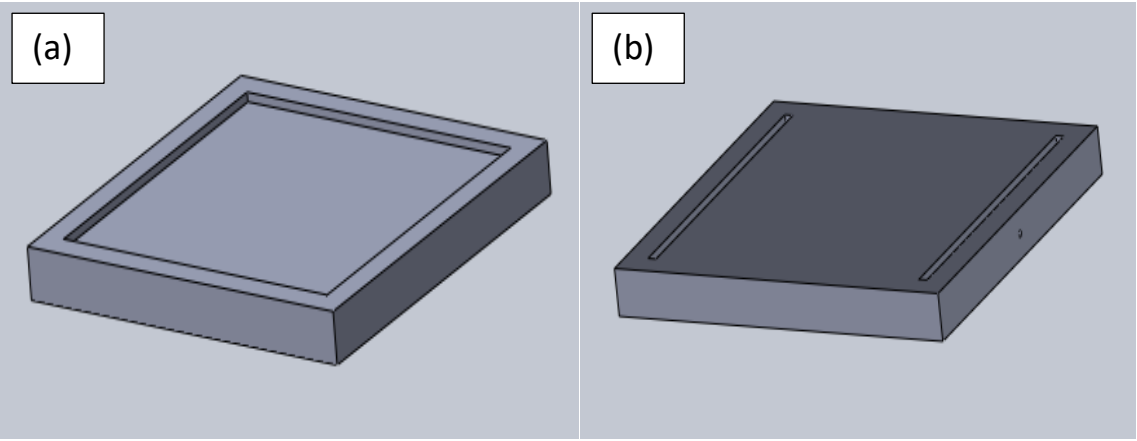

Figure 33: (a)base part mould and (b) top part mould.

Teflon film, (CAB Foods), was first placed onto the mould cavity to prevent the cured resin from sticking to the mould. Then, the hemp yarns were aligned by hand in the female mould cavity before the matrix/hardener epoxy system was poured in the mould cavity. Afterwards, the mixture was placed under pressure at 20 MPa using a hydraulic press, HY–JACK (10500C), for 5 hours, as shown in Figure 34, cured at ambient temperature for 19 hours and finally post-cured at 80°C for 8 hours.

Figure 34: Experimental set up.

3.8 Composite characterization

The influence of the alkali, silanization and maleic anhydride treatment on the mechanical properties was measured, using a Zwick machine (1484), by running tensile and flexural tests. Thermogravimetric analysis to probe composite thermal stability was tested, using a Netzsch (STA 409 CD) apparatus, on the untreated and treated hemp-filled epoxy composites.

3.8.1 Mechanical properties

The tensile properties of the hemp yarn reinforced epoxy composites were tested according to ASTM D638. Three samples per composite parts were tested. The tensile load on each specimen was applied at 0° axes with a speed of 5 mm/min. A class-C extensometer was used during the test.

The flexural properties of the hemp yarn reinforced epoxy composites were tested according to ASTM D790. The 3-point flexural test was performed on 3 test specimens, for each composite part, with a rate of crosshead motion of Z = 0.65 mm/min and a span-to-depth ratio of 16:1 (64:4).

The samples were cut from void free areas or areas with the lowest visible voids on the composite surface plates as shown in Figure 35. The composite parts were sent to Waterjet Technology where the tensile and flexural test specimens were sectioned using an ultra-high pressure waterjet equipped with a 1 mm high speed cutting beam (water & abrasive). The dog bones shaped sample tensile test specimen's area was 165 × 19 mm^2 with a gauge section of 57 × 13 mm^2. The rectangular flexural test specimen's area was 73 × 13 mm^2.

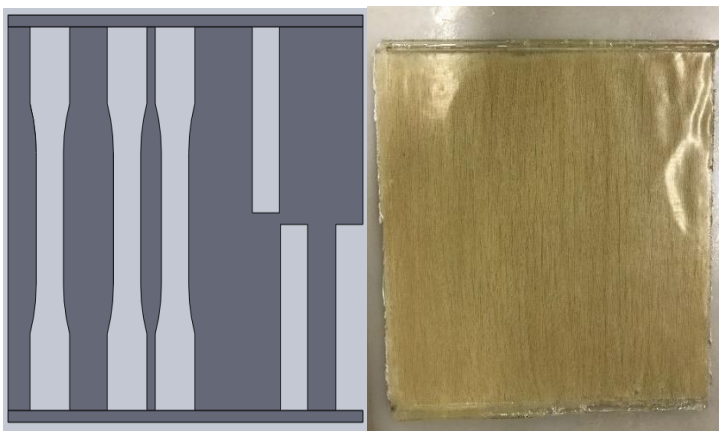

Figure 35: Sampling for tensile & flexural test specimens.

3.8.2 Thermogravimetric analysis (TGA)

The thermal stability behaviour of the fibres and composites was investigated according ASTM E1131. Samples with masses ranged between 40 mg and 49 mg were placed in an aluminium oxide crucible. Thermogravimetric analysis of the weight loss as a function of increasing temperature, was performed at a heating rate of 10^{o}C/min from 20^{o}C to 900^{o}C under argon (Air Liquide) with a flow rate of 50 mL/min. Temperature calibration was carried out using 4 samples of pure metals with known melting points, 156.6^{o}C, 271.4^{o}C, 660.3^{o}C and 1064.2^{o}C for the melting of indium, bismuth, aluminium and gold, respectively.

3.8.3 Scanning electron microscopy of composites

Scanning electron microscopy analysis was performed to investigate the failure zone of the tensile and flexural specimens. The samples were coated with gold and then placed in the SEM for an investigation of pulled out fibres, poor and good fibre/matrix interfaces, voids and yarn to yarn interfaces.

3.9 Mechanical properties prediction

The mechanical properties of the different hemp yarn reinforced epoxy composites were predicted using the general rule of mixtures (ROM). By assuming that the hemp yarns were perfectly aligned, and the composite was voids free, the rule of mixtures was used to predict the tensile strength and modulus of the composites using the equations below:

$$\sigma \text{ comp} = \sigma_{fibre} \times V_{fibre} + \sigma_{matrix} \times V_{matrix}$$

where σ_{fibre} is the strength of the fibre, σ_{matrix} the strength of the matrix, V_{fibre} volume of the fibre and V_{matrix} the volume of the matrix, with σ comp the strength of the composite.

$$E_{comp} = E_{fibre} \times V_{fibre} + E_{matrix} \times V_{matrix}$$

where E_{fibre} is the strength of the fibre, E_{matrix} the strength of the matrix and $E_{comp\ the}$ the modulus of the composite.

The strength and modulus of the fibres were obtained from the mechanical test results of the fibres.

4 Results and discussion

4.1 Characterization of the hemp fibres and yarns

4.1.1 Observation of the hemp fibres and yarns

Under polarized light microscopy, the plant inter-structure helped to differentiate fibre bundles from single fibres by the presence of two columns in between the cell walls as shown in Figure 36 (a), circled area a. The two columns are separated by the lighter cell wall of the single fibre on the right side. Additionally, twisted single fibres/columns as shown in Figure 36 (circled area b), also allowed the presence of the fibre bundles to be confirmed and to be differentiated from single fibres as shown in Figure 36 (a). Furthermore, the presence of a single fibre end separated from another single fibre, as shown in Figure 36 (circled area c), confirmed that this was a fibre bundle.

Almost all the specimens observed under polarized light microscopy displayed dislocations, which are present in the fibre cell wall and generated by the difference between the angle formed by the microfibrils relative to the fibre axis and the angle found in the surrounding cell wall (Thygesen, Eder and Burgert, 2007). They are generally known as nodes, kinks, kink bands, slip planes, or clusters of dislocations. Under polarized light, dislocations can be visualized as light bands traversing the fibre (Hughes, 2012) (Thygesen, Eder and Burgert, 2007). These light bands were found in the hemp fibres (Figure 36). Dislocations and clusters of dislocations displayed by some fibres were lighter than those presented by other fibres as shown in Figure 36 (a) and (b). The origin of dislocations in hemp fibres is not clearly understood but it has been reported to be generally caused by the action of extracting single fibres from natural fibres or excessive compressing stress, that may have been introduced while spinning single fibres during the formation of yarns (Hughes, 2012) (Thygesen, Eder and Burgert, 2007). It has also been said that a higher number of dislocations in plant fibres negatively affects their mechanical properties, moisture behaviour and fibre/matrix adhesion in composite materials (Dai and Fan, 2011) (Thygesen and Eder, 2007)(Thygesen, Bilde-Sørensen and Hoffmeyer, 2006). In this research, it is possible that dislocations could have been introduced during the formation of hemp yarns by the action of spinning single fibres or fibre bundles, or the effect of pulling warp and weft yarn form the woven fabric.

Figure 37 (C) presents the yarn structure of the as-received yarn hemp fibres used for this research. The yarn structure was investigated under scanning electron microscopy to better

understand the mechanical properties of hemp yarns during yarn rupture. Also investigated were the surface morphology and twist per cm of the yarns. Compared to other yarn structure, (Figure 37(A), (B) and (D)), the yarn structure used for this study was found to be a ring spun yarn structure with right-handed angle to the yarn axis twist direction known as the Z-twist (Chattopadhyay, 2010). Variations of both fibre twist angles and the cross section along the individual fibres were also observed. In addition, the surface morphology of hemp fibres revealed the presence of a rough surface, which could have been introduced by a likely pre-treatment on the hemp yarns, mercerization in this case. The fibre morphology was then compared to the surface morphology of untreated hemp yarns characterized by Madsen *et al.*, 2007 and Mwaikambo, 2016, as shown in Figure 38 (A & B) and Figure 3 (D & E), respectively. The as-received hemp yarns (Figure 38, F) revealed a rougher surface morphology than the untreated hemp yarns characterized by Madsen *et al.*, 2007 (Figure 38, A & B).

Figure 38 (D), (E) and (F) showed images of untreated (Mwaikambo, 2016), NaOH-treated (Mwaikambo, 2016) and as-received (this study) hemp fibres, respectively. Additionally, it can be noted that the untreated hemp fibres (Figure 38 (D)) depicts a less rough topography compared to the two others. On the contrary, Figure 38 (E) is as rough as Figure 38 (F). The rougher surface was introduced by the action of NaOH that removed an important amount of fibre components such as lignin and hemicellulose by breaking their inter- and intra-linkages to cellulose (Mwaikambo, 2016). This then suggested that the as-received hemp yarns used for this study (Figure 38 (F)), had been pre-treated, likely mercerized.

The as-received hemp used for this study showed non-circular cross-sectional shapes in the different single fibres as shown in Figure 38 (G).

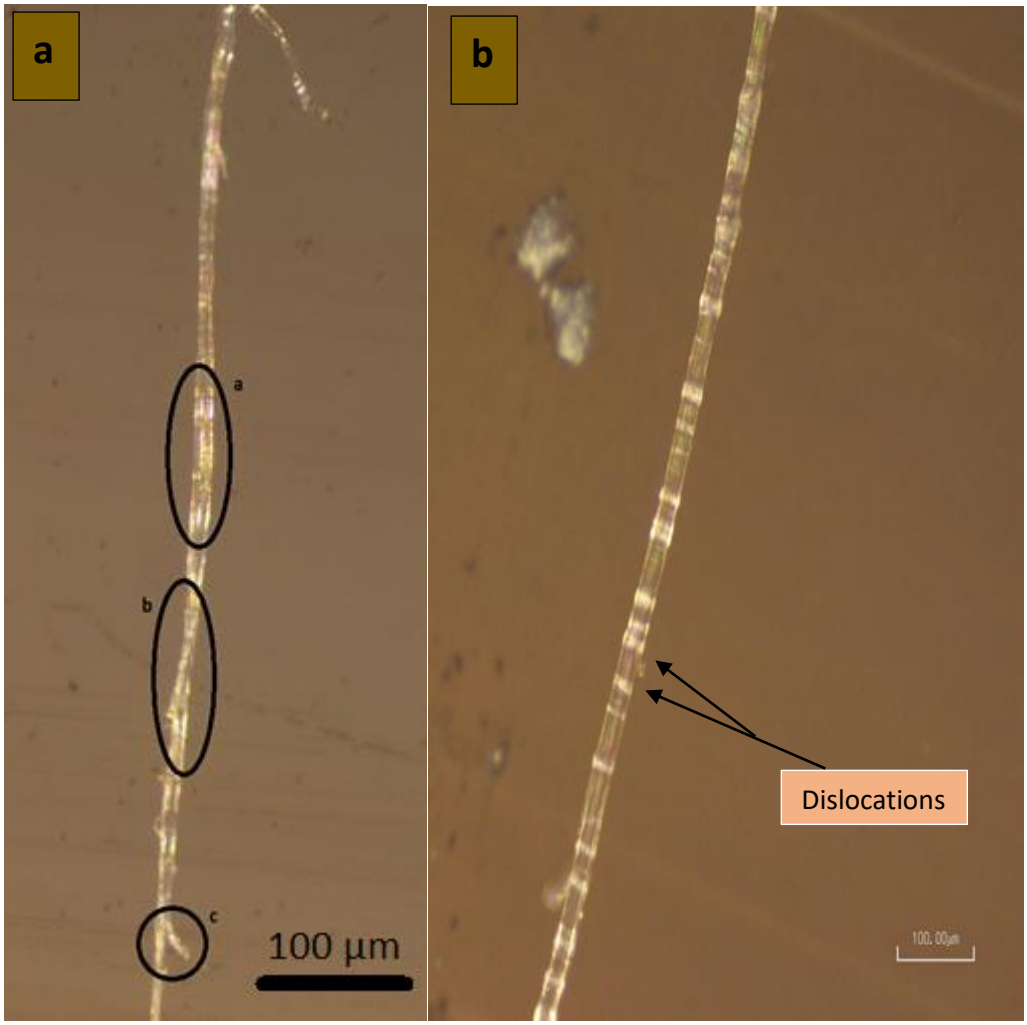

Figure 36: Light polarized microscopy of a multi-column bundle fibre (a) and a single weft fibre showing dislocations (b).

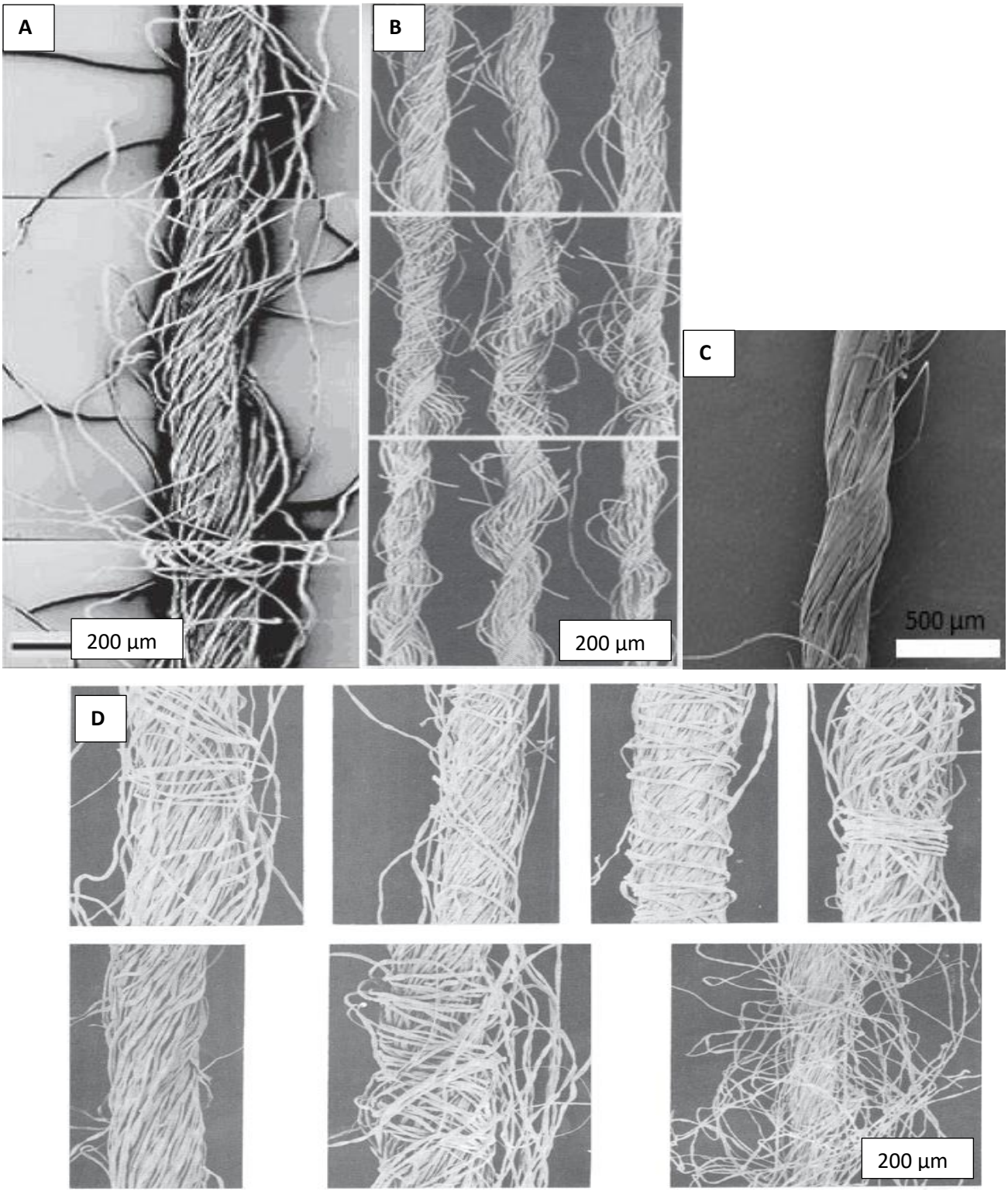

Figure 37: (A) SEM images of Ring spun yarn surface structure (Tyagi, 2010); (B) SEM images of Air-jet spun yarn surface structure (Tyagi, 2010); (C) SEM image of received Hemp surface structure (This study); and (D) Different SEM images of rotor spun yarns (Tyaa, 2010).

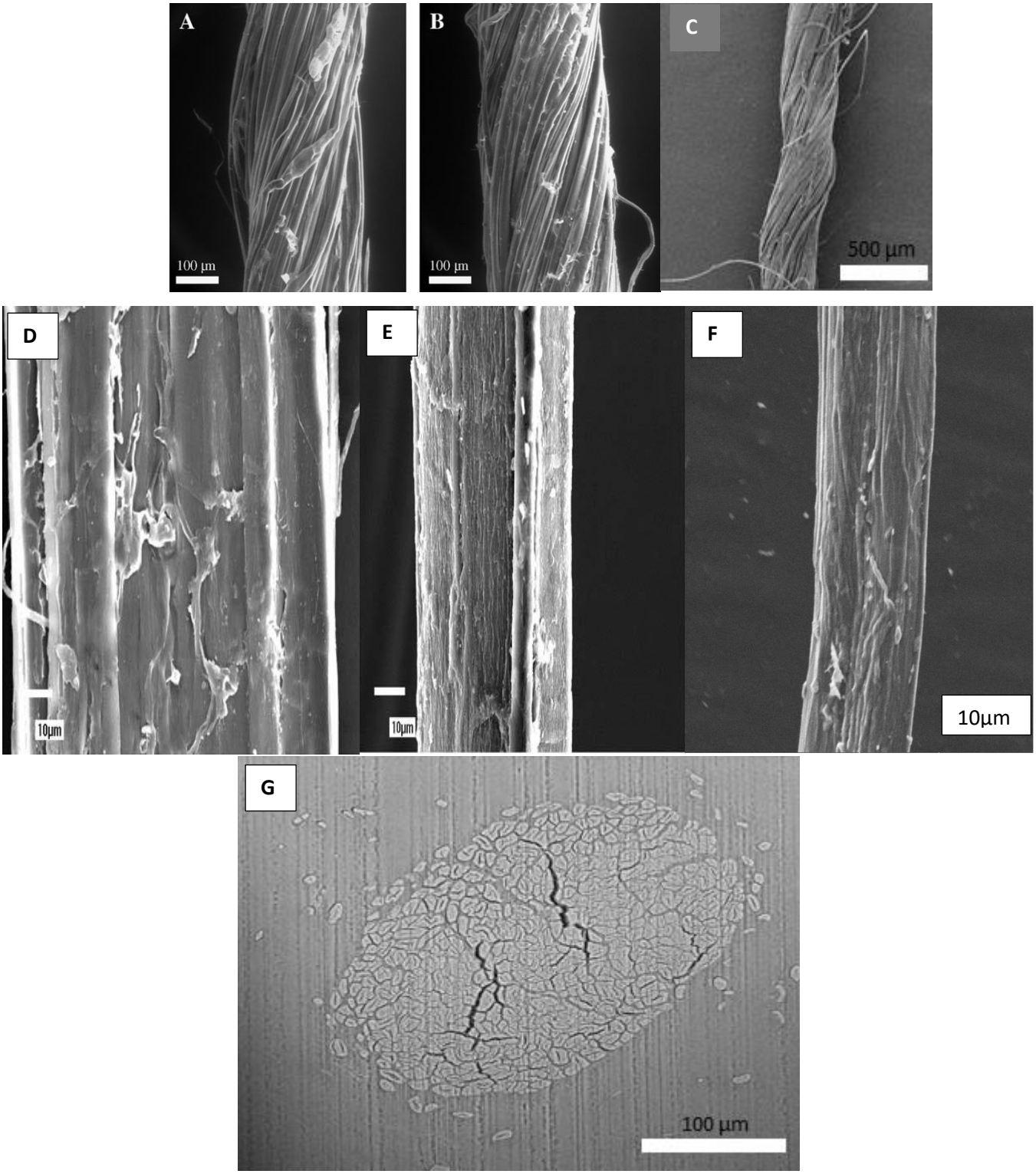

Figure 38: (A) &(B) SEM micrographs of untreated hemp fibres; (C) surface structure of as-received hemp (this study); Higher magnification micrographs of (D) untreated hemp fibre; (E) NaOH-treated hemp fibre; (F) as-received hemp fibre; and (G) non-circular cross-sectional shapes of as-received hemp (This study).

4.1.2 Fibre density and linear density

The fibre density measurements obtained using the pycnometer method are presented in table 7. The three measurement of the fibre density were performed using six sets, three for the weft and the other three for the warp yarns using approximately 20 mg of weft and warp yarns of 25 cm length. The linear density of the hemp yarns was determined in Tex, defined as the mass in grams of one kilometre yarn (Gokarneshan, Varadarajan and Senthil Kumar, 2013). For each type of yarn, three sets of 10 yarns, with length ranged from 16.4 to 27.9 cm, were used to determine the linear density. Like the fibre densities, the linear densities were expressed in term of the overall means ± standard deviation of the mean and are presented in table 7.

	Measurements				
	1	2	3	Mean	Std dev.
	Weft				
Fibre density (g/cm^3)	1.42	1.41	1.43	1.42	0.02
Linear density (Tex)	132.8	137.2	131.1	133.7	2.6
	Warp				
Fibre density (g/cm^3)	1.43	1.47	1.45	1.45	0.02
Linear density (Tex)	125.1	138.9	127.4	130.5	7.4

Table 7: Measurement of fibre density and linear density.

The fibre densities of the hemp yarns showed small differences, see table 7, with their mean ± standard deviation, 1.42 ± 0.02 and 1.45 ± 0.02 for the weft and warp hemp yarns, respectively. However, the calculated densities are in total agreement with the reported densities of natural hemp fibres, which are reported to be ranged from 1.4 to 1.5 g/cm^3 (Moyeenuddin A Sawpan, Pickering and Fernyhough, 2011).

The calculated average linear densities, 133.7 and 130 .5 tex for the weft and warp hemp yarns, respectively, had coefficient of variations of 11.6% and 12.6% for weft and warp hemp yarns, respectively. Rijavec, Janjić and Ačko, 2017, also determined the linear density of hemp fibres and found it ranged from 149.8 to 220.5 tex with coefficient of variations between 26% and 52%. These values are slightly higher than those reported here.

4.2 X-ray diffraction analysis

To investigate any changes regarding to the crystallinity index of as-received and treated hemp yarns, XRD spectra were recorded. All the X-ray diffractograms displayed the same curve pattern with different intensities.

Figure 39 and 40 presents the X-ray diffractograms of the weft and warp hemp yarns. They reveal the presence of the maximum intensity of diffraction of the cellulose-I crystallographic plane (200, at 2 θ between 24-28°) and the minimal intensity between the 200 and 110 peaks (I_{am}) at 2θ = 21.22°. The crystallinity index of weft and warp hemp yarns were calculated, based on the Segal Method, and the results reported in table 8.

	Hemp yarns					
	Weft			Warp		
	I (am)	I (200)	CI (%)	I (am)	I (200)	CI
As-received	8.26	63.44	86.98	6.6	43.22	84.73
Alkalized	12.39	126.88	90.23	10.45	80.22	86.97
Silanized	10.79	92.38	88.31	9.32	77.49	87.97
Maleic-Anhydride-treated	9.39	87.75	89.29	9.39	66.68	85.91

Table 8: Crystallinity indexes of received, alkalized, silanized and maleic anhydride-treated weft and warp hemp yarns.

The crystallinity indices showed the following order: alkalized (90.23%) > maleic anhydride-treated (89.29%) > silanized (88.31) > as-received (86.98%) for the weft hemp fibres; and silanized (87.97%) > alkalized (86.97%) > maleic anhydride-treated (85.91) > as-received (84.73%) for the warp hemp yarns.

The as-received fibres, already mercerized, presented a crystallinity index of 86.96% and 84.73% for weft and warp hemp yarns, respectively. Similar crystallinity indexes were also found in the literature for alkali-treated hemp fibres, with values ranged from 49% to 92%. However, crystallinity indexes of untreated hemp fibres have been reported to be ranged from 35% to 88% (Hajiha, Sain and Mei, 2014) (Moyeenuddin A Sawpan, Pickering and Fernyhough, 2011) (Stevulova *et al.*, 2014) (Arbelaiz *et al.*, 2005)(Mwaikambo and Ansell, 1999). The high crystallinity index is consistent with the as-received yarns having undergone a treatment, prior to use, that had removed material responsible for increasing the amorphous content of hemp fibres. Mercerization would be one such treatment. The alkalization of the weft and warp hemp yarns revealed an increase of the crystallinity index

from 86.98% and 84.73% to 90.23% and 86.97% for weft and warp hemp yarns, respectively. The sodium hydroxide, used for the alkalization of the yarns, removed further amorphous material such as any residual waxes, pectin and likely hemicellulose from the hemp yarns.

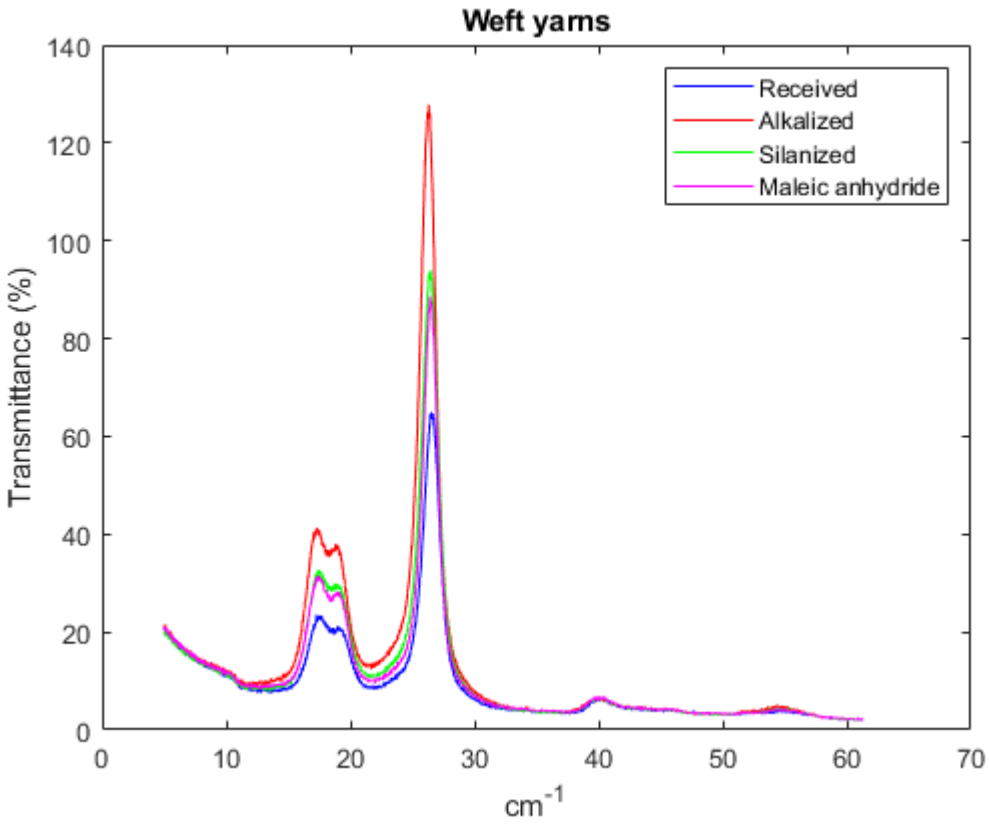

Figure 39: X-ray diffractograms of the as-received weft hemp yarns.

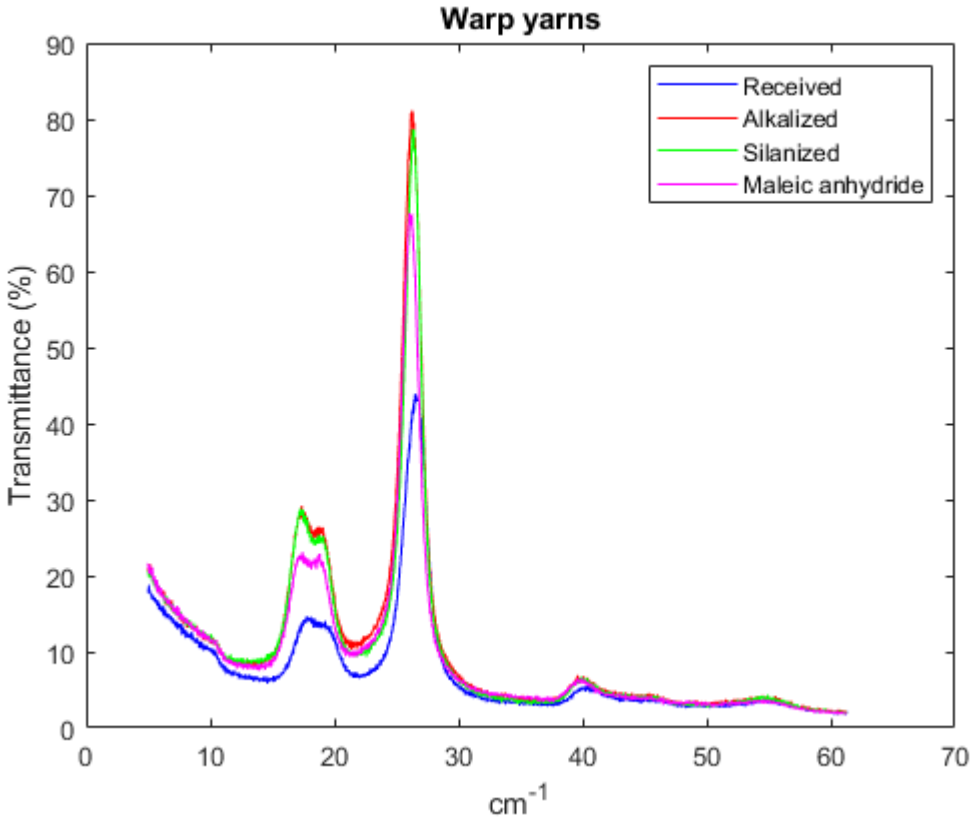

Figure 40: X-ray diffractograms of the as-received warp hemp yarns.

This contributed a better orientation of the crystalline cellulose region, and hence, increasing the crystallinity index. This was also observed by other researchers (Palanivel *et al.*, 2017)(Hajiha, Sain and Mei, 2014) (Moyeenuddin A Sawpan, Pickering and Fernyhough, 2011) (Stevulova *et al.*, 2014) (Arbelaiz *et al.*, 2005)(Mwaikambo and Ansell, 1999). The amount of crystallinity index increase was small because the index of the as-received yarns was large to begin with. There was already very little amorphous material to be removed.

Although, the differences were not significant, the silanized hemp yarns showed higher crystallinity indexes compared to the as-received hemp yarns. For the weft hemp yarns, the alkalized yarns showed the highest crystallinity index followed by that of the maleic anhydride-treated hemp yarns that was higher than that of the silanized hemp yarns. However, the trend was different for the warp hemp yarns that depicted the highest crystallinity index for the silanized hemp yarns followed by the alkalized and the maleic anhydride hemp yarns. It is reported that the reaction between silane and maleic anhydride reagents with cellulose occurs in the amorphous or at the edges of crystalline cellulose

regions (Moyeenuddin A Sawpan, Pickering and Fernyhough, 2011) (Tserki *et al.*, 2005). The coupling agents first react with the chain ends on the surface of crystallites, as they cannot diffuse into crystalline region, resulting in the opening of some of the hydrogen-bonded cellulose chains (Tserki *et al.*, 2005). This then results in some conversion of crystalline to amorphous cellulose. Moreover, the reagent diffuses into this newly produced amorphous section, reacting with the crystalline cellulose and simultaneously generating more amorphous cellulose (Tserki *et al.*, 2005). A small decrease in crystallinity indexes from alkali-treated to alkali/silane-treated hemp fibres was also reported by Sawpan, Pickering and Fernyhough, 2011. Nonetheless, the overall increase seen here is small but may be due to the organic solvents used dissolving some amorphous components.

4.3 Tensile properties of untreated and treated hemp yarns

As one of the methods used to monitor the effect of the chemical treatments on the hemp yarns, tensile tests, generating the material response to the applied tension load and load-displacement curves, were recorded. The load-displacement curves of the warp and weft yarns initially showed a gradual increase in slope with a non-linear section before the curves became linear as shown in Figure 41.

Since two type of yarns were being characterized, a differentiation between the strength of warp and weft hemp yarns was then necessary before one could be chosen for further experiments in producing composites.

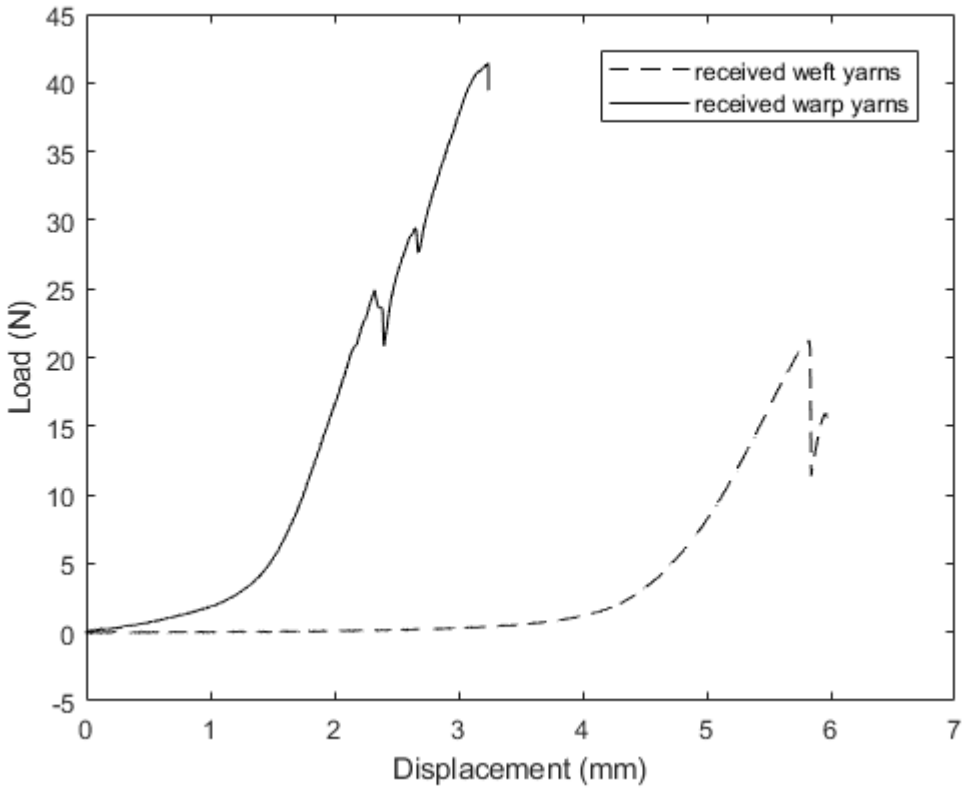

Figure 41: Load versus displacement curve of the received weft and warp hemp yarn.

As depicted in the above figure, the curves showed variability in the length of the non-linear part between the as-received and treated weft and warp hemp yarns. The warp yarns were always to the left compared to the weft because warp yarns were tighter than weft yarns. This was confirmed by the twist angle of the measurement made on the warp and weft yarns, which showed twist angles of 8° to 26° and 25° to 36° for the warp hemp yarns and weft hemp yarns, respectively.

Moreover, the above-mentioned variability led to scatter in the determination of stress-strain curves. To eliminate these differences, the linear part of the curve had to be extended to the x-axis using the linear regression (Figure 42) (Madsen *et al.*, 2007)**.** The point of intersection was then taken into consideration in the determination of strain (ε) as shown below:

$$\varepsilon = \frac{\Delta l + I}{l_0}$$

where Δl is the displacement, I the intercept and l_0 the gauge length.

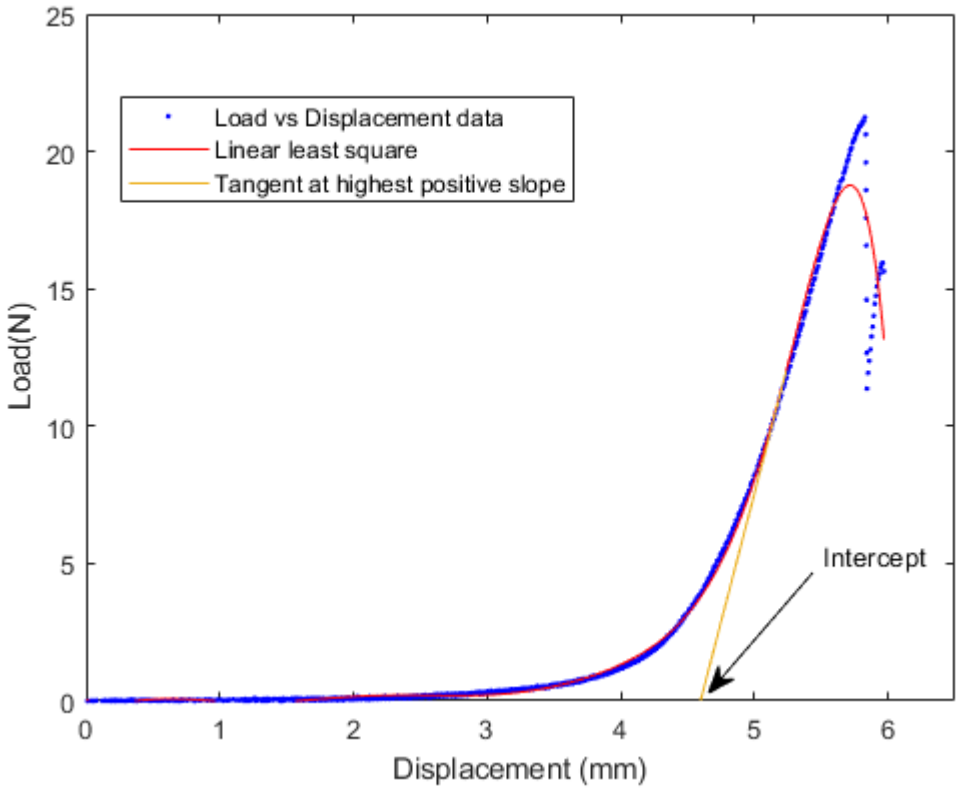

Figure 42: Load vs displacement curve showing load vs displacement data, linear least square, the intercept and the tangent at highest slope.

The apparent cross-sectional area, used to determine the stress of the hemp yarns, was calculated from the mean fibre density and the linear density using equation below:

$$\text{Filament diameter } (d_f) = 11.89 \times 10^{-4} \left(\frac{w}{\rho}\right)^{1/2} \text{ (Chattopadyay, 2010)}$$

where w = fibre linear density (denier) and ρ = fibre density (g/cm^3).

The filament diameters were first calculated before the yarn cross-sectional areas were determined and found to be 40748 and 41244 µm^2 for the warp and weft hemp yarns, respectively. The calculated cross-sectional areas lay within the range of typical hemp fibres of 30000 – 40000 µm^2 that corresponds to 200 – 350 single fibres per yarn cross-section found by other authors (Madsen *et al.*, 2007).

The stress and strain values were then calculated using the apparent cross-sectional area and the stress vs strain curves of the warp and received hemp yarns were then plotted, (Figure 43). When it comes to mechanical properties of fibres such as those presented in this study,

high variability in the results often reflects the natural heterogeneity of natural fibres (del Borrello *et al.*, 2020).

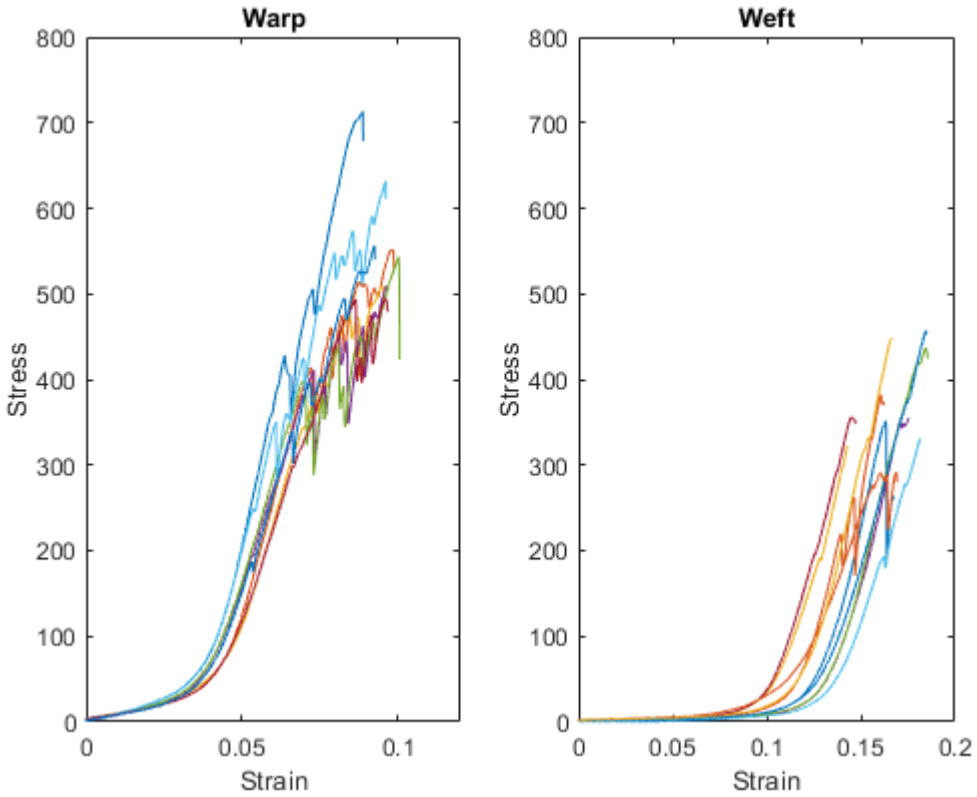

Figure 43: Received warp and weft hemp yarns stress vs strain curves.

The hemp yarns, as-received, revealed a difference in tensile properties between the warp and weft yarns. The tensile strength of warp hemp yarns, with an overall mean of 799± 109 MPa, was found to be superior to the that of the weft hemp yarns with an overall mean of 503 ± 118 MPa. These value fall in the range of the tensile properties of reported alkali-treated yarns, 436-1110 MPa (Sunny, Pickering and Lim, 2020). This comparison is reported since the as-received hemp fibres were likely mercerized. The observed difference in tensile properties was probably a consequence of the variability in the linear density and twist angle of the warp and weft hemp yarns. It was reported that the higher the linear density, the higher the tensile properties (Ma *et al.*, 2016; Alias *et al.*, 2018). However, since no significant difference, statistically, was observed between the weft hemp yarns with the higher density depicted the lower tensile strength compared to the warp hemp yarns (133.67 Tex vs 130.5 Tex, for the weft and warp hemp yarns, respectively), hence, no clear effect of the linear density was

observed. The correlation between the twist angle and the tensile was in agreement with the outcome of the study performed by Shah, Schubel and Clifford, 2013, which stated that the higher the twist angle, the lower the mechanical properties of twisted plant yarns, as shown in Figure 44. As a result of their improved mechanical properties, the warp hemp yarns of the as-received fabric were chosen over the pulled weft hemp yarns and further research was carried forth with warp yarns only.

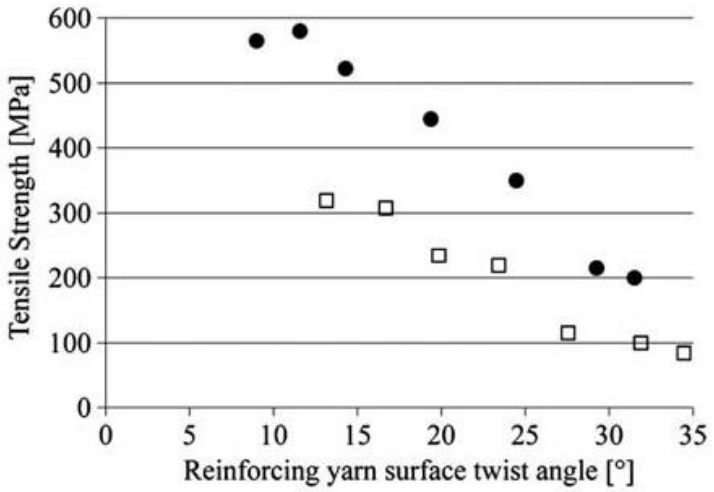

Figure 44: Correlation between the twist angle and the tensile strength (Shah, Schubel and Clifford, 2013).

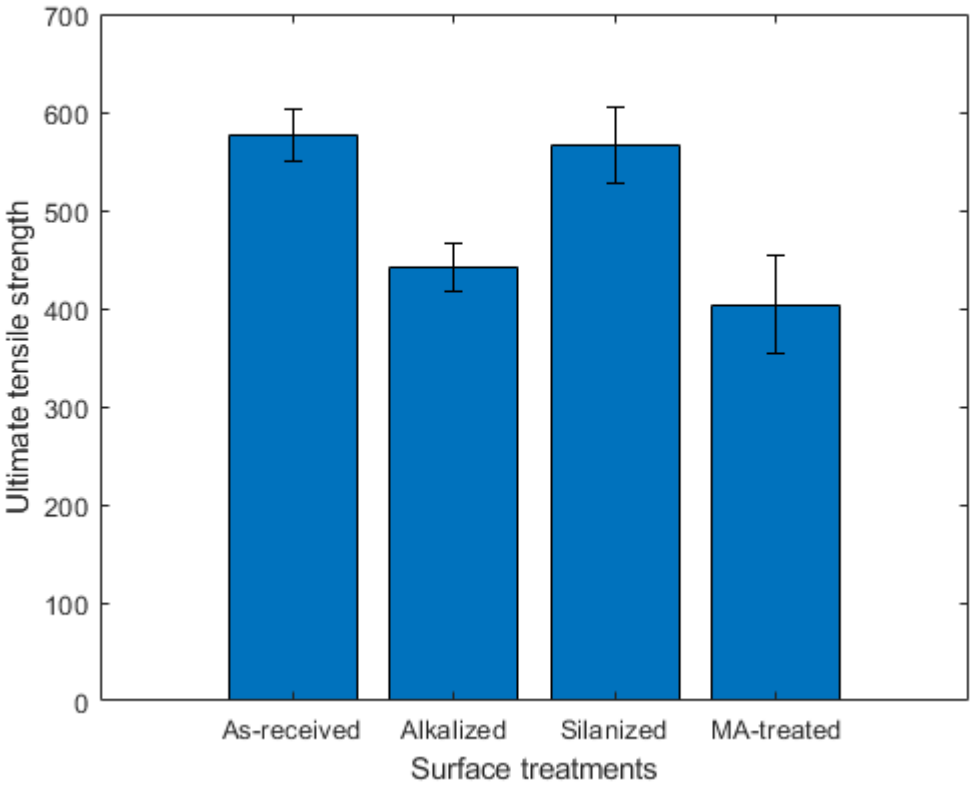

Figure 45: Tensile strengths of the as-received and treated hemp yarns.

Figure 45 presents the average strength of as-received and treated hemp yarns. The alkali treatment appeared to reduce the strength, whereas the silane treatment appeared to make no statistically significant difference to the strength. The order of the average tensile strength: as-received (799 ± 109 MPa) > silane-treatment (753 ± 140 MPa) > maleic anhydride-treatment (562 ± 139 MPa) > alkali- treatment (518 ± 101 MPa).

Usually, a yarn is made up of fibres. The tensile strength of a spun yarn depends on several factors such as the fibre properties, the yarn structural geometry and the spinning parameters. The last two factors are known not to be affected during the chemical treatments of the yarns, hence, attention had to be paid to the fibre properties that were altered during the surface treatments of the yarns. Additionally, the yarn tensile strength is also influenced by the yarn hairiness (Tyagi, 2010).

Tyagi, 2010, reported that the yarn strength proportionally increases with an increase in twist until it reaches the optimum twist (the twist at which the yarn strength is the highest) before it falls with further increases in twist (Tyagi, 2010). Therefore, the yarn strength is governed

by a twist-strength relationship influenced by the combined effect of fibre slippage and fibre obliquity or yarn twist (Figure 46). At low twist level, the twist-strength relationship is governed by the resistance of fibres to slippage. However, as the twist level increases the resistance to slippage reaches a steady maximum, causing the yarn to reach its maximum strength, hence, introducing the fibre obliquity factor to the contribution of the yarn strength. Once the fibre obliquity contributes to the twist-strength relationship, it causes a decrease in yarn strength (Tyagi, 2010).

Sodium hydroxide is known to break inter- and intra-cellulosic linkages, which results in the removal of hemicellulose and lignin. This makes the fibres finer by reducing their diameter. As a result, during the yarn elongation, finer fibres increase the frictional slippage, which reduces the optimum twist level and hence increase the maximum strength of the yarn (Tyagi, 2010) (Sari *et al.*, 2017). Additionally, NaOH is well known to remove the cementing components (i.e. hemicellulose, lignin and pectin) increasing the order of crystallite cellulose chains, while the reagent from the silane and maleic anhydride treatment reacts with either the non-crystalline cellulose and the edge of crystalline cellulose end chains increasing the effectiveness of amorphous cellulose (Moyeenuddin A Sawpan, Pickering and Fernyhough, 2011). This influences the mechanical properties of hemp yarns.

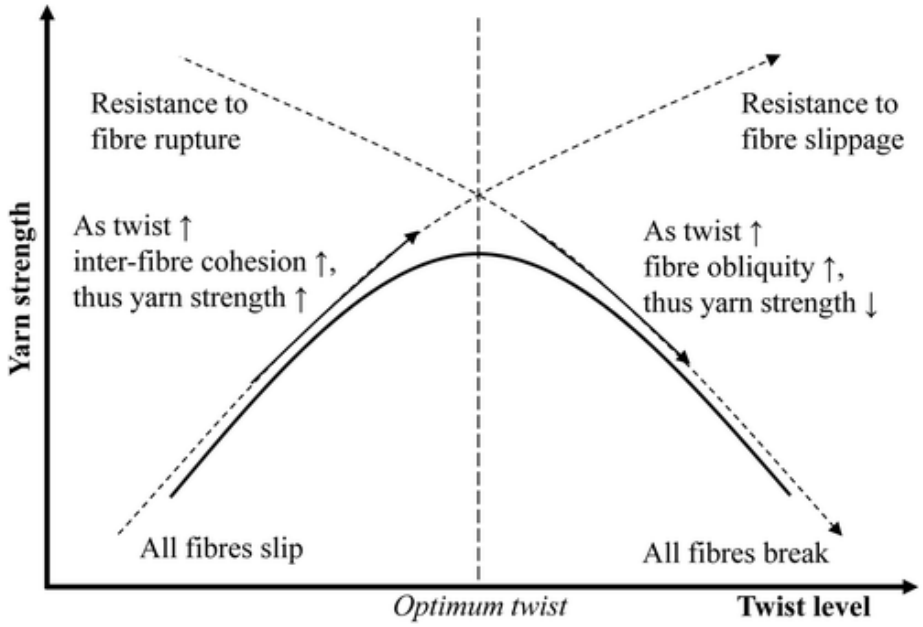

Figure 46: Relation between the yarn strength and twist level.

Considering all the above-mentioned effects of the different chemical treatments on the strength of the hemp fibres, the as-received hemp yarns should have shown a different order average of their tensile strength pattern if they had not been subjected to any prior surface treatment.

Contrary to the increase of the tensile strength of untreated hemp fibres/yarns, which has been reported after an alkalisation (Hajiha et al., 2014) (Mwaikambo, 2016) (Sawpan et al., 2011), the hemp yarns (alkali-treated in this study) showed a decrease in strength as shown in Figure 45. Indeed, under the characterization section of this paper, it was demonstrated that the as-received hemp had already undergone a pre-treatment, likely an alkali treatment. The decrease in strength after the alkali treatment was likely caused by an excess dose of caustic soda on the pre-treated hemp yarns. This resulted in the removal of more materials from the hemp fibres, which damaged the fibre surface by increasing roughness (Figure 47 (b)) and hence, reducing their mechanical properties. Hamidon *et al.* studied the effect of different concentration of NaOH after the alkali treatment of bast fibres. Their study revealed that higher percentage of alkali concentration caused excess delignification of natural fibre, which makes the fibre weaker and hence, decreases its mechanical properties (Hamidon *et al.*, 2019). The silane treatment of hemp yarns was carried out in a mildly acidic solution. The mildly acidic solution could serve as a catalyst during the cleavage of the β-1,4-glycosidic bonds between the two anhydro-glucose units causing the scission of cellulosic chains, hence, slightly lowering the tensile strength compared to the strength of the as-received hemp yarns (Moyeenuddin A Sawpan, Pickering and Fernyhough, 2011) (Arbelaiz *et al.*, 2005).

The maleic anhydride (MA) treated hemp fibers showed a decrease in tensile properties compared to the as-received (NaOH-treated) hemp yarns. Similar effects have also been reported, in the literature, where bast fibers treated with MA (maleic anhydride) in a xylene solvent under heat revealed a decrease in tensile strength. The heating in presence of xylene was postulated to be responsible for the weakening of interfibrillar interaction in cellulose, hence, reduced the tensile properties (Moyeenuddin A Sawpan, Pickering and Fernyhough, 2011). Maleic anhydride also produces a small amount acidity on reaction with the surface as the result of the formation of carboxylic acid groups which could further have contributed to the effect.

The formation of a layer on the fibre surface by the deposition of the silane and maleic anhydride solution during the silanization and the maleic anhydride treatment is reported to be responsible for the smoothening of the fibre surface compared to the alkali-treated hemp yarns as shown in Figure 47 (a, b, c and d). According to Tyagi, 2010, every factor that does not contribute to the increase in the resistance to friction during slippage negatively affects the tensile properties of a yarn. It is likely that the smooth surface obtained after the silane and maleic anhydride-treated hemp fibres may have contributed to the non-resistance to slippage and, hence to the reduction of the tensile properties compared to the as-received yarns. Interestingly dislocation kinks can be seen in the SEM micrograph (d) below.

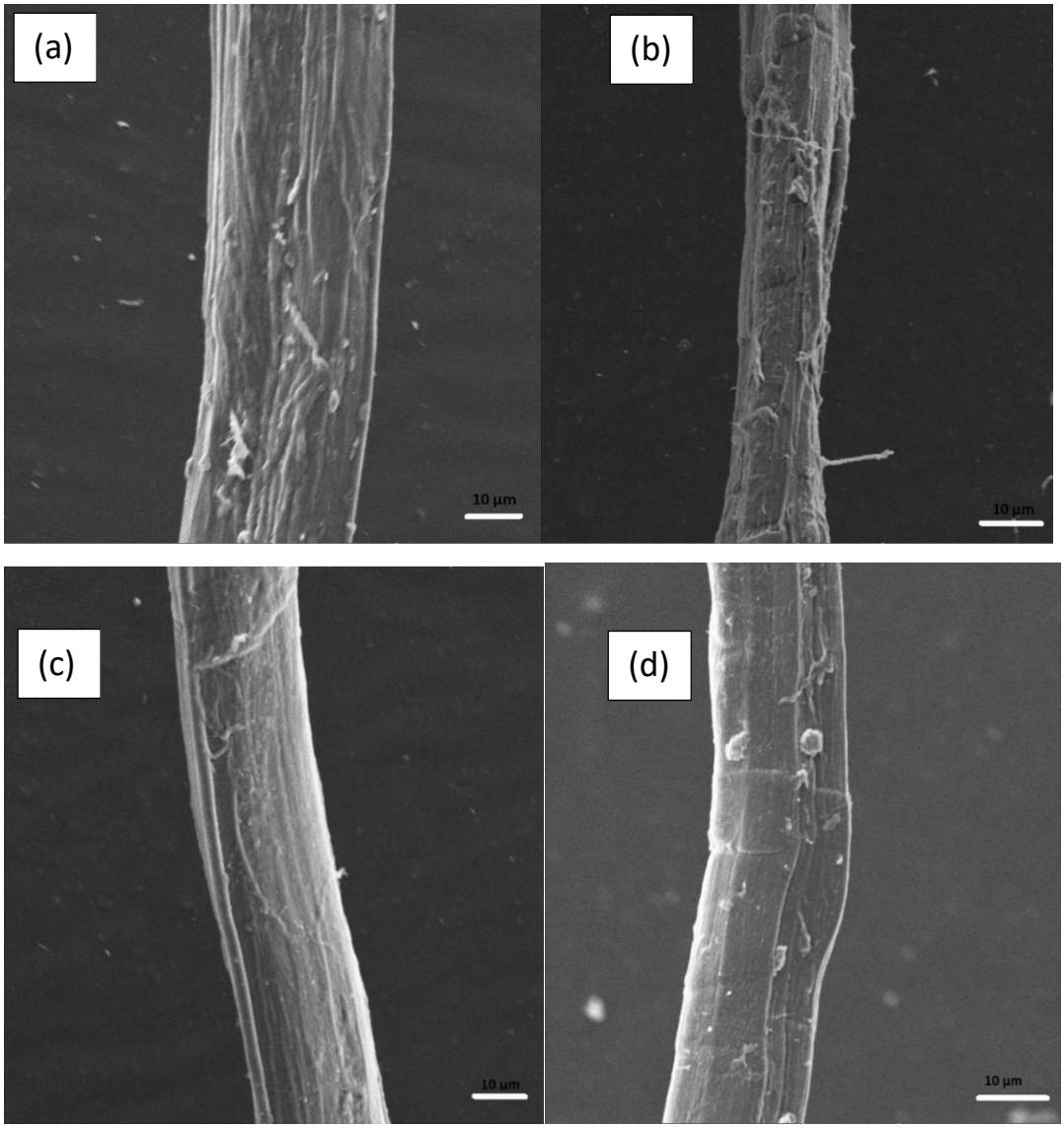

Figure 47: SEM micrographs of as-received (a), alkali-(b), maleic anhydride-(c) and silane-treated (d) hemp yarns.

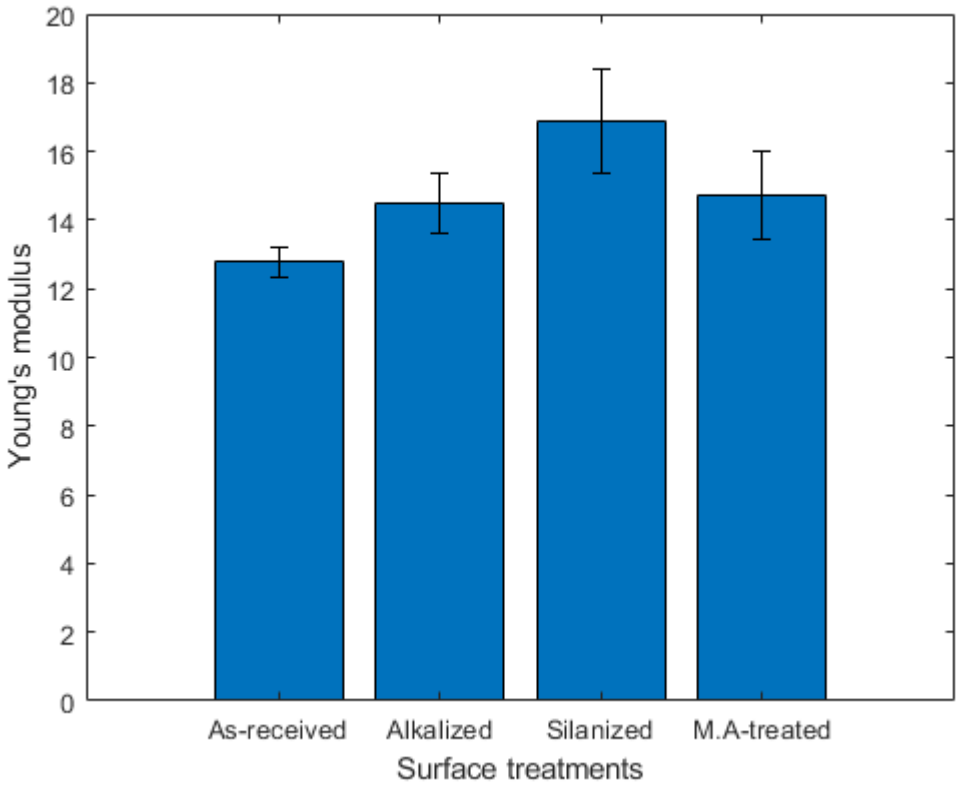

Figure 48: Young's modulus of the as-received, alkali-, silane- and Maleic anhydride (M.A)-treated hemp yarns.

Figure 48 presents the elastic modulus of the as-received and chemically treated hemp yarns. Unlike the tensile strength data, the as-received material had the lowest Young's modulus. Young's modulus of the silane-treated, 16.9 ± 4.3 GPa, was slightly higher than that of the maleic anhydride-treated hemp yarns, 14.7 ± 2.6 GPa, which showed a non-significant difference compare with the Young's modulus of the alkali-treated hemp yarns, 14.5 ± 2.6 GPa. The as-received hemp yarns showed the lowest stiffness with a Young's modulus of 12.8 ± 1.3 GPa. The trend displayed by the observed values was in agreement with that observed by other researchers for untreated and further treated hemp fibres (Moyeenuddin A Sawpan, Pickering and Fernyhough, 2011)(Sunny, Pickering and Lim, 2020). The difference in tensile modulus was probably due to the different mechanical interaction at the fibre interfaces that was affected by the different chemical treatments applied on the fibres. The deposition of the silane molecules on the surface of the as-received hemp fibres likely formed a slightly better interface that may have affected the inter-connection of fibres at their interfaces compare with the deposition of the maleic anhydride and the action of the sodium hydroxide solution

on the as-received hemp fibres that seemed to have similar effect on the resistance to slippage at the fibre interface. This likely explains the observed trend in Figure 48. It should be noted that the moduli reported are for fibre yarns which are less than those reported in the literature for individual fibres (30-70 GPa) (Manaia, Manaia and Rodriges, 2019).

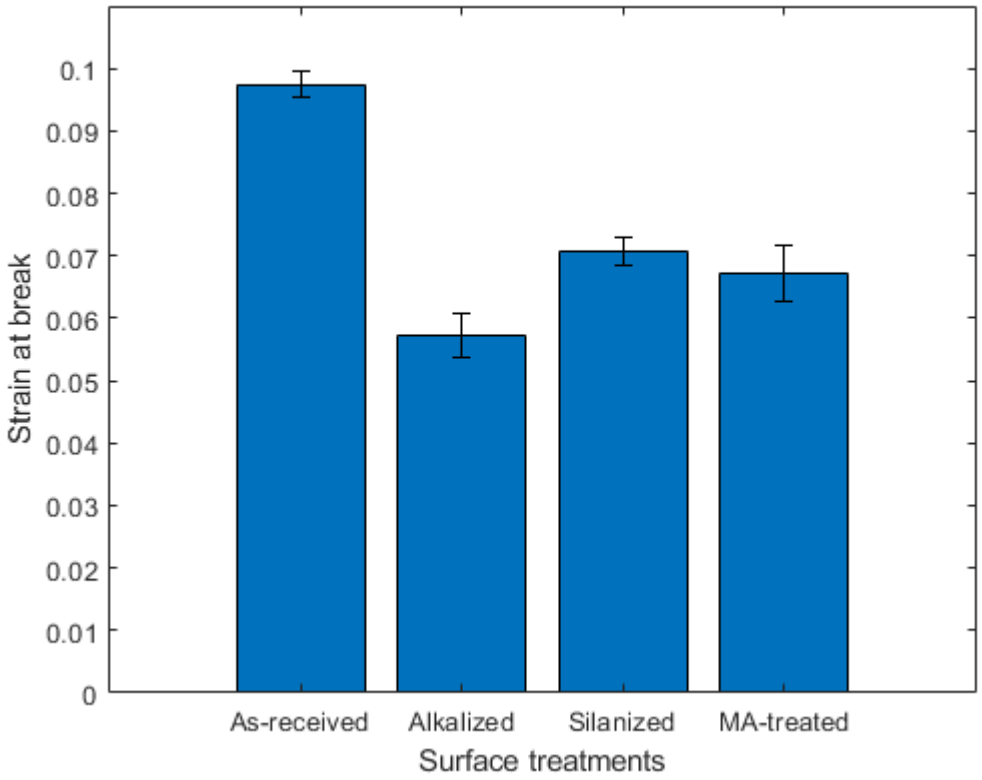

Figure 49: Strain at break of the as-received and alkali-, silane- and maleic anhydride- (M.A) treated hemp yarns.

Figure 49 presents the strain at break of the as-received, and alkali-, silane- and maleic anhydride- (M.A) treated hemp yarns which are respectively 0.09 ± 0.01 MPa, 0.05 ± 0.01 MPa, 0.07 ± 0.01 MPa and 0.06 ± 0.01 MPa. Generally, the chemical treatments lower the resistance to deformation in the fibres. The alkali treatment caused more damages to the microfibrils lowering the shear resistance at the fibre interfaces and this led to a decrease in the strain at break. The silane and maleic anhydride molecules by creating a new layer on the as-received fibres seemed to have retained some of the fibres' ductility by slightly increasing their shear resistance, resulting in a slightly increase of the failure strain compared to the alkalized hemp yarns. However, the as-received hemp fibres, pre-alkalized, likely had a slight

amount of non-lignocellulose components and further chemical treatments brought about damage to the as-received hemp yarns. Therefore, this decreases their overall extensibility.

4.4 Fourier transform infrared spectroscopy analysis

The FTIR analysis performed to characterize the effectiveness of the chemical treatments on the hemp yarns revealed differences at some characteristic bands on the cellulose backbone, as depicted on all FTIR spectra, figure 50. Differences on the spectra, due to the alteration of the cellulose backbone, were observed in the transmittance percentage and at certain FTIR bands on the spectra of the alkali-, silane- and maleic anhydride-treated hemp fibres compared to the received hemp fibres.

Figure 51 presents the spectrum of the as-received hemp fibres, the peak at around 3335 cm^{-1}, corresponds to the axial OH stretching in cellulose and hemicellulose (Dai and Fan, 2010). The peak at around 2899 cm^{-1} corresponds to symmetrical -CH stretching found in cellulose and hemicellulose (Dai and Fan, 2010; Stevulova *et al.*, 2014). The band appearing at around 1623 cm^{-1} likely represents the OH bending of absorbed water. CH_2 rocking vibration from the cellulose were also present in the hemp fibres at 1317 cm^{-1}. The peak at 1280 cm^{-1} indicates the presence of C=O of acetyl groups or G-ring stretching present in lignin (Fan, Dai and Huang, 2012)(Sunny, Pickering and Lim, 2020)(Hajiha, Sain and Mei, 2014). Inter-molecular linkages (likely due to β-glycosidic linkages) were also observed between the sugar units in cellulose and possible hemicellulose by the presence of the C-C stretching at 1048 cm^{-1} and the asymmetrical out of phase ring stretching at 915cm^{-1} (Hajiha, Sain and Mei, 2014)(Dai and Fan, 2010). However, some characteristic peaks of lignin and hemicellulose from untreated hemp fibres spectra, such as the 1723cm^{-1} peak, generated by the absorption of carbonyl (C=O) present in hemicellulose, were not found on the as-received hemp fibres/yarns spectra. This suggests that the presence of hemicellulose is low (Manaia, Manaia and Rodriges, 2019)(Pothan *et al.*, 2002). This is consistent with the X-ray diffraction data that indicated a high crystallinity index, a marker for high cellulose content. Additionally, no weak bands were found at around 2109 cm^{-1} on the spectra of the as-received hemp fibres (Moyeenuddin A Sawpan, Pickering and Fernyhough, 2011)(Dai and Fan, 2010)(Hajiha, Sain and Mei, 2014).

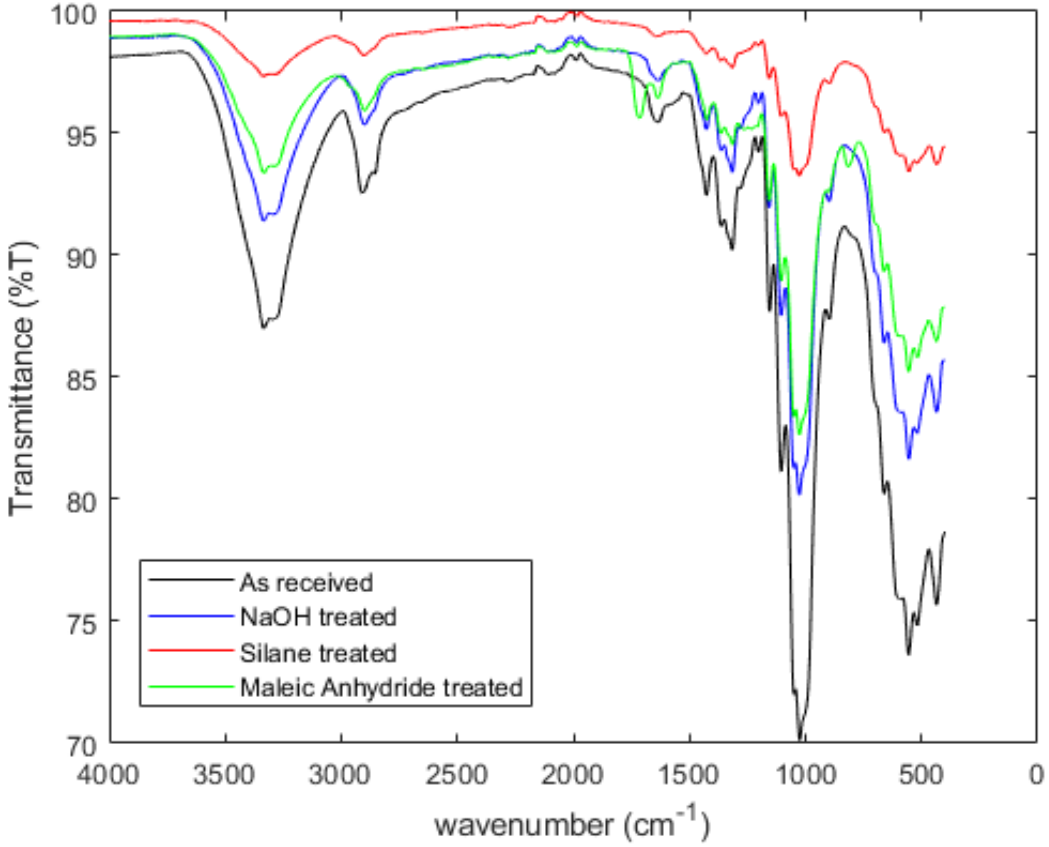

Figure 50: FTIR spectrum of the as-received and treated hemp yarns.

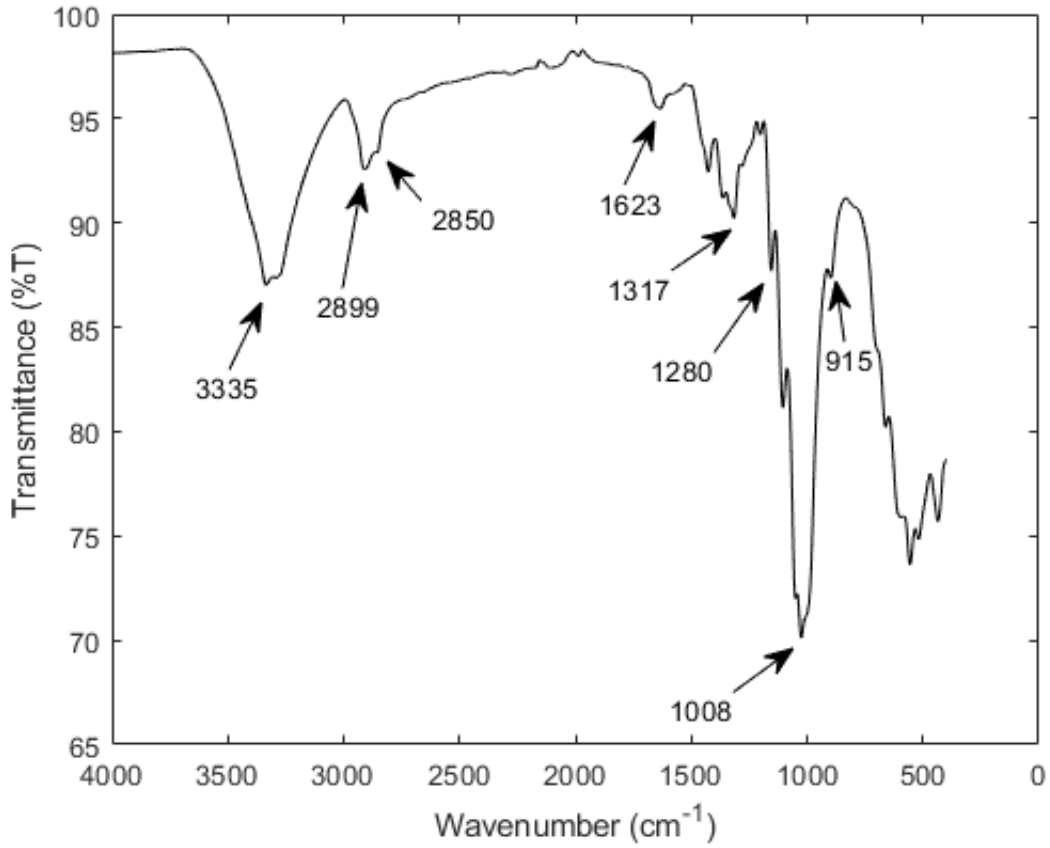

Figure 51: FTIR spectra of the as-received hemp yarns.

Figure 50 presents the infrared spectroscopy profiles of as-received and alkali-treated hemp fibres show similar at some major characteristic bands. However, the decrease in peak intensities, with ratios of absorbance of 0.97, 0.99, 0.98 and 0.93 at the peaks 3335 cm^{-1}, 2899 cm^{-1}, 1317 cm^{-1} and 1008 cm^{-1}, respectively. The decrease in peak intensities was also observed by other researchers and confirms the further removal of any remaining hemicellulose and lignin by the alkali treatment (Sunny, Pickering and Lim, 2020). The small shoulder band seen at 2899 cm^{-1}, –CH stretching, in the received hemp fibres was not found on the alkali-treated hemp fibres. It is possible that the –CH was hidden since it has been reported to be found in cellulose and hemicellulose (Dai and Fan, 2010; Stevulova *et al.*, 2014).

As also observed by Suardana, Piao and Lim, 2011, and Sgriccia, Hawley and Misra, 2008, the FTIR of the silanized hemp fibre did not reveal any significant difference compare to the FTIR of the as-received hemp fibres (Figure 50). Contrary to the findings of Sawpan *et al*., 2011, in

regard with the characteristic peaks of the silanization of natural fibres, resulting from the reaction between silane and cellulose, that are usually observed 708 cm^{-1} for Si-O-Si symmetric stretching, and at 1203 cm^{-1} for Si-O-C stretching (Lu, Swan and Ferguson, 2012), no clear peaks were observed around these wavenumbers as shown in Figure 50**.** However, all FTIR spectra including the as-received yarns displaced an absorbance band at 1200 cm^{-1} and a shoulder between 780 and 700 cm^{-1}. It is quite possible that these bands obscured any bands due to the adsorption of silane. Such obscuration of silane bands, except at very high concentrations of silane, was observed by Sepe *et al.*, 2018. To confirm the presence of the silane in the silanized hemp yarns, an EDS analysis was performed on the as-received and silane-treated hemp yarns. The results revealed the presence of traces of silicon that increased from an average percentage of 0.20 in the as-received hemp to 0.33 in the silanized hemp, as shown in Figure 52. It should be noted that the silicon content would remain low because little more than a monolayer of silane is expected.

Figure 50 also presents spectra of as-received and maleic anhydride-treated hemp fibres, revealed the appearance of new peaks at 1714 cm^{-1} and 1638 cm^{-1} representing, respectively, the ν(C=O) stretching of the ester carboxyl group and the ν(-C=C-) conjugated with the carboxyl group of the maleic anhydride incorporated on the hemp fibres. This provided evidence of the effective maleation of the hemp fibres by the maleic anhydride solution (Hong *et al.*, 2008). Additionally, the decrease in intensity at 3334 cm^{-1} and the disappearance of the shoulder band at 2854 cm^{-1} , assigned to either cellulose and hemicellulose (Dai and Fan, 2010; Stevulova *et al.*, 2014), were also noticed. According to Sawpan, Pickering and Fernyhough, 2011, and Hong *et al.*, 2008, this was likely caused by the reaction between the fibres and the maleic anhydride reagent.

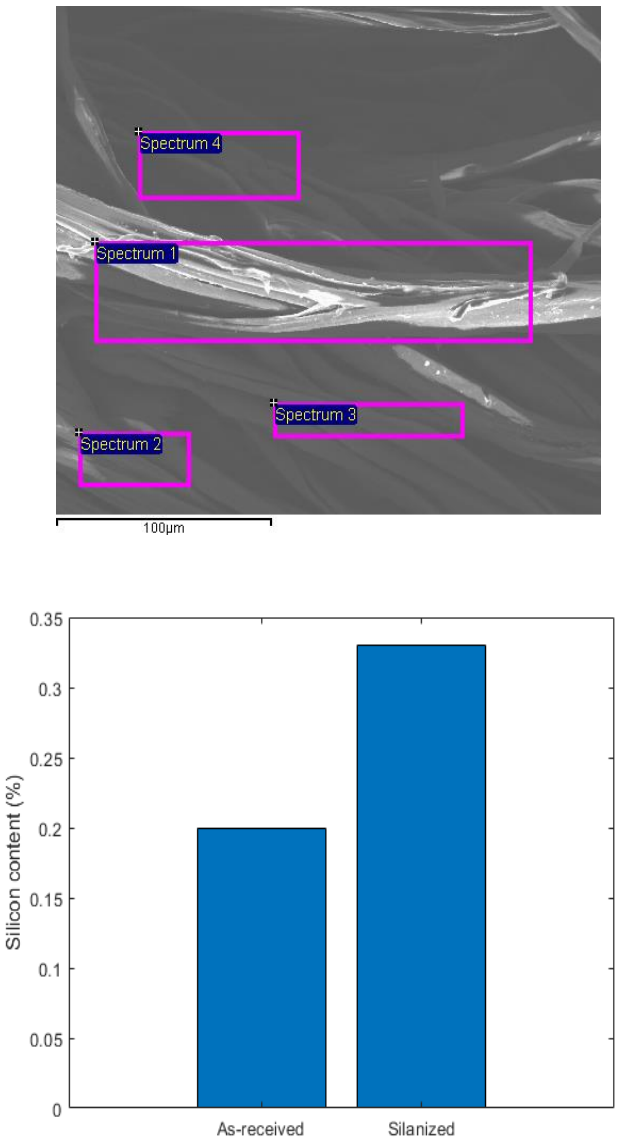

Figure 52: SEM micrograph showing places where the EDS was performed and EDS of the as-received and silanized hemp fibres vs the silicon.

4.5 Thermal gravimetric analysis

Figure 53 and 54 present the thermogravimetric analysis results of the received and treated hemp yarns.

The results of the thermogravimetric and the derivative thermogravimetric (TG/DTG) curves of the as-received hemp yarns are shown in Figure 53. The degradation of the as-received hemp yarn and alkali-treated hemp yarns showed the same pattern, displaying three degradation stages after a first degradation peak between 30°C and 150°C, which corresponds to the evaporation of moisture of approximately 5% from the hemp yarns. This was also observed by other researchers (S. Ouajai and Shanks, 2005). The degradation of the as-received hemp yarns starts at approximately 250°C, preceding the extrapolated onset at 325°C (15.28% loss) of the major weight loss, which peaked at approximately at 350°C (42.54%). The degradation then finished at around 550°C. Cellulose starts to degrade at 275°C and ends at 550°C; lignin degradation was found to start around 300°C and end at 450°C. Similar thermal behaviour of hemp fibres have also been reported in the literature (Kaczmar, Pach and Burgstaller, 2011) (S. Ouajai and Shanks, 2005). The residual mass was found to be 16.8%. Little evidence, if any, of hemicellulose, pectin and wax degradation was observed. This again is consistent with the fact that the as-received yarns had undergone a treatment which removed these components prior to the use of the yarns in this study. Such a sharp degradation as observed here was seen by Sunny, Pickering and Lim, 2020, when hemicellulose and other components were removed by alkalization.

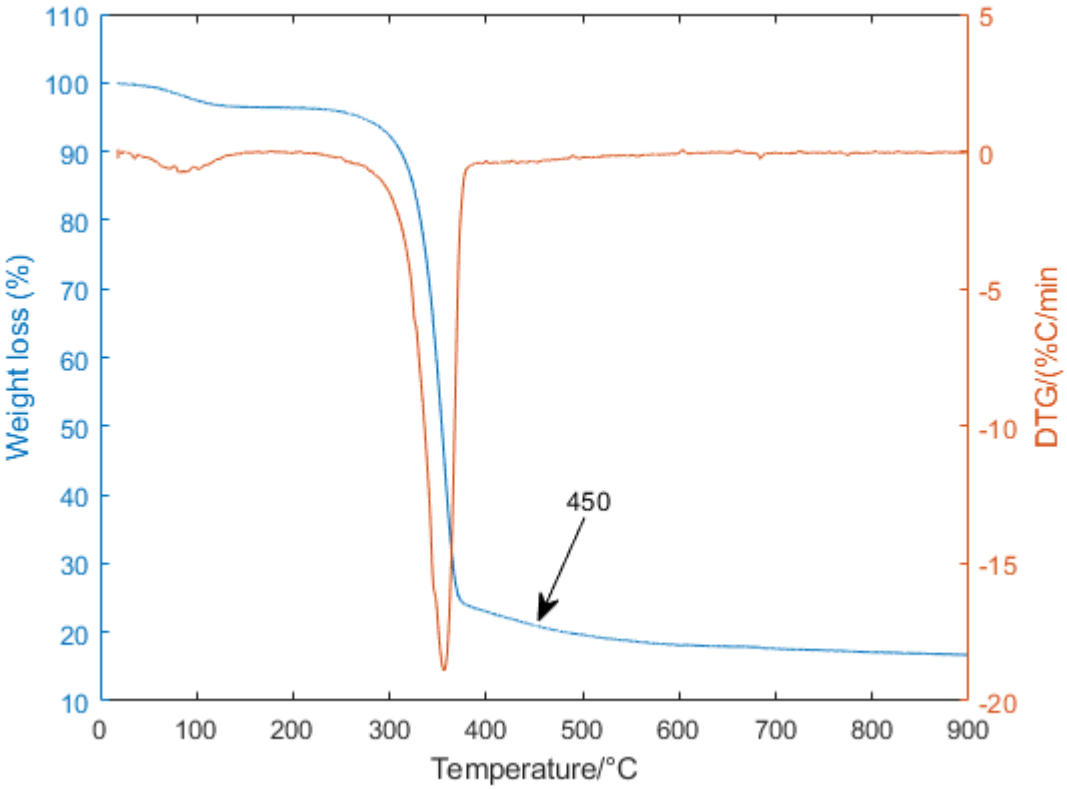

Figure 53: DTG/TG curves of the as-received hemp fibre yarn.

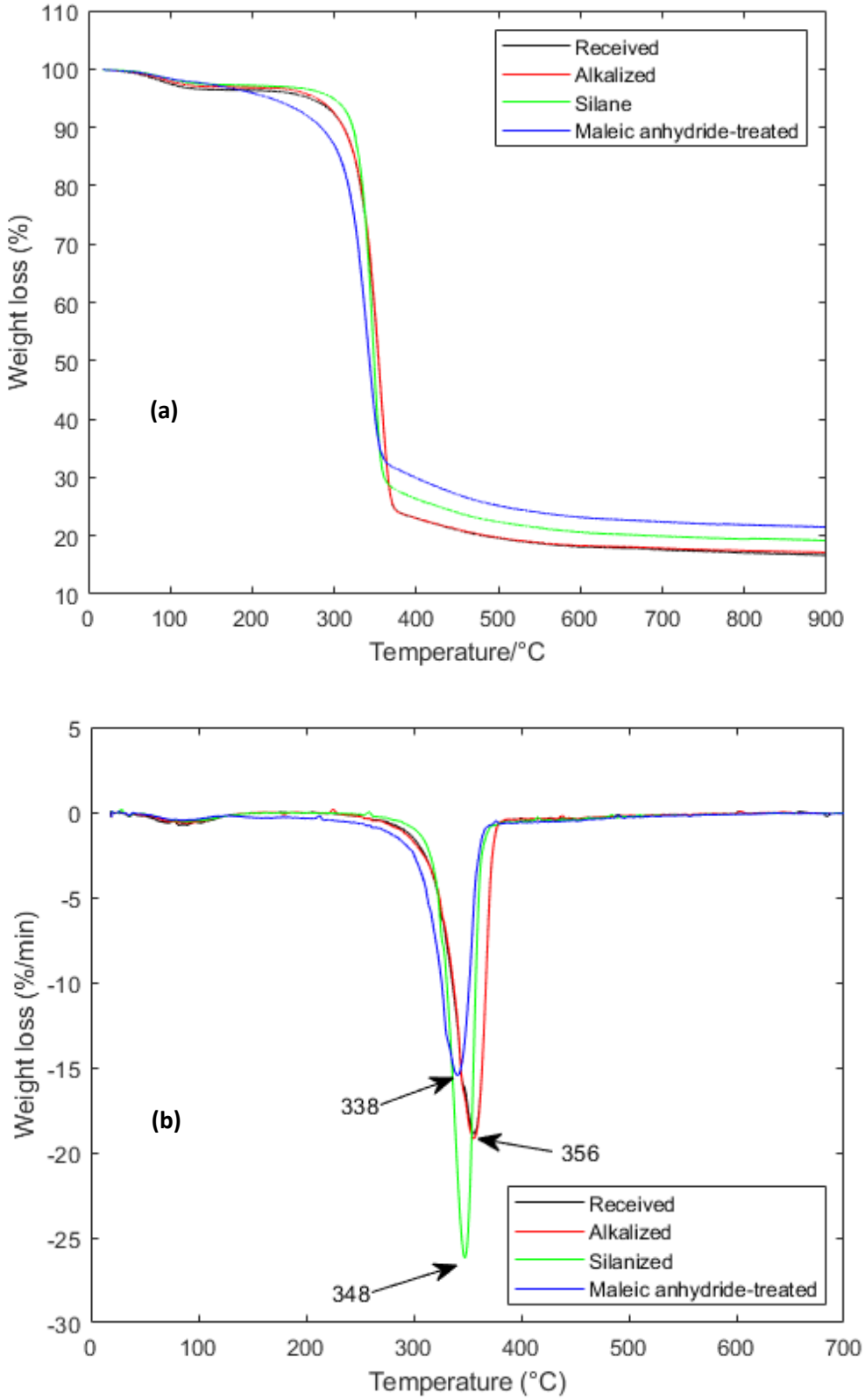

Figure 54: TG (a) and DTG (b) curves of the as-received and treated hemp yarns (top image) and DTG curves of the as-received and treated hemp yarns.

The TG/DTG curves of the silane and maleic anhydride-treated hemp fibres (Figure 54) depicted a slight reduction in temperature at the inflection peak of the mass loss to 348°C and 338°C, compared to the inflection peak temperature of the as-received and alkali-treated hemp fibres that was the same, 356°C.

Being the main component responsible for the mechanical and thermal properties of natural fibres (Fuqua, Huo and Ulven, 2012), cellulose consists of amorphous and crystalline regions. In contrast to crystalline regions, amorphous regions tend to easily degrade when exposed to heat (Stevulova *et al.*, 2014). The degradation is then mainly influenced by the resistance of crystalline regions to heat, which depends on the crystallinity index (Stevulova *et al.*, 2014). The higher the crystalline index, the higher the resistance to heat, hence, the better the thermal behaviour (Stevulova *et al.*, 2014). The 10% mass loss temperatures of the as-received, alkali-, silane- and maleic anhydride-treated hemp yarns were found to be at 311.2°C, 311.01°C, 322.6°C and 283.2°C, respectively. Taking into consideration the slightly different crystallinity index of the hemp yarns, calculated form the XRD peaks, 84,73%, 86,97%, 87,97% and 85,91%, corresponding to the as-received hemp, alkali-, silane- and maleic anhydride-treated hemp yarns. It can be seen that the maleic anhydride seemed to have a negative effect compared with the silane treatment. This was also observed by Ouajai and Shanks, 2005. The 10% mass loss temperature indicated a relative thermal stability with silane-treated hemp yarns being relatively more stable than the as-received and alkali-treated hemp followed by the maleic anhydride-treated hemp fibres with the worst stability. The decomposition of maleic anhydride treated polymers has been noted by a number of authors. The earlier decomposition has been ascribed to decarboxylation reactions (Karami *et al.*, 2019)(Świtała-Zeliazkow, 2001). The absence of significant hemicellulose shoulder in all the TG/DTG curves at 275°C is a further indication that the hemp hemicellulose content is low.

4.6 Characterization of composites

4.7 FTIR spectroscopy

Figure 55 presents the FTIR spectra of the neat epoxy and the 10% as-received/treated hemp yarns reinforced epoxy composites. The FTIR spectra did not show any significant changes except characteristic bands for the epoxy resin. The FTIR broad band at 3396 cm^{-1} was assigned to the O–H stretching of hydroxyl groups in epoxy resin. This can also be due to the N-H stretch derived from the hardener (Xu *et al.*, 2018). A slight change in the shape of the -OH stretch might be indicative of interaction between the cellulosic fibres and the epoxy matrix.

The adsorption band at 3044 cm^{-1} corresponding to the C–H of the epoxide ring in the epoxy resin. The stretching C=C of aromatic ring and C–C of aromatic of epoxy groups was found at 1608 cm^{-1} and 1508 cm^{-1}, respectively. The adsorption bands at 936 cm^{-1} and 826 cm^{-1} respectively corresponded to the C–O and C–O–C stretching of oxirane groups. The stretching C–N and wag N–H bands at 1281 cm^{-1} and 754 cm^{-1} revealed the presence of primary and secondary amines in the neat epoxy and all the composites that acted as crosslinking points during the chain growth polymerization of the epoxide groups by the amine hardeners. However, the spectra of the hemp yarns reinforced epoxy composites revealed a decrease in band intensities compared with the spectrum of the neat epoxy with a ratio of absorbance of 0.98 at most of the characteristic peaks. It is apparent that the ATR technique is reporting the overall epoxy matrix's FTIR response. This is likely because fibres are not present at the surface in significant quantities. Furthermore, it must also be borne in mind that the fibres constitute just 10% of the composites in these FTIR spectrographs hence their contribution would be proportionately low.

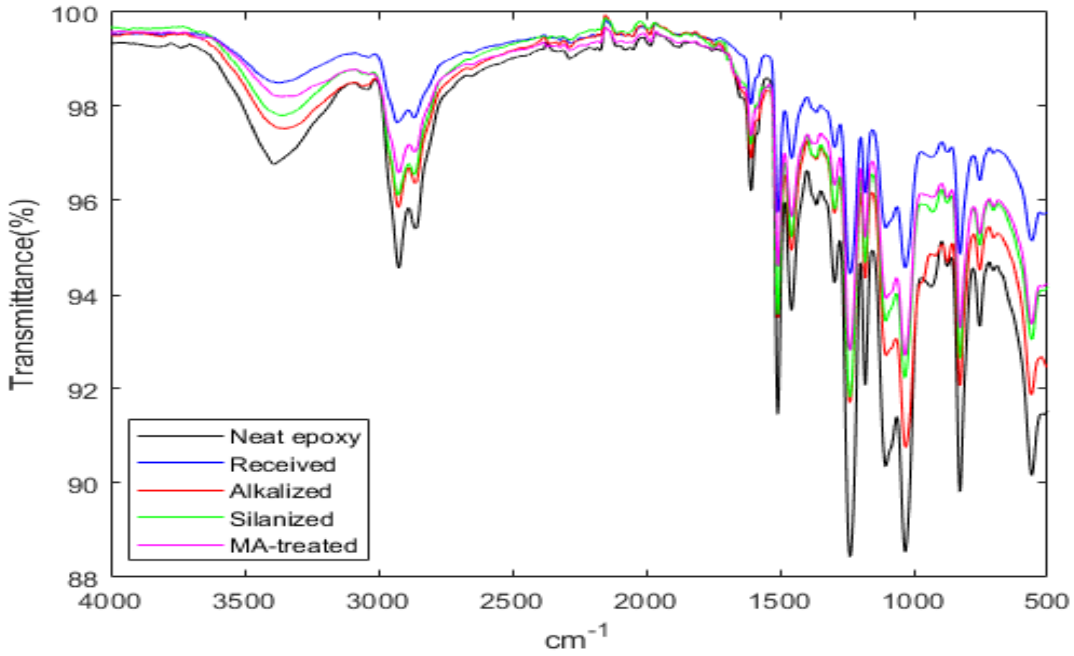

Figure 55: FTIR spectra of the neat epoxy, as-received and treated hemp yarn reinforced epoxy composites.

4.8 Thermogravimetric analysis

Figure 56 - 59 present the thermogravimetric analysis results of the neat epoxy and all the hemp yarn reinforced epoxy composites with a fibre content of 10%.

Figure 56 presents the results of the thermogravimetric and the derivative thermogravimetric (TG/DTG) curves of the neat epoxy. The degradation of the neat epoxy and all the hemp yarn filled epoxy composites showed the same pattern, displaying three degradation stages. The first stage, which corresponds to the evaporation of moisture from the polymer/composite material, occurred within the range of 0-260°C. The second stage is characterized by the beginning of the degradation of the epoxy matrix at 309 °C (extrapolated onset temperature), started above 290°C and ended at 496°C. The most important weight loss occurred during this stage and corresponded to the degradation of the epoxy/hardener system. Additionally, the highest rate of mass change occurred at 363°C (48.53%). The degradation of the remaining components occurred during the third stage, which started at 496°C. The residual mass was found to be 11.2%. However, in addition to the above description, the TG curves of the hemp yarns reinforced epoxy composites revealed the presence of some characteristic peaks ascribed to the degradation of the main lignocellulosic components.

The decomposition of the three main lignocellulosic components occurred in the temperature range of 275 - 550 °C. Cellulose, starts to degrade at 275°C, and ends at 550°C; lignin degradation has been found to start around 300°C and end at 450°C. This follows the degradation of the main cellulosic components in the as-received and treated hemp yarns and confirms the relative thermal behaviour observed after the thermogravimetric analysis of the hemp yarns. Other researchers also observed similar thermal behaviour in different hemp fibres reinforced polymer composites (Ouajai and Shanks, 2005), (Kaczmar, Pach and Burgstaller, 2011), (Oza *et al.*, 2014), (Bachtiar *et al.*, 2019).

The first significative weight losses depicted on the TG/DTG curves occurred at 316.3°C, 316.7°C, 317.4°C and 316.4°C for the as-received, NaOH, silane- and maleic anhydride-treated hemp reinforced epoxy composites at 10% fibre loading, respectively, as sown in Figure 57 (b). These peaks were all the same and similar behaviour were also observed at 15 and 20% fibre loading, as shown in Figure 58(b) and 59(b), respectively. However, the maleic anhydride-treated

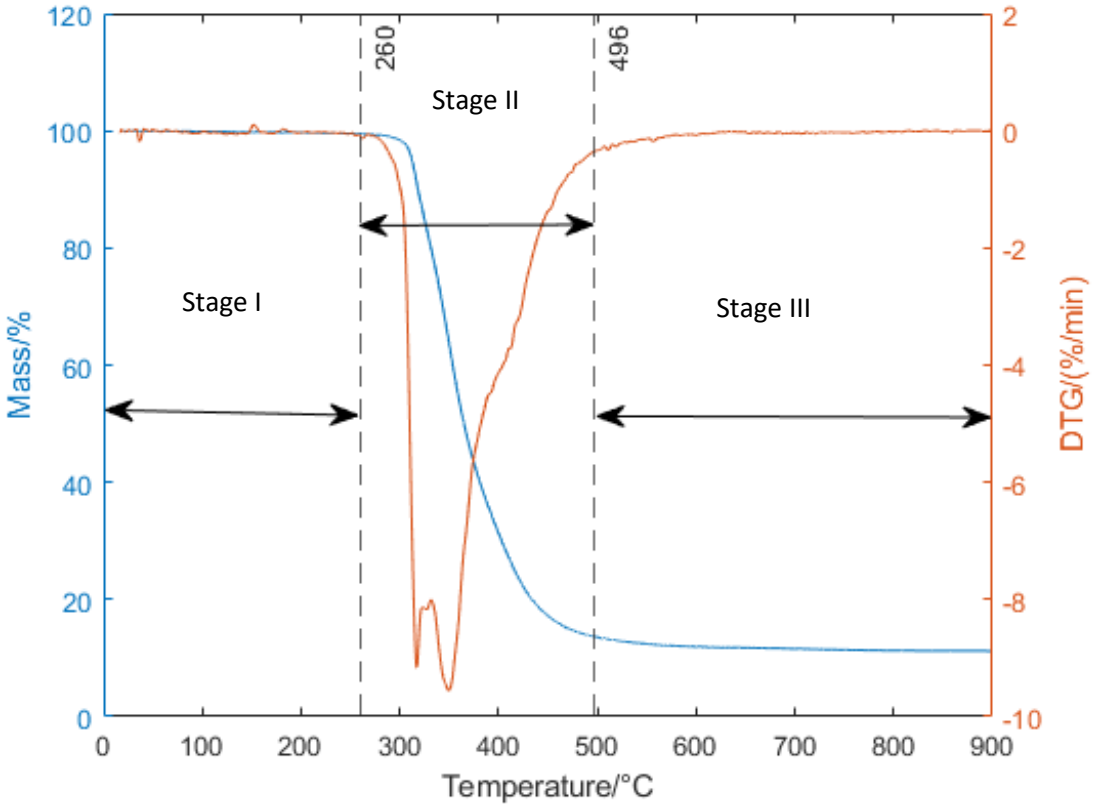

Figure 56: Thermogravimetric and the derivative thermogravimetric (TG/DTG) curves of the neat epoxy.

hemp reinforced composites H and L showed slightly different values. At 15% H seemed to be slightly thermal stable than the other composites while the contrary was observed at 20%. This was so surprising since similar effect as that observed at 10% was also expected. It is no surprise that the composites are less stable than the neat epoxy since the fibre decomposes at a slightly lower temperature than the main epoxy. Additionally, it is no surprise that increased loadings will cause even earlier initial decomposition to a greater extent.

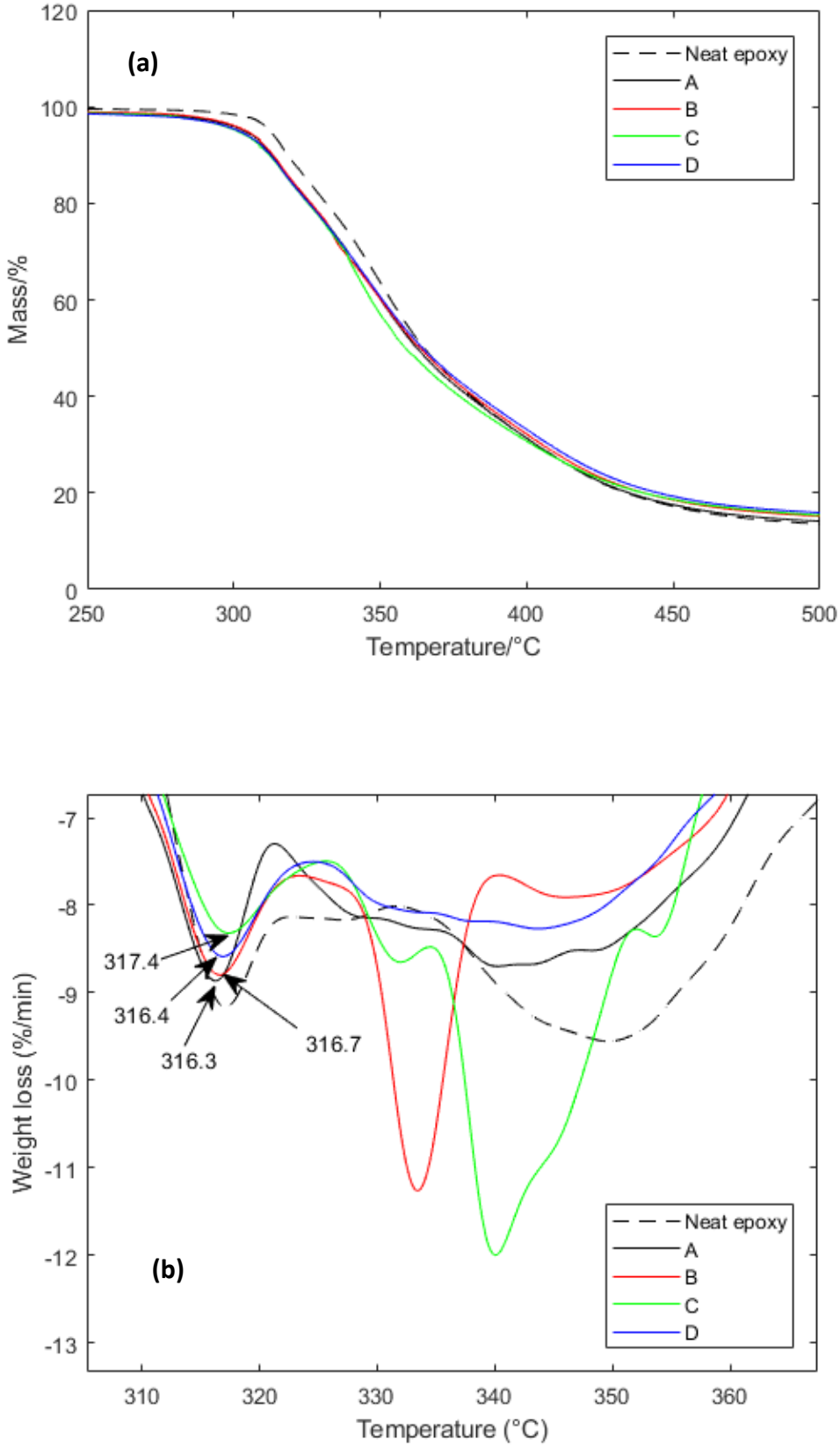

Figure 57: TG (a) and DTG (b) curves of the neat, as-received and treated hemp yarn reinforced epoxy composites, 10% fibre loading.

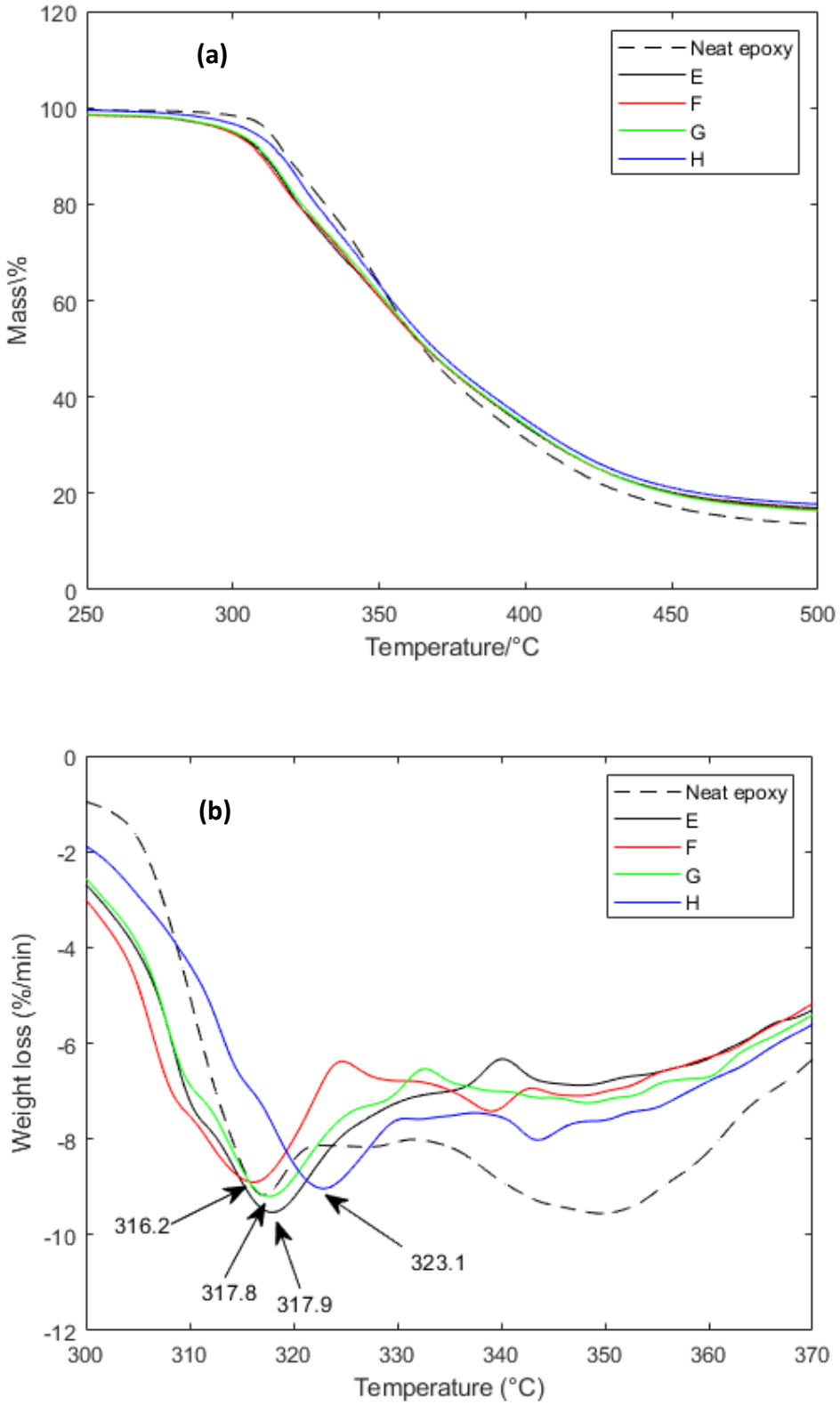

Figure 58: TG (a) and DTG (b) curves of the neat, as-received and treated hemp yarn reinforced epoxy composites, 15% fibre loading.

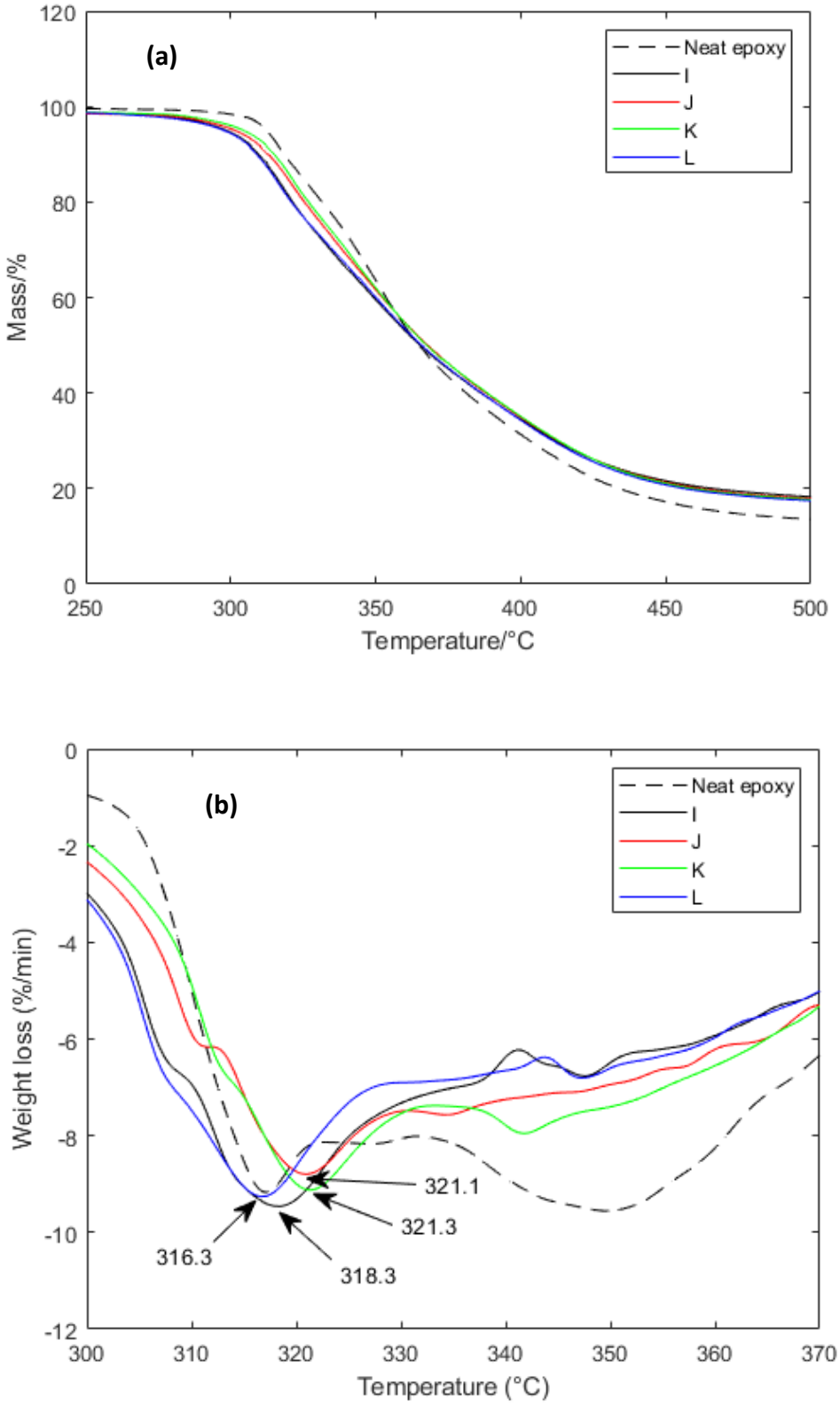

Figure 59: TG (a) and DTG (b) curves of the neat, as-received and treated hemp yarn reinforced epoxy composites, 20% fibre loading.

4.9 Mechanical properties of composites

4.9.1 Tensile properties

At the outset, it should be noted that there are often significant uncertainties associated with the measurement of mechanical properties of composites such as those in this study. This may be due to natural variability in the fibres but in this study is also a result of varying degrees of misalignment of the fibres. However, it is expected that this variability will be reduced by averaging.

Figure 60 (a) presents the ultimate tensile strength of the neat epoxy and the general trends of the as-received and treated hemp fibres reinforced epoxy composites at 10%, 15% and 20% fibre loading. The neat epoxy displayed the lowest tensile strength 55.80 ± 7.02 MPa compare with all the reinforced epoxy composites. The effect of the alkalization and silanization of the fibres on the alkali-treated and silane-treated hemp reinforced epoxy composites was statistically significant according to their tensile strength values 61.79 ± 0.12 MPa and 64.82 ± 3.56 MPa (at 10% fibre loading) for the alkali- and silane-treated hemp yarn reinforced epoxy composites. The maleic anhydride-treated hemp yarn reinforced composites weakened the tensile properties of the as-received hemp yarn reinforced epoxy composites 56.62 ± 3.25 MPa, at 10% fibre loading. With the maleic anhydride-treated hemp yarn reinforced epoxy composites displaying the lowest tensile strength at 20% (56.62 ± 3.25 MPa), the reinforced composites also followed the same trend, with higher strength, than at 10%, 76.16 ± 5.81 MPa, 73.24 ± 3.68 MPa, 72.26 ± 4.28 MPa for the silane, as-received, alkali-treated hemp yarn reinforced epoxy composites, respectively. The increase in strength at 15% fibre content was also observed with the maleic anhydride having the lowest tensile strength 60.40 ± 2.16 MPa. The silane treatment at 20% loading shows the highest tensile strength and this was probably due to the combined effect of the better fibre/matrix and the highest loading which improved the composite resistance to load. As a result, this enhanced the mechanical properties.

The alkali- and silane treatments did not have a considerable impact on the tensile strength on their respective composites compare to the tensile strength of the as-received hemp reinforced epoxy composite at all the fibre contents. Although the alkalization and silanization are mainly reported to improve the tensile strength of plant fibre reinforced epoxy composites (Sepe *et al.*, 2016, 2018)(Tanasă *et al.*, 2020), extensive alkalization has been

shown to deteriorate the structure of the microfibrils of cellulose, causing poor fibre/matrix adhesion. This reduces the load transfer capacity of the composites and hence may have contributed to the reduced tensile strength observed in this study for further alkalization treatment of the as-received fibres. It should, however, be noted that although the further alkalized fibres were the weakest tested, they did not produce the weakest composites. Similar effect of a further alkalization on hemp fibres was also observed on the tensile properties of the alkali-treated hemp fibre reinforced polyester composite (Kabir, 2012) (Sepe *et al.*, 2016).

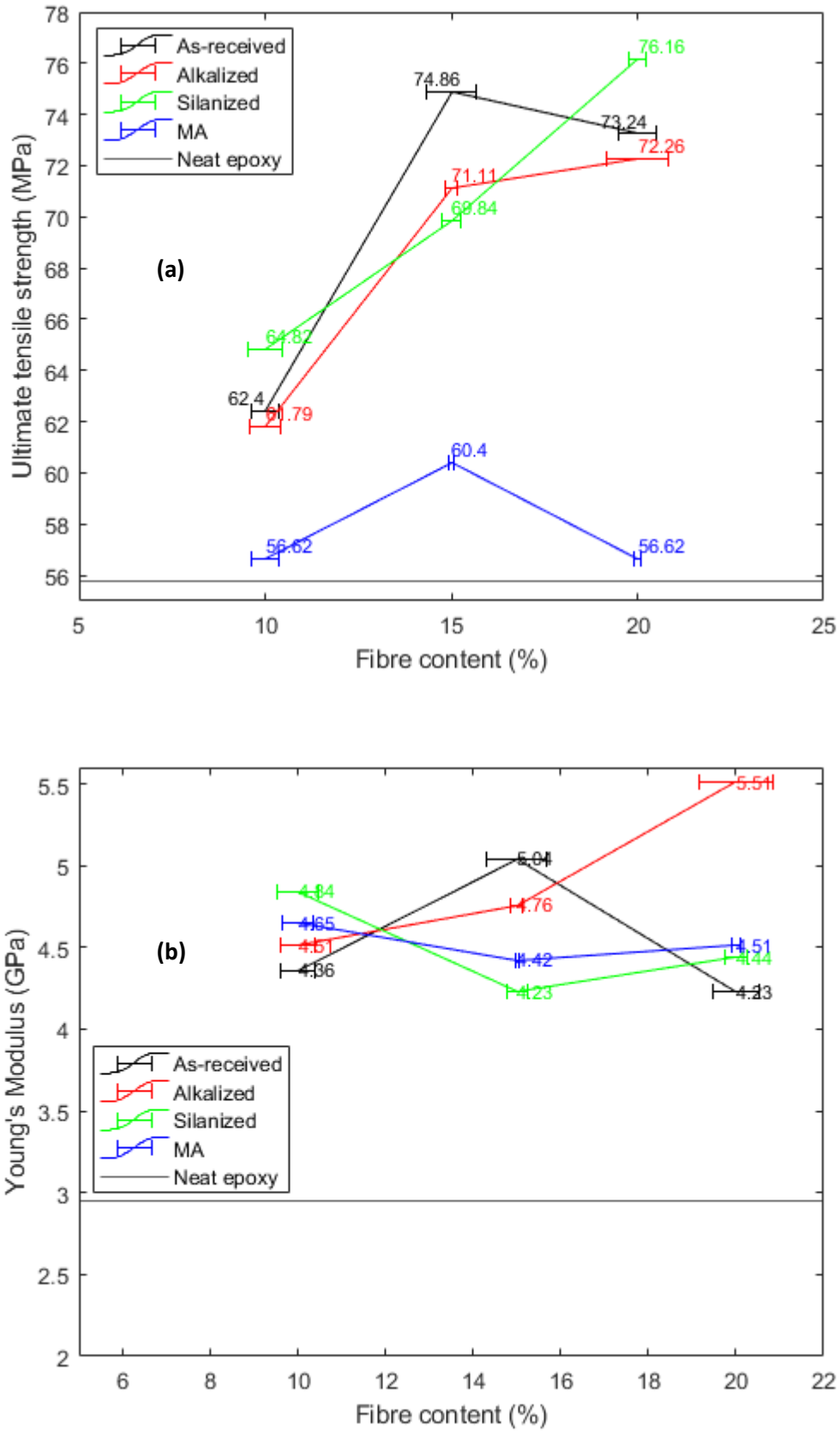

Figure 60: General trends of ultimate tensile strength (a) and the Young's modulus (b).

The silane coupling agent are expected to have reacted with hydroxyl groups from the fibres on one end and the matrix on the other end. The already mercerized fibres may have not had enough free hydroxyl groups that could have reacted with the silane molecules. Furthermore, the non-exposure to heat that did not allow a proper condensation reaction between the fibre and the silanol groups may have contributed to the formation of an overall weaker fibre/matrix interface than initially expected.

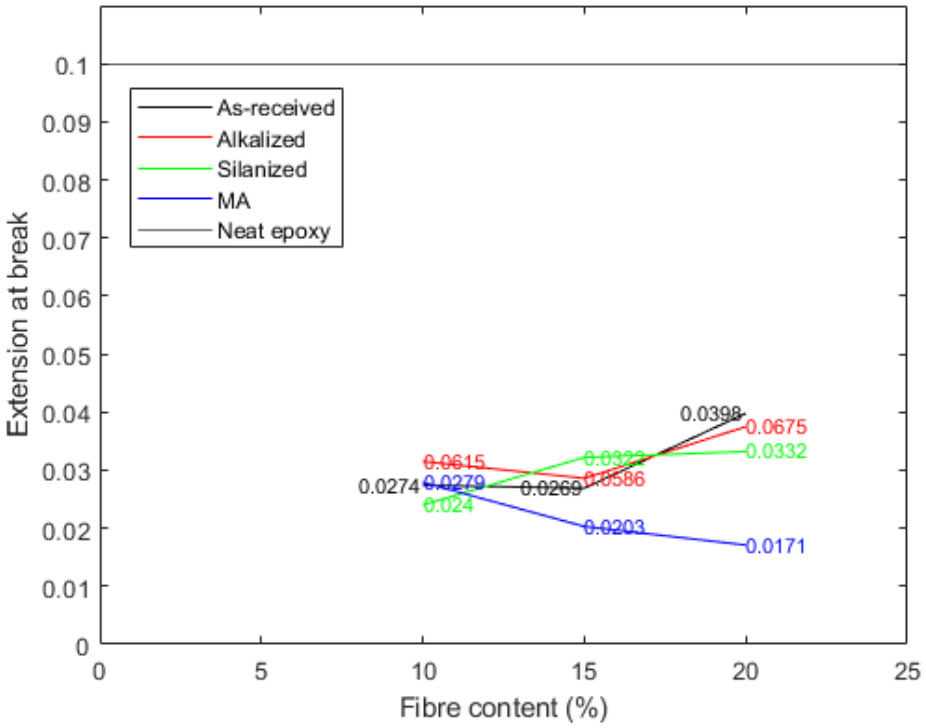

Figure 61: Extension at break of the neat epoxy, as-received and treated hemp yarn reinforced epoxy composites.

The maleic anhydride showed the lowest tensile strength compared to the other composites. It is believed that internal reaction between fibre and matrix at the interface may have caused this. This was also observed by Sepe *et al.*, 2018, and Bodur, Bakkal and Sonmez, 2016. It was previously noted that the maleic anhydride fibres had one of the lowest tensile strengths of the fibre types under investigation.

The Young's modulus of the as-received and treated hemp reinforced epoxy composites showed higher values compare to that of the neat epoxy, 2.946 ± 0.317 GPa as was the case for the tensile strengths (Figure 60 (b)). This isn't surprising given that the fibres have higher

modulus than the neat epoxy. The Young's modulus generally showed similar trends as that of the tensile strengths. The elastic modulus of the silane and maleic anhydride yarns reinforced epoxy composites was slightly higher than that of alkali-treated followed by the received hemp reinforced epoxy composite, at 10%. In general, however, maleic anhydride-treated fibres had the lowest modulus. Surprisingly, despite the higher modulus of the silanized and maleic anhydride-treated fibres, this result was not translated to the composites. This suggested that the strength of the interfaces between these treated surfaces were inferior to the interfaces formed with the alkalized (including the as-received) fibres.

The elongations at break of the as-received, alkali- and silane- treated hemp yarns reinforced epoxy composites did not show any significant difference, though they were lower than that of the matrix as shown in Figure 61. This was probably due to the effect of the fibres on the ultimate tensile strength and modulus, which caused an increase in stiffness and therefore reduced the elongation at break of the composites. Additionally, the different inter-linkages between the fibre and the matrix at the different fibre/matrix interfaces present in the different composites, which probably enabled the composites to easily react to deformation. While the alkali and silane treatment did not impact the extension at break of their respective composites, at all the fibre loadings, compared with the as-received hemp yarns reinforced epoxy composites. In general, the maleic anhydride compatibilizer degraded the elongation of the maleic anhydride-treated hemp epoxy composite, compare to the other composites, due to the effect of the maleic anhydride at the fibre surface, which may have reduced the capacity of the overall load transfer and decreased its capacity to resist to deformation. This was also reported by Ku *et al.*, 2011.

In general, it was found that across all the properties (tensile strength, Young's modulus and extension at break) the maleic anhydride-treated fibres performed the worst. Interestingly, the maleic anhydride-treated fibres showed the least dependence of the properties on the loading of fibres added.

4.9.2 Flexural properties

Figure 62 presents the flexural strength of the neat epoxy and the general trends of the as-received and treated hemp fibres reinforced epoxy composites at 10%, 15% and 20% fibre loading. The neat epoxy depicted the lowest flexural strength 167.25 ± 7.02 MPa compare with all the reinforced epoxy composites. The chemical treatments on the as-received hemp yarns did not show any considerable differences in the flexural strengths of the alkali-, silane- and maleic anhydride-treated hemp yarn reinforced epoxy composites respectively 202.57 ± 22.11 MPa, 211 ± 3.94 MPa, and 188.65 ± 4.84 MPa, although they were slightly higher than that of the as-received hemp yarn reinforced epoxy composites, 184.65 ± 2.03 MPa at 10% fibre loading. At 15% fibre loading, the flexural strength values were still slightly different although they were higher than those of the 10% fibre loading. The as-received, alkali- and silane-treated hemp yarn reinforced epoxy composites flexural values were respectively 220.69 ± 6.63 MPa, 234.28 ± 5.78 MPa and 204.26 ± 7.61 MPa, while the maleic anhydride-treated hemp reinforced epoxy composite had a flexural strength of 167.25 ± 8.02 MPa. At 20% fibre loading the flexural strength values depicted the same pattern as that of the 10% fibre loading but with slightly lower. At the top, the alkali- and silane-treated hemp yarn reinforced epoxy composites present similar values: 211.34 ± 12.07 MPa and 211.30 ± 40.39 MPa, respectively. At the bottom, the as-received hemp yarn reinforced epoxy composite showed slightly higher flexural strength,166.98 ± 27.23 MPa, than the maleic anhydride-treated hemp yarn reinforced epoxy composite 167.24 ± 19.63 MPa. Peaking behaviour in flexural strength and modulus as seen here for alkalized (strength and modulus) and as-received (strength) samples has also been reported for alkali treated fibres by (Xu *et al.*, 2018). The maleic anhydride treatment did not affect the flexural strength at 10% and 20% fibre loading significantly and weakened the flexural strength at 15% fibre loading compared to the flexural strengths of the as-received, alkali- and silane-treated hemp yarn reinforced epoxy composites. It is likely that the coupling of the fibres and the matrix caused by the silane molecules may have induced a better adhesion between the fibre and the matrix, although significant changes in flexural strength were observed. This enabled the composite to have similar load transfer capacity as the as-received and alkali-treated hemp yarn reinforced epoxy composites. The maleic anhydride treatment ended up weakening the flexural strength across all fibre loadings. As before this is ascribed to a likely weak interface

between these fibres and the epoxy. It is possible that the carboxylic acid groups on the surface did not react well with the epoxy matrix.

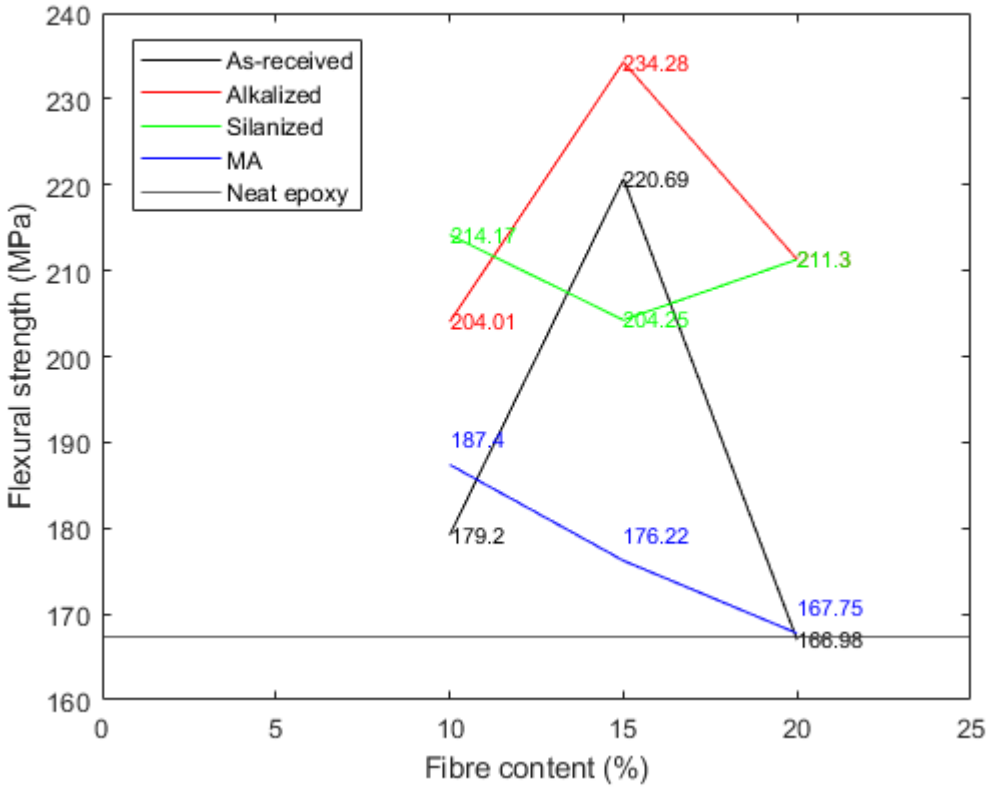

Figure 62: Flexural strength of the neat epoxy, as-received and treated hemp yarn reinforced epoxy composites.

The flexural modulus of the received and treated hemp reinforced epoxy composites showed higher values compare to that of the neat epoxy, 2.9458 ± 0.3166 GPa, like for the Young's modulus (Figure 63 (a)). The flexural modulus almost showed a different trend compare with that of the flexural strength. Although not statistically significant, the stiffness of the alkali-, silane- and maleic anhydride-treated hemp yarn reinforced epoxy composites were slightly higher than that of the as-received hemp yarns reinforced epoxy composite. This was probably due to the differences in the inter and intra linkages present in the hemp yarn reinforced epoxy composites according to the different chemical treatments the fibres were exposed to.

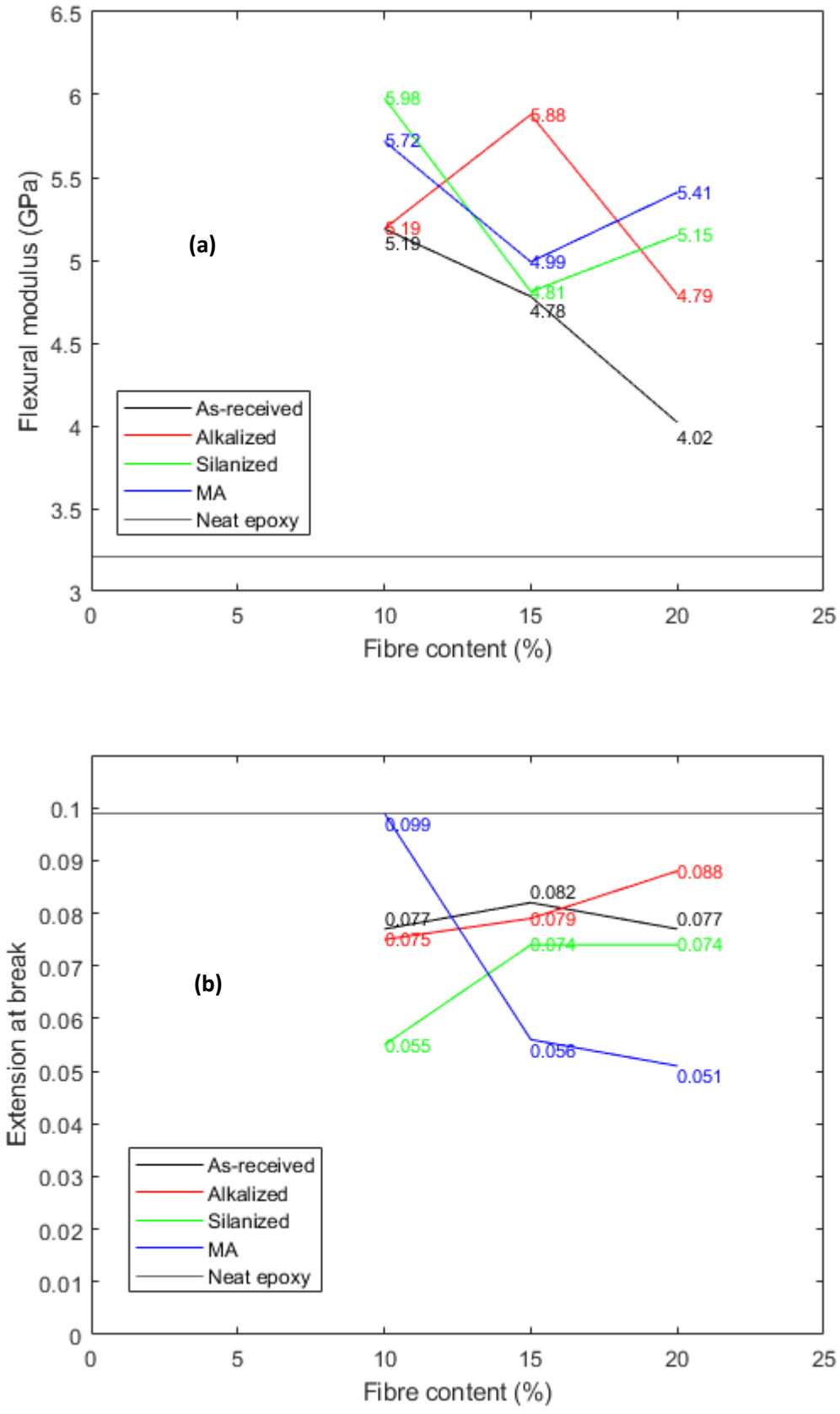

Figure 63: Flexural modulus (a) and extension at break (b) of the neat epoxy, as-received and treated hemp.

The elongations at break (Figure 63 (b)), of the as-received, alkali- and silane- treated hemp yarns reinforced epoxy composites showed lower values than that of the neat epoxy except for the maleic anhydride-treated hemp yarn epoxy composite at 10%. The maleic anhydride treatment on the as-received hemp depicted less resistance to deformation at 15% and 20% fibre loading, whereas the alkalization and silanization of the as-received treatment did not have any significant impact on the epoxy composite compare with the as-received hemp yarn epoxy composite. This difference may have been assigned to either the fibre loading or the presence of the different fibre/matrix interfaces resulting from the respective chemical treatments. The worsening of the resistance to deformation displayed by the maleic anhydride-treated hemp yarn reinforced epoxy composite was also observed by Ku *et al.*, 2011.

4.9.3 Microscopy

Depending on the way the load is applied on a material, different modes of failures can be observed. Below are the SEM micrographs of fracture tensile specimens for the as-received, alkali-, silane- and maleic anhydride-treated epoxy composites as shown in Figure 64 (a), 64 (b), 64 (c) and 64 (d), respectively, at 10% fibre loading. The fracture zones in the as-received and alkali-treated hemp yarn reinforced epoxy composites show similar features and better fibre distribution in the matrix compare than the silane- and maleic anhydride-treated hemp yarns reinforced epoxy composites. All the composites failed in a brittle mode presenting fibre pulled out and fracture bands in the matrix. The differences in the fibre distribution in the matrix generating the level of fibre/matrix interfaces, which are responsible of the load transfer within the material, may have caused differences in the capacity of load bearing in the composites. However, Figure 64 (a) presents less fibre-matrix debonding, revealing an overall better fibre to matrix bonding compared to the other composites. This explains the differences in mechanical properties that were not statistically different in the as-received, alkali and silane-treated hemp reinforced epoxy composites. Compared to the first three composites (Figure 64 (d)), it can be seen that the SEM micrograph of the maleic anhydride-treated hemp reinforced epoxy composite depicts more significant fibre-matrix debonding and holes left by pulled-out fibres revealing low interfacial bonding between the fibre and the matrix. Additionally, considerable cracks along the matrix can also be observed. This is

consistent with the tensile properties of the maleic anhydride hemp yarn-reinforced composites. This weak interface explains why the maleic-anhydride-treated fibre composites failed at lower tensile strengths than the other composites.

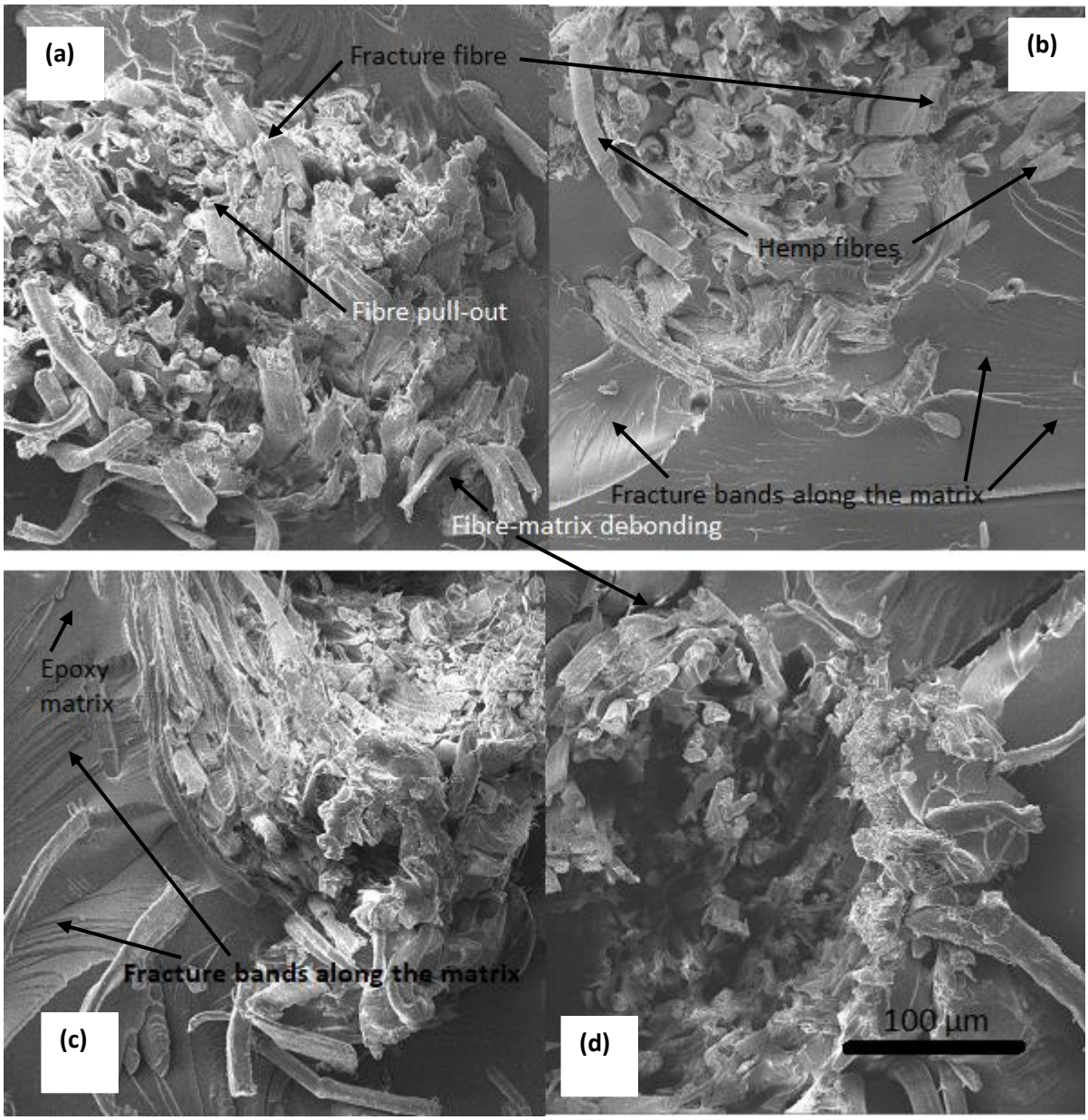

Figure 64: SEM micrographs of tensile test specimen of the as-received (a), alkali-(b), silane (c) and maleic anhydride-(d) treated hemp yarn reinforced epoxy composites at 10% fibre loading.

The SEM micrographs of fracture flexural specimens for the as-received, alkali-, silane- and maleic anhydride-treated epoxy composites may be found in Figure 65 (a), 65 (b), 65 (c) and 65 (d) respectively. This was also observed at higher fibre loading. No distinctive differences were observed on the SEM micrographs. The fracture bands along the matrix, the bending fibres and fibre-matrix debonding were shown on the images. However, the as-received and the maleic anhydride-treated hemp yarn reinforced epoxy composites appeared not to retain as many hemp fibres as the alkali- and silane-treated hemp yarn reinforced epoxy composites. This was likely caused by the nature of the fibre/matrix interfaces formed in the respective composites and may explain the trend showed on the flexural strength whereby the alkali- and silane-treated hemp yarn reinforced epoxy composites seemed to display slightly better responses to the applied flexural load. Furthermore fibre-matrix debonding is again apparent in the maleic-anhydride treated fibre composites.

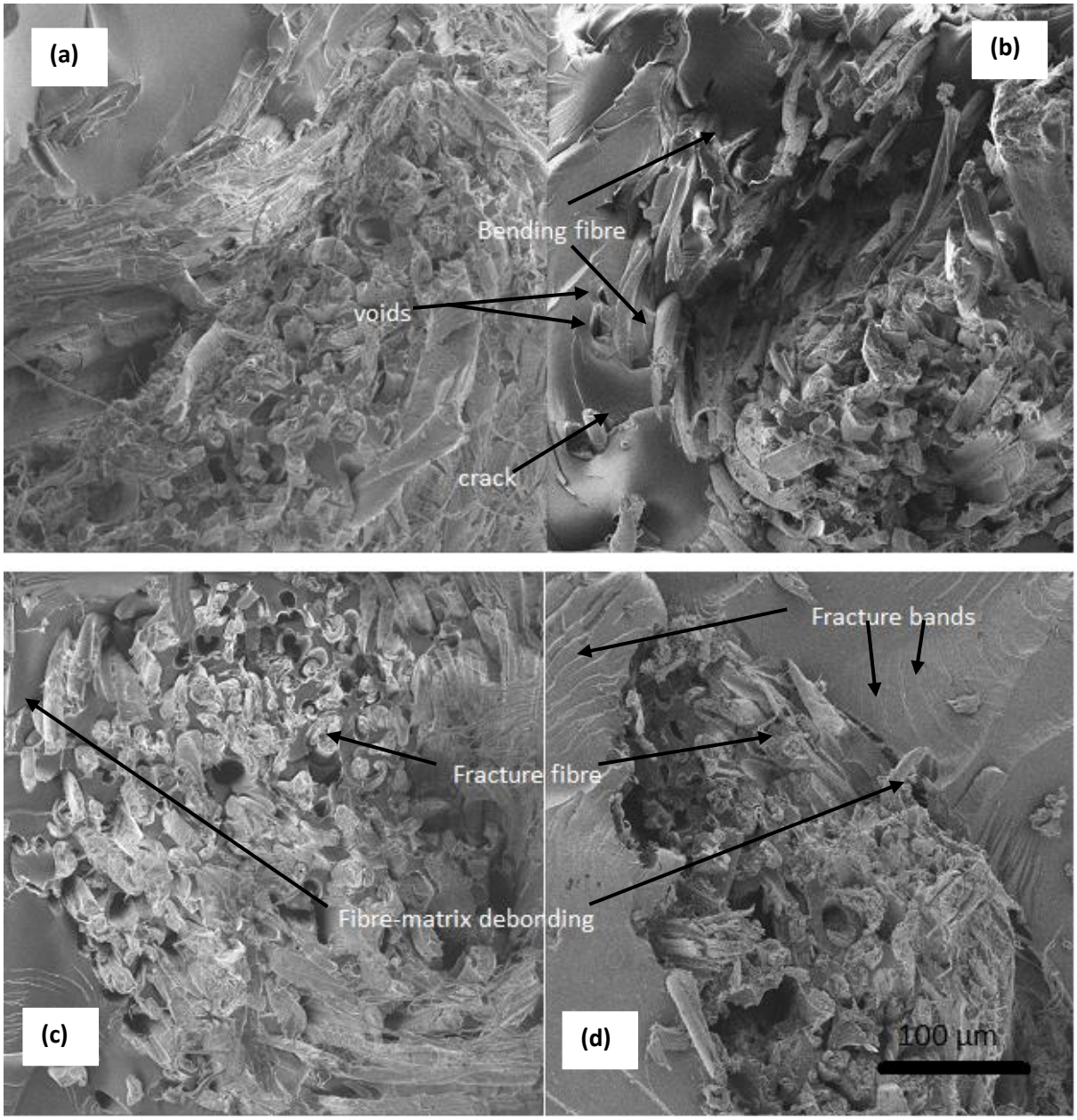

Figure 65: SEM micrographs of flexural test specimen of the as-received (top left), alkali-(top right), silane (bottom left) and maleic anhydride-(bottom right) treated hemp yarn reinforced epoxy composites at 10% fibre loading.

4.9.4 Mechanical properties prediction

The tensile strength of the composite and the elastic modulus were determined at the different fibre loadings and the computed values as shown in Figure 66 and 67.

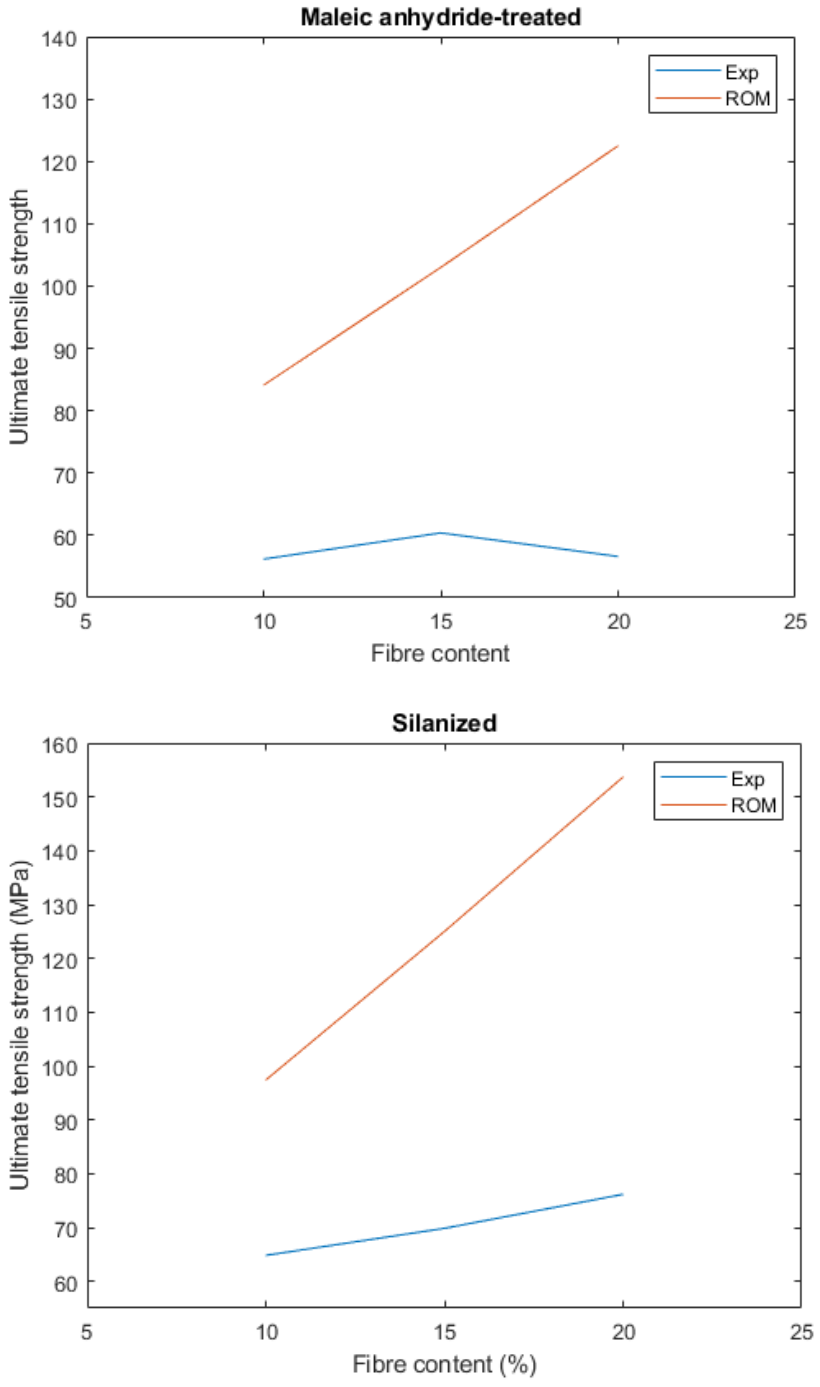

Figure 66: Predicted and experimental tensile strength of maleic anhydride and silane-treated hemp yarn reinforced epoxy composites.

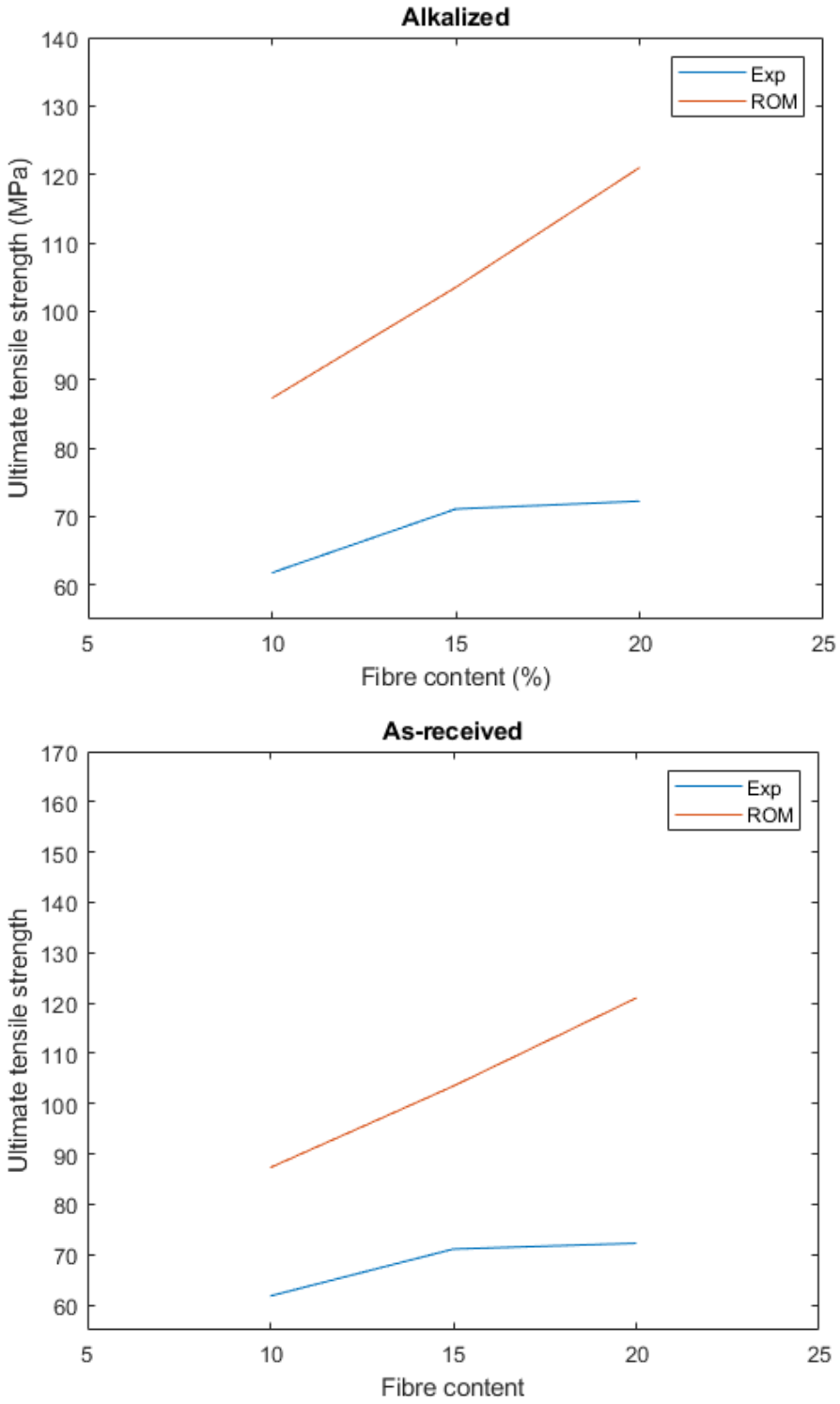

Figure 67: Predicted and experimental tensile strength of the as-received and alkalized hemp yarn reinforced epoxy composites.

Generally, the predicted strength of the as-received and alkali-treated hemp epoxy reinforced composites followed the same pattern and seem to have similar values. This may explain why the alkalization did not cause significant changes on the reinforced fibres epoxy composite.

However, the experimental values of the silane-treated hemp yarn reinforced epoxy composite appeared to be the only composite that followed the predicted values pattern although that of the experimental were lower. As expected, the maleic anhydride-treated hemp yarn reinforced epoxy composite did not follow the pattern of the predicted values. The differences observed may have occurred due to the type of interfaces present in the different composites as it was shown in the microscopy section.

All the composite experimental tensile strengths deviated from the theoretical models. This was probably due to the fact that the presence of voids in composites is not considered in models. Additionally, the misalignment of the fibres in the composites could have also impacted the experimental values.

5 Conclusion

The microscopy characterization of the as-received hemp yarns revealed the presence of warp and weft hemp yarns which both contained defects such as dislocations, known to affect mechanical properties of natural plant fibres. SEM characterization helped identified the Z-twist direction in the hemp yarns, which allowed their classification under the ring spun yarns group. The warp and weft hemp yarns showed no significant differences between their fibre densities and linear densities. These were consistent with densities found in the literature.

The tensile measurement on the already pre-treated hemp yarns revealed an average higher tensile strength for the warp hemp yarns compared with the weft hemp yarns. This helped choose the warp hemp yarns for further composite manufacture, which appeared to be choice worthy for the continuation of the research.

The as-received yarns were assessed as being pre-treated, likely by mercerization. The evidence for this was a high crystallinity index (determined by XRD), absence of bands characteristic of hemicellulose in the FTIR spectrum and a sharp decomposition observed in the TGA thermogram. The decomposition of the material was observed below 300^{o}C with the exception of the evaporation of moisture. These were all in contrast to what has been reported for raw hemp yarn in the literature.

The modification of the surface of the as-received warp hemp yarns was accomplished by means of an alkalization, a silanization and a maleic anhydride treatment. The effectiveness of the surface treatments was assessed using XRD, FTIR, TGA methods and performing tensile testing. The chemical treatments had a small impact on the crystallinity index as measured by XRD. This was likely because the crystallinity index of the as-received hemp yarns was already high, leaving little scope for further increase in the crystallinity of the yarns.

The alkalization and the maleic anhydride treatment of the as-received hemp yarns displayed clear changes to the FTIR spectra. This was especially true of the maleic anhydride treatment where new bands characteristic of carboxylate acids/esters and double bonds were observed. By contrast the silanized hemp yarns did not show any clear characteristic peaks from the silane. It is suggested that these were obscured by other bands in the FTIR spectra. Similar results have been reported in the literature at the concentrations of silane used. To confirm

silanization an increase in silicon content was detected using an energy dispersive X-ray spectroscopy.

The different interfaces generated by the above-mentioned surface treatments affected the thermal stability of the treated hemp yarns assessed by means of TGA. The silane treated hemp yarns were more thermally stable than the alkali-treated hemp yarns followed the as-received hemp yarns. The maleic anhydride treated hemp yarns showed the lowest thermal stability. The poorer maleic anhydride treated yarn stability was ascribed to possible decarboxylation reactions.

The tensile strength of the as-received hemp yarn was higher than that of the silane-treated hemp yarns, which was higher than the maleic anhydride treated hemp yarns followed by the alkali-treated hemp yarns. This was attributed to the different effect of the chemical treatments that removed the remaining non-lignocellulose components. This negatively affected the state of the hemp fibres and therefore the microfibril angle. As, a result the resistance to fibre-slippage was reduced which impacted the mechanical properties.

The thermogravimetric analysis of the neat epoxy revealed that the as-received and treated hemp reinforced epoxy composites were less thermally stable than the neat epoxy. The thermal stability of the treated hemp yarn epoxy composites did not show any significant difference at all the fibre loadings. Because the fibre loadings were low, it is not surprising that the bulk of the decomposition was due to the epoxy resin which consequently had the largest effect on the thermal stability of the composites.

The interfaces formed by the chemical treatments differently affected the tensile and flexural properties of the treated hemp yarn epoxy composites. All chemical treatments on the as-received yarns increased the tensile and flexural properties of the epoxy but, in general, they were not higher than the tensile and flexural properties of composites made with the as-received hemp yarns. Generally, the alkalization and silanization seemed not to have significant impact on the as-mercerized, already pre-treated, hemp reinforced epoxy composites. However, the maleic anhydride treatment worsened the properties of the hemp reinforced epoxy composites. Scanning electron microscopy revealed that the likely reason for the poor behaviour of the maleic anhydride treated yarn composites was poor matrix-

fibre adhesion. Evidence was seen of fibre-matrix debonding/delamination in the case of this set of samples which was not seen in the other composites.

The as-received and treated-hemp yarn reinforced epoxy composites revealed lower strengths that the predicted ones. This was probably caused by the mis-orientation I the fibres. It was seen on the predicted graph that there were no significant changes in tensile strength of the as-received hemp by the alkalization, silanization and maleic-anhydride-treated on the mechanical properties of their respective composites. So the experimental values insignificances were not surprising although some appeared to be worse than others.

Generally, this study showed that no significant improvement could be brought to already mercerized hemp yarns. A further alkalization on the hemp yarns slightly decreased the mechanical properties of the epoxy compare with the as-received hemp yarn reinforced epoxy composites. The silanization of the hemp yarn did not significantly impact the mechanical properties of its composite compare with the already mercerized, as-received, hemp yarn epoxy composites while the maleic anhydride treatment worsened the mechanical properties of the composites. The fact that very little improvement, if at all, was seen was that the as-received fibres already displayed high crystallinity with much of the non-cellulosic material having been removed. The changes brought about by further alkalization would have been small and may have worsened the strength of the fibres as explained. Silanization may not have been successful because of poor condensation of the fibre because no elevated temperature was used during the hydrolysis of silane. The poor behaviour of maleic anhydride as a couple agent is worth further study.

6 Recommendations

The work performed on already mercerized treated hemp yarns may have produced different results if proceeded with completely untreated hemp fibres. Therefore, future work should be performed on such fibres. An approach would be to begin with untreated hemp-fibres. These should be treated for 5h with 6wt% NaOH solution as done in this study. The time of exposure would then be extended to create different levels of alkalization. Thus, alkalization should take place for 5h, 10h, 15h, 20h and 25h. This would better mimic the effect of a pre-treatment that led to as-treated fibres similar to those used in this study. It would also provide fibres of different crystallinities so the effect of alkalization and crystallinity could be better probed. As an alternative, the temperature of alkalization for constant exposure time could be varied to achieve different degrees of mercerization. In this study, alkalization was performed at room temperature. Higher temperature alkalization across the temperature range 25-100^{o}C would be expected to give different crystallinities. Care would, however, need to be taken in such a study to account for damage done to the fibres by elevated temperatures. Silanization should also be performed at each level of alkalization.

Moisture sorption measurements on the fibres and the composites should be done for a better understanding of its influence in the composites. Additionally, the determination of the critical length for the analytical modelling of the mechanical properties of hemp reinforced polymer composites could be investigated.

Furthermore, investigating the effects of the surface treatments on the mechanical properties of hemp fibre reinforced polymer should be enlarged to more than one matrix to better understand the effect of the chemical treated at their different fibre/matrix. In this study the Sicomin SD8100/SR8224 system was employed. This system had relatively high tensile strength. A system with lower tensile strength may have enhanced differences between the treatment methods more.

Only one silane was employed, 3-aminopropyltriethoxysilane (APS). This silane was chosen because it contained the amine functional group like the hardener used. Another approach would be to have used a silane with an epoxy group attached. An example would be (3-glycidyloxypropyl)trimethoxysilane (GPTMS) with which some authors have reported some success.

For operational reasons, the loadings of fibres were limited to 10, 15 and 20wt%. This range could be extended to at least 30%. This would allow more data points to be used for modelling.

The poor performance of maleic anhydride treated fibres deserves further studies. This result was in contrast to results reported for polyester-based composites. This might be the result of a number of factors which require exploration. Is it a general phenomenon observed with epoxy-based systems or just the system studied? Is it a result of the very high crystallinity in this study? This could be tied to the recommendation above of repeating the study at different levels of pre-alkalization.

7 References

Agbor, V. B. *et al.* (2011) 'Biomass pretreatment: Fundamentals toward application', *Biotechnology Advances*, 29(6), pp. 675–685. doi: 10.1016/j.biotechadv.2011.05.005.

Akil, H. M. *et al.* (2011) 'Kenaf fiber reinforced composites: A review', *Materials and Design*, 32(8–9), pp. 4107–4121. doi: 10.1016/j.matdes.2011.04.008.

Ali, A. *et al.* (2018) 'Hydrophobic treatment of natural fibers and their composites—A review', *Journal of Industrial Textiles*, 47(8), pp. 2153–2183. doi: 10.1177/1528083716654468.

Alias, A. H. *et al.* (2018) 'Evaluation of kenaf yarn properties as affected by different linear densities for woven fabric laminated composite production', *Sains Malaysiana*, 47(8), pp. 1853–1860. doi: 10.17576/jsm-2018-4708-25.

Anwar, Z., Gulfraz, M. and Irshad, M. (2014) 'Agro-industrial lignocellulosic biomass a key to unlock the future bio-energy: A brief review', *Journal of Radiation Research and Applied Sciences*, 7(2), pp. 163–173. doi: 10.1016/j.jrras.2014.02.003.

Arbelaiz, A. *et al.* (2005) 'Flax fiber surface modifications: Effects on fiber physico mechanical and flax/polypropylene interface properties', *Polymer Composites*, 26(3), pp. 324–332. doi: 10.1002/pc.20097.

Aziz, S. H. and Ansell, M. P. (2004) 'The effect of alkalization and fibre alignment on the mechanical and thermal properties of kenaf and hemp bast fibre composites : Part 1 – polyester resin matrix', 64, pp. 1219–1230. doi: 10.1016/j.compscitech.2003.10.001.

Bachtiar, E. V. *et al.* (2019) 'Thermal stability, fire performance, and mechanical properties of natural fibre fabric-reinforced polymer composites with different fire retardants', *Polymers*, 11(4). doi: 10.3390/polym11040699.

Bakar, A. *et al.* (2015) 'Review of the Compression Moulding of Natural Fiber-Reinforced Thermoset Composites: Material Processing and Characterisations', *Pertanika Journal of Tropical Agricultural Science*, 38(4), pp. 533–547.

Batzer, H. and Lohse, F. (1976) 'Epoxy Resins.', *Kunstst Ger Plast*, 66(10), pp. 50–53.

Baxter, R. *et al.* (2008) 'A process for producing pulp from lignocellulosic-containing material', 39(5), pp. 561–563.

Beckermann, G. W. and Pickering, K. L. (2008) 'Engineering and evaluation of hemp fibre reinforced polypropylene composites', *Indian Journal of Natural Products and Resources*, 7(6), p. 515. doi: 10.1016/j.compositesa.2008.03.010.

Benkhelladi, A., Laouici, H. and Bouchoucha, A. (2020) 'Tensile and flexural properties of polymer composites reinforced by flax, jute and sisal fibres', *International Journal of Advanced Manufacturing Technology*, 108(3), pp. 895–916. doi: 10.1007/s00170-020-05427-2.

Bhattacharyya, D., Subasinghe, A. and Kim, N. K. (2015) *Natural fibers*, *Multifunctionality of Polymer Composites*. Elsevier Inc. doi: 10.1016/B978-0-323-26434-1.00004-0.

Bledzki, A. K. *et al.* (2008) 'The effects of acetylation on properties of flax fibre and its polypropylene composites', *Express Polymer Letters*, 2(6), pp. 413–422. doi: 10.3144/expresspolymlett.2008.50.

Bodur, M. S., Bakkal, M. and Sonmez, H. E. (2016) 'The effects of different chemical treatment methods on the mechanical and thermal properties of textile fiber reinforced polymer composites', *Journal of Composite Materials*, 50(27), pp. 3817–3830. doi: 10.1177/0021998315626256.

del Borrello, M. *et al.* (2020) 'Manufacturing and characterization of hemp-reinforced epoxy composites', *Polymer Composites*, 41(6), pp. 2316–2329. doi: 10.1002/pc.25540.

Cao, Y., Wang, W. and Wang, Q. (2014) 'Application of mechanical model for natural fibre reinforced polymer composites', *Materials Research Innovations*, 18, pp. S2354–S2357. doi: 10.1179/1432891714Z.000000000431.

Carrier, M. *et al.* (2011) 'Thermogravimetric analysis as a new method to determine the lignocellulosic composition of biomass', *Biomass and Bioenergy*, 35(1), pp. 298–307. doi: 10.1016/j.biombioe.2010.08.067.

De Carvalho Mendes, C. A. *et al.* (2015) 'Chemical, physical, mechanical, thermal and morphological characterization of corn husk residue', *Cellulose Chemistry and Technology*, 49(9–10), pp. 727–735. Available at: http://www.scopus.com/inward/record.url?eid=2-s2.0-84961256771&partnerID=tZOtx3y1.

Chang Hong, R. wood (2004) 'A Review on Natural Fibre- Based Composites-Part I: Structure, Processing and Properties of Vegetable Fibres', *Journal of Natural Fibers*, 1(2), pp. 37–41. doi: 10.1300/J395v01n02.

Chattopadhyay, R. (2010) 'Introduction: Types of technical textile yarn', *Technical Textile Yarns*, pp. 3–55. doi: 10.1533/9781845699475.1.3.

Chattopadyay, R. (2010) 'Introduction: types of technical textile yarn 1'. doi: 10.1533/9781845699475.1.3.

Cho, D., Kim, H. J. and Drzal, L. T. (2013) 'Surface treatment and characterization of natural fibers: Effects on the properties of biocomposites', *Polymer Composites, Biocomposites*, 3, pp. 133–177. doi: 10.1002/9783527674220.ch4.

Dai, D. and Fan, M. (2010) 'Characteristic and Performance of Elementary Hemp Fibre', *Materials Sciences and Applications*, 01(06), pp. 336–342. doi: 10.4236/msa.2010.16049.

Dai, D. and Fan, M. (2011) 'Investigation of the dislocation of natural fibres by Fourier-transform infrared spectroscopy', *Vibrational Spectroscopy*, 55(2), pp. 300–306. doi: 10.1016/j.vibspec.2010.12.009.

Dhandapani, S., Nayak, S. K. and Mohanty, S. (2016) 'Surface modification of oil palm fruit bunch and fibre reinforcement effect on bio-based polyester matrix composites: Dynamic, morphological, thermal and mechanical properties', *Journal of Elastomers and Plastics*, 48(5), pp. 456–479. doi: 10.1177/0095244315580458.

Douglas W, R. (1987) 'Pulp Bleaching Technology', *Tappi press*, pp. 39–52.

Duval, A. and Lawoko, M. (2014) 'A review on lignin-based polymeric, micro- and nano-structured materials', *Reactive and Functional Polymers*, 85, pp. 78–96. doi: 10.1016/j.reactfunctpolym.2014.09.017.

Fa, O. (2013) *Biofi ber reinforced polymer composites for structural applications*.

Fan, M., Dai, D. and Huang, B. (2012) 'Fourier Transform Infrared Spectroscopy for Natural Fibres', *Fourier Transform - Materials Analysis*. doi: 10.5772/35482.

Faruk, O. *et al.* (2012) 'Biocomposites reinforced with natural fibers: 2000-2010', *Progress in Polymer Science*, 37(11), pp. 1552–1596. doi: 10.1016/j.progpolymsci.2012.04.003.

Fortea-Verdejo, M. *et al.* (2017) 'Plant fibre-reinforced polymers: where do we stand in terms of tensile properties?', *International Materials Reviews*, 62(8), pp. 441–464. doi:

10.1080/09506608.2016.1271089.

French, A. D. (2014) 'Idealized powder diffraction patterns for cellulose polymorphs', *Cellulose*, 21(2), pp. 885–896. doi: 10.1007/s10570-013-0030-4.

Fuqua, M. A., Huo, S. and Ulven, C. A. (2012) 'Natural fiber reinforced composites', *Polymer Reviews*, 52(3–4), pp. 259–320. doi: 10.1080/15583724.2012.705409.

Gokarneshan, N., Varadarajan, B. and Senthil Kumar, C. B. (2013) 'Calculations in fabric testing', *Mechanics and Calculations of Textile Machinery*, pp. 334–346. doi: 10.1533/9780857095527.2.334.

Gurunathan, T., Mohanty, S. and Nayak, S. K. (2015) 'A review of the recent developments in biocomposites based on natural fibres and their application perspectives', *Composites Part A: Applied Science and Manufacturing*, 77, pp. 1–25. doi: 10.1016/j.compositesa.2015.06.007.

Haghdan, S. and Smith, G. D. (2015) 'Natural fiber reinforced polyester composites: A literature review', *Journal of Reinforced Plastics and Composites*, 34(14), pp. 1179–1190. doi: 10.1177/0731684415588938.

Hajiha, H., Sain, M. and Mei, L. H. (2014) 'Modification and Characterization of Hemp and Sisal Fibers', *Journal of Natural Fibers*, 11(2), pp. 144–168. doi: 10.1080/15440478.2013.861779.

Hamidon, M. H. *et al.* (2019) 'Effects of fibre treatment on mechanical properties of kenaf fibre reinforced composites: A review', *Journal of Materials Research and Technology*, 8(3), pp. 3327–3337. doi: 10.1016/j.jmrt.2019.04.012.

Hari, P. K. (2012) 'Types and properties of fibres and yarns used in weaving', *Woven Textiles: Principles, Technologies and Applications*, pp. 3–34. doi: 10.1533/9780857095589.1.3.

Hintz, H. L. and Lawal, S. A. (2018) 'Pulping and Bleaching ☆', *Reference Module in Materials Science and Materials Engineering*, (January), pp. 1–7. doi: 10.1016/B978-0-12-803581-8.11233-0.

Ho, M. P. *et al.* (2012) 'Critical factors on manufacturing processes of natural fibre composites', *Composites Part B: Engineering*, 43(8), pp. 3549–3562. doi: 10.1016/j.compositesb.2011.10.001.

Hong, C. K. *et al.* (2008) 'Mechanical properties of maleic anhydride treated jute fibre/polypropyiene composites', *Plastics, Rubber and Composites*, 37(7), pp. 325–330. doi: 10.1179/174328908X314334.

Hughes, M. (2012) 'Defects in natural fibres: Their origin, characteristics and implications for natural fibre-reinforced composites', *Journal of Materials Science*, 47(2), pp. 599–609. doi: 10.1007/s10853-011-6025-3.

Huijgen, W., Bermudez, L. and Bakker, R. (2010) *Literature review of physical and chemical pretreatment processes for lignocellulosic biomass*, *Biosynergry*.

Jain, D., Mukherjee, A. and Kwatra, N. (2014) 'Local micromechanics of moisture diffusion in fiber reinforced polymer composites', *International Journal of Heat and Mass Transfer*, 76, pp. 199–209. doi: 10.1016/j.ijheatmasstransfer.2014.04.031.

Kabir, M. M. *et al.* (2012) 'Chemical treatments on plant-based natural fibre reinforced polymer composites: An overview', *Composites Part B: Engineering*, 43(7), pp. 2883–2892. doi: 10.1016/j.compositesb.2012.04.053.

Kabir, M. M. (2012) 'Effects of Chemical Treatments on Hemp Fibre Reinforced Polyester Composites', *PhD*, (September), pp. 1–205.

Kaczmar, J. W., Pach, J. and Burgstaller, C. (2011) 'The chemically treated hemp fibres to reinforce polymers', *Polimery/Polymers*, 56(11–12), pp. 817–822. doi: 10.14314/polimery.2011.817.

Kalita, P. *et al.* (2009) 'Determination and comparison of kinetic parameters of low density biomass fuels', *Journal of Renewable and Sustainable Energy*, 1(2), p. 023109. doi: 10.1063/1.3126936.

Karaduman, Y. *et al.* (2018) 'Interfacial Modification of Hemp Fiber–Reinforced Composites', *Natural and Artificial Fiber-Reinforced Composites as Renewable Sources*. doi: 10.5772/intechopen.70519.

Karami, Z. *et al.* (2019) 'Bio-based thermoset alloys from epoxy acrylate, sesame oil- and castor oil-derived resins: Renewable alternatives to vinyl ester and unsaturated polyester resins', *Polymers from Renewable Resources*, 10(1–3), pp. 27–44. doi: 10.1177/2041247919863633.

Karim, M. R. A. *et al.* (2020) 'Natural fibres as promising environmental-friendly reinforcements for polymer composites', *Polymers and Polymer Composites*. doi: 10.1177/0967391120913723.

Komuraiah, A., Kumar, N. S. and Prasad, B. D. (2014) 'Chemical Composition of Natural Fibers and its Influence on their Mechanical Properties', *Mechanics of Composite Materials*, 50(3), pp. 359–376. doi: 10.1007/s11029-014-9422-2.

Ku, H. *et al.* (2011) 'A review on the tensile properties of natural fiber reinforced polymer composites', *Composites Part B: Engineering*, 42(4), pp. 856–873. doi: 10.1016/j.compositesb.2011.01.010.

Kuruvila, J., Sabu, T. and Pavithran, C. (1996) 'Effect of chemical treatment of the tensile properties of short sisal fibre-reinforced polyethylene composites', *Obstetrical and Gynecological Survey*, 37(3), pp. 5139–5149. doi: 10.1097/00006254-197803000-00022.

Lan, Y. (2018) 'Waxes', *Encyclopedia of Food Chemistry*, pp. 312–316. doi: 10.1016/B978-0-08-100596-5.22344-5.

Lascano, D. *et al.* (2019) 'Optimization of the curing and post-curing conditions for the manufacturing of partially bio-based epoxy resins with improved toughness', *Polymers*, 11(8). doi: 10.3390/polym11081354.

Lee, H. V., Hamid, S. B. A. and Zain, S. K. (2014) 'Conversion of lignocellulosic biomass to nanocellulose: Structure and chemical process', *Scientific World Journal*, 2014. doi: 10.1155/2014/631013.

Li, X., Tabil, L. G. and Panigrahi, S. (2007a) 'Chemical treatments of natural fiber for use in natural fiber-reinforced composites: A review', *Journal of Polymers and the Environment*, 15(1), pp. 25–33. doi: 10.1007/s10924-006-0042-3.

Li, X., Tabil, L. G. and Panigrahi, S. (2007b) 'Chemical treatments of natural fiber for use in natural fiber-reinforced composites: A review', *Journal of Polymers and the Environment*, 15(1), pp. 25–33. doi: 10.1007/s10924-006-0042-3.

Liu, M. *et al.* (2017) 'Targeted pre-treatment of hemp bast fibres for optimal performance in biocomposite materials: A review', *Industrial Crops and Products*, 108(July), pp. 660–683. doi: 10.1016/j.indcrop.2017.07.027.

Lu, N., Swan, R. H. and Ferguson, I. (2012) 'Composition, structure, and mechanical properties of hemp fiber reinforced composite with recycled high-density polyethylene matrix', *Journal of Composite Materials*, 46(16), pp. 1915–1924. doi: 10.1177/0021998311427778.

Ma, H. *et al.* (2016) 'Effect of linear density and yarn structure on the mechanical properties of ramie fiber yarn reinforced composites', *Composites Part A: Applied Science and Manufacturing*, 87, pp. 98–108. doi: 10.1016/j.compositesa.2016.04.012.

Madsen, B. *et al.* (2007) 'Hemp yarn reinforced composites – I . Yarn characteristics', 38, pp. 2194–2203. doi: 10.1016/j.compositesa.2007.06.001.

Madsen, B. and Lilholt, H. (2003) 'Physical and mechanical properties of unidirectional plant fibre composites-an evaluation of the influence of porosity', *Composites Science and Technology*, 63(9), pp. 1265–1272. doi: 10.1016/S0266-3538(03)00097-6.

Manaia, J. P., Manaia, A. T. and Rodriges, L. (2019) 'Industrial hemp fibers: An overview', *Fibers*, 7(12), pp. 1–16. doi: 10.3390/?b7120106.

Mansaray, A. E. and Ghaly, K. . . (1999) 'Kinetics of the Thermal Degradation of Rice Husks in Nitrogen Atmosphere', *Energy Sources*, 21(9), pp. 773–784. doi: 10.1080/00908319950014335.

Maschio, G. *et al.* (1997) 'A new method to determine the composition of biomass by thermogravimetric analysis', *The Canadian Journal of Chemical Engineering*, pp. 127–133. doi: 10.1002/cjce.5450750120.

Medina, L. A. and Dzalto, J. (2018) '1.11 Natural Fibers', *Comprehensive Composite Materials II*, 1, pp. 269–294. doi: 10.1016/B978-0-12-803581-8.09877-5.

Mehta, G. *et al.* (2006) 'Effect of fiber surface treatment on the properties of biocomposites from nonwoven industrial hemp fiber mats and unsaturated polyester resin', *Journal of Applied Polymer Science*, 99(3), pp. 1055–1068. doi: 10.1002/app.22620.

Mishra, S. and Naik, J. B. (1998) 'Absorption of steam and water at ambient temperature in wood polymer composites prepared from agro-waste and novolac', *Journal of Applied Polymer Science*, 68(9), pp. 1417–1421. doi: 10.1002/(SICI)1097-4628(19980531)68:9<1417::AID-APP5>3.0.CO;2-E.

Mishra, S. and Naik, J. B. (2005) 'Effect of treatment of maleic anhydride on mechanical properties of natural fiber: Polystyrene composites', *Polymer - Plastics Technology and Engineering*, 44(4), pp. 663–675. doi: 10.1081/PTE-200057814.

Mohammed, L. *et al.* (2015) 'A Review on Natural Fiber Reinforced Polymer Composite and Its Applications', *International Journal of Polymer Science*, 2015. doi: 10.1155/2015/243947.

Moigne, N. Le *et al.* (2018) *Surfaces and Interfaces in Natural Fibre Reinforced Composites Fundamentals , Modifications and Characterization*. doi: 10.1007/978-3-319-71410-3.

Mwaikambo, L. Y. (2016) 'Mechanical properties of alkali treated plant fibres and their potential as reinforcement materials . I . hemp fibres', (July). doi: 10.1007/s10853-006-5075-4.

Mwaikambo, L. Y. and Ansell, M. P. (1999) 'The effect of chemical treatment on the properties of hemp, sisal, jute and kapok for composite reinforcement', *Angewandte Makromolekulare Chemie*, 272(4753), pp. 108–116. doi: 10.1002/(sici)1522-9505(19991201)272:1<108::aid-apmc108>3.3.co;2-0.

Nishino, T. (2004) 'Natural fibre sources', *Green Composites: Polymer Composites and the Environment*, pp. 49–80. doi: 10.1016/B978-1-85573-739-6.50007-5.

Nishino, T. (2013) 'Preparation, microstructure, and properties of biofibers', *Polymer Composites, Biocomposites*, 3, pp. 109–131. doi: 10.1002/9783527674220.ch3.

Ouajai, S. and Shanks, R. A. (2005) 'Composition, structure and thermal degradation of hemp cellulose after chemical treatments', *Polymer Degradation and Stability*, 89(2), pp. 327–335. doi: 10.1016/j.polymdegradstab.2005.01.016.

Ouajai, Sirisart and Shanks, R. A. (2005) 'Morphology and structure of hemp fibre after bioscouring', *Macromolecular Bioscience*, 5(2), pp. 124–134. doi: 10.1002/mabi.200400151.

Oza, S. *et al.* (2014) 'Effect of surface treatment on thermal stability of the hemp-PLA composites: Correlation of activation energy with thermal degradation', *Composites Part B: Engineering*, 67, pp.

227–232. doi: 10.1016/j.compositesb.2014.06.033.

Palanivel, A. *et al.* (2017) 'Dynamic mechanical analysis and crystalline analysis of hemp fiber reinforced cellulose filled epoxy composite', *Polimeros*, 27(4), pp. 309–319. doi: 10.1590/0104-1428.00516.

Pickering, K. L., Efendy, M. G. A. and Le, T. M. (2016) 'A review of recent developments in natural fibre composites and their mechanical performance', *Composites Part A: Applied Science and Manufacturing*, 83, pp. 98–112. doi: 10.1016/j.compositesa.2015.08.038.

Pothan, L. A. *et al.* (2002) 'Influence of chemical treatments on the electrokinetic properties of cellulose fibres', *Journal of Adhesion Science and Technology*, 16(2), pp. 157–178. doi: 10.1163/156856102317293687.

Puglia, D., Biagiotti, J. and Kenny, J. M. (2005) 'A Review on Natural Fibre- Based Composites — Part II - Application of Natural Reinforcements in Composite Materials for Automotive Industry', *Journal of Natural Fibers*, 1(3), pp. 23–65. doi: 10.1300/J395v01n03.

Rijavec, T., Janjić, S. and Ačko, D. K. (2017) 'Oživljanje navadne konoplje Cannabis sativa L. var. sativa v Sloveniji: Raziskava zelene konoplje', *Tekstilec*, 60(1), pp. 36–48. doi: 10.14502/Tekstilec2017.60.36-48.

Rohen, L. A. *et al.* (2017) 'Hemp Fiber Density Using the Pycnometry Technique', pp. 423–428. doi: 10.1007/978-3-319-51382-9.

Roumeli, E. *et al.* (2015) 'Effect of maleic anhydride on the mechanical and thermal properties of hemp/high-density polyethylene green composites', *Journal of Thermal Analysis and Calorimetry*, 121(1), pp. 93–105. doi: 10.1007/s10973-015-4596-y.

Salit, M. S. *et al.* (2015) *Manufacturing of natural fibre reinforced polymer composites*, *Manufacturing of Natural Fibre Reinforced Polymer Composites*. doi: 10.1007/978-3-319-07944-8.

Sari, N. H. *et al.* (2017) 'The Effect of Sodium hydroxide on Chemical and Mechanical Properties of Corn Husk Fiber'.

Sawpan, Moyeenuddin A., Pickering, K. L. and Fernyhough, A. (2011) 'Effect of fibre treatments on interfacial shear strength of hemp fibre reinforced polylactide and unsaturated polyester composites', *Composites Part A: Applied Science and Manufacturing*, 42(9), pp. 1189–1196. doi: 10.1016/j.compositesa.2011.05.003.

Sawpan, Moyeenuddin A, Pickering, K. L. and Fernyhough, A. (2011) 'Effect of various chemical treatments on the fibre structure and tensile properties of industrial hemp fibres', *Composites Part A*, 42(8), pp. 888–895. doi: 10.1016/j.compositesa.2011.03.008.

Sepe, R. *et al.* (2016) 'Mechanical properties of hemp fibre/epoxy composites. Influence of fibre chemical treatments', *ECCM 2016 - Proceeding of the 17th European Conference on Composite Materials*, (June), pp. 26–30.

Sepe, R. *et al.* (2018) 'Influence of chemical treatments on mechanical properties of hemp fiber reinforced composites', *Composites Part B: Engineering*, 133, pp. 210–217. doi: 10.1016/j.compositesb.2017.09.030.

Sgriccia, N., Hawley, M. C. and Misra, M. (2008) 'Characterization of natural fiber surfaces and natural fiber composites', *Composites Part A: Applied Science and Manufacturing*, 39(10), pp. 1632–1637. doi: 10.1016/j.compositesa.2008.07.007.

Shah, D. U. *et al.* (2012) 'Determining the minimum , critical and maximum fibre content for twisted yarn reinforced plant fibre composites', *COMPOSITES SCIENCE AND TECHNOLOGY*, 72(15), pp. 1909–

1917. doi: 10.1016/j.compscitech.2012.08.005.

Shah, D. U., Schubel, P. J. and Clifford, M. J. (2013) 'Modelling the effect of yarn twist on the tensile strength of unidirectional plant fibre yarn composites', *Journal of Composite Materials*, 47(4), pp. 425–436. doi: 10.1177/0021998312440737.

Shahzad, A. (2013) 'A study in physical and mechanical properties of hemp fibres', *Advances in Materials Science and Engineering*, 2013. doi: 10.1155/2013/325085.

Shih, Y. F. *et al.* (2012) 'Plant fibers and wasted fiber/epoxy green composites', *Composites Part B: Engineering*, 43(7), pp. 2817–2821. doi: 10.1016/j.compositesb.2012.04.044.

Slopiecka, K., Bartocci, P. and Fantozzi, F. (2011) 'Thermogravimetric analysis and kinetic study of poplar wood pyrolysis', *Applied Energy*, 97(May), pp. 491–497. doi: 10.1016/j.apenergy.2011.12.056.

Sood, M. and Dwivedi, G. (2018) 'Effect of fiber treatment on flexural properties of natural fiber reinforced composites: A review', *Egyptian Journal of Petroleum*. doi: 10.1016/j.ejpe.2017.11.005.

Stevulova, N. *et al.* (2014) 'Properties characterization of chemically modified hemp hurds', *Materials*, 7(12), pp. 8131–8150. doi: 10.3390/ma7128131.

Suardana, N. P. G., Piao, Y. and Lim, J. K. (2011) 'Mechanical properties of HEMP fibers and HEMP/PP composites: Effects of chemical surface treatment', *Materials Physics and Mechanics*, 11(1), pp. 1–8.

Sunny, T., Pickering, K. L. and Lim, S. H. (2020) 'Alkali treatment of hemp fibres for the production of aligned hemp fibre mats for composite reinforcement', *Cellulose*, 27(5), pp. 2569–2582. doi: 10.1007/s10570-019-02939-3.

Swain, P. T. R. and Biswas, S. (2017) 'Abrasive Wear Behaviour of Surface Modified Jute Fiber Reinforced Epoxy Composites', *Materials Research*, 20(3), pp. 661–674. doi: 10.1590/1980-5373-mr-2016-0541.

Świtała-Zeliazkow, M. (2001) 'Thermal degradation of copolymers of styrene with dicarboxylic acids I. Alternating styrene-maleic acid copolymer', *Polymer Degradation and Stability*, 74(3), pp. 579–584. doi: 10.1016/S0141-3910(01)00198-7.

Taib, R. M. *et al.* (2004) 'Alkali Extracted Steam Exploded Acacia mangium Wood Fiber as Reinforcing Material for Polypropylene Based Composites', *Journal of Natural Fibers*, 1(1), p. 2010. doi: 10.1300/J395v01n01.

Tanasă, F. *et al.* (2020) 'Modified hemp fibers intended for fiber-reinforced polymer composites used in structural applications—A review. I. Methods of modification', *Polymer Composites*, 41(1), pp. 5–31. doi: 10.1002/pc.25354.

Thygesen, A. *et al.* (2011) 'Cellulosic fibers: Effect of processing on fiber bundle strength', *Journal of Natural Fibers*, 8(3), pp. 161–175. doi: 10.1080/15440478.2011.602236.

Thygesen, L. G., Bilde-Sørensen, J. B. and Hoffmeyer, P. (2006) 'Visualisation of dislocations in hemp fibres: A comparison between scanning electron microscopy (SEM) and polarized light microscopy (PLM)', *Industrial Crops and Products*, 24(2), pp. 181–185. doi: 10.1016/j.indcrop.2006.03.009.

Thygesen, L. G. and Eder, Æ. M. (2007) 'Dislocations in single hemp fibres — investigations into the relationship of structural distortions and tensile properties at the cell wall level', pp. 558–564. doi: 10.1007/s10853-006-1113-5.

Thygesen, L. G., Eder, M. and Burgert, I. (2007) 'Dislocations in single hemp fibres-investigations into the relationship of structural distortions and tensile properties at the cell wall level', *Journal of Materials Science*, 42(2), pp. 558–564. doi: 10.1007/s10853-006-1113-5.

Trache, D. *et al.* (2016) 'Microcrystalline cellulose: Isolation, characterization and bio-composites application—A review', *International Journal of Biological Macromolecules*, 93, pp. 789–804. doi: 10.1016/j.ijbiomac.2016.09.056.

Tserki, V. *et al.* (2005) 'A study of the effect of acetylation and propionylation surface treatments on natural fibres', *Composites Part A: Applied Science and Manufacturing*, 36(8), pp. 1110–1118. doi: 10.1016/j.compositesa.2005.01.004.

Tyagi, G. K. (2010) 'Yarn structure and properties from different spinning techniques', *Advances in Yarn Spinning Technology*, pp. 119–154. doi: 10.1533/9780857090218.1.119.

Usmani, M. A. *et al.* (2017) *Biomass-based composites from different sources: Properties, characterization, and transforming biomass with ionic liquids*, *Lignocellulosic Fibre and Biomass-Based Composite Materials: Processing, Properties and Applications*. doi: 10.1016/B978-0-08-100959-8.00004-4.

Van De Velde, K. and Kiekens, P. (1999) 'Wettability of natural fibres used as reinforcement for composites', *Angewandte Makromolekulare Chemie*, 272(4761), pp. 87–93. doi: 10.1002/(SICI)1522-9505(19991201)272:1<87::AID-APMC87>3.0.CO;2-Q.

Wang, B., Sain, M. and Oksman, K. (2007) 'Study of structural morphology of hemp fiber from the micro to the nanoscale', *Applied Composite Materials*, 14(2), pp. 89–103. doi: 10.1007/s10443-006-9032-9.

Wang, H., Kabir, M. and Kong, H. (2013) 'Chemical Treatments on Hemp Fibre Composites', pp. 2–3.

Wang, W., Sain, M. and Cooper, P. A. (2006) 'Study of moisture absorption in natural fiber plastic composites', *Composites Science and Technology*, 66(3–4), pp. 379–386. doi: 10.1016/j.compscitech.2005.07.027.

Xie, Y. *et al.* (2010) 'Composites : Part A Silane coupling agents used for natural fiber / polymer composites : A review', *Composites Part A*, 41(7), pp. 806–819. doi: 10.1016/j.compositesa.2010.03.005.

Xu, Y. le *et al.* (2018) 'Mechanical and thermal properties of a room temperature curing epoxy resin and related hemp fibers reinforced composites using a novel in-situ generated curing agent', *Materials Chemistry and Physics*, 203, pp. 293–301. doi: 10.1016/j.matchemphys.2017.10.004.

8 Appendix

Tensile modulus predictions graphs

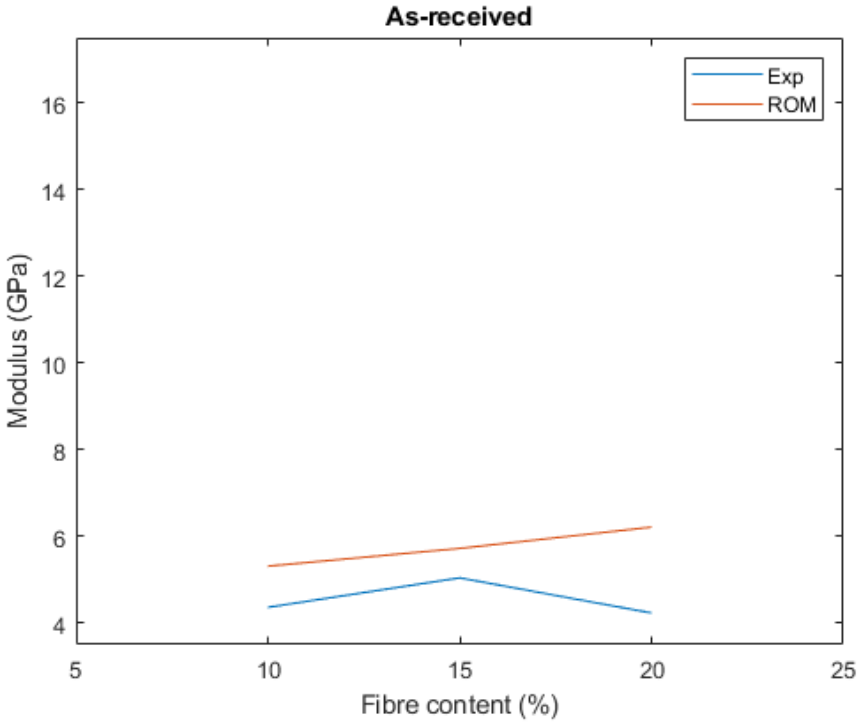

As-received hemp yarn reinforced epoxy composite.

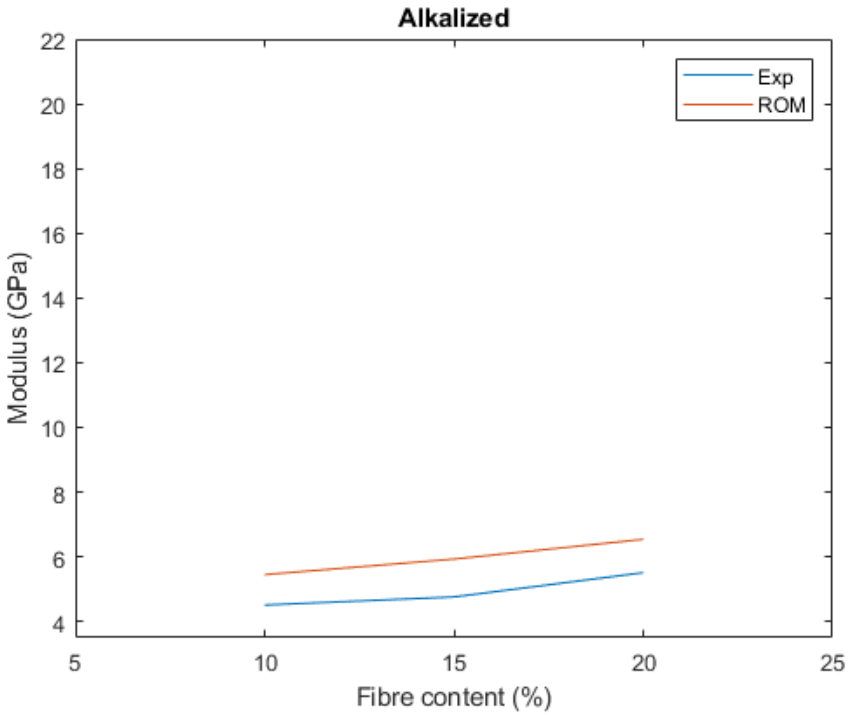

Alkalized hemp yarn reinforced epoxy composite.

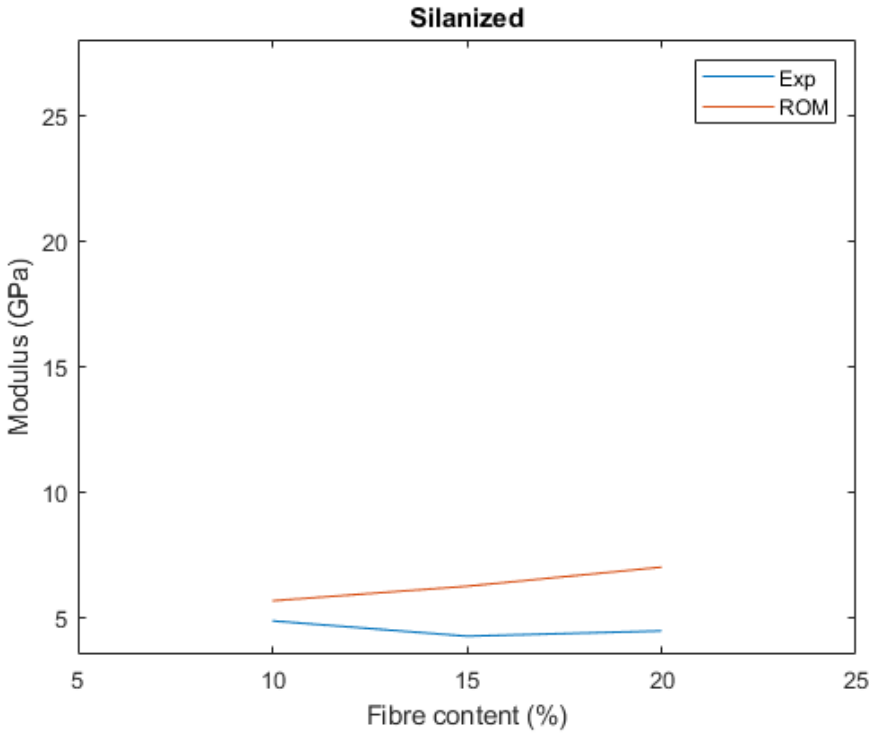

Silanized hemp yarn reinforced epoxy composite.

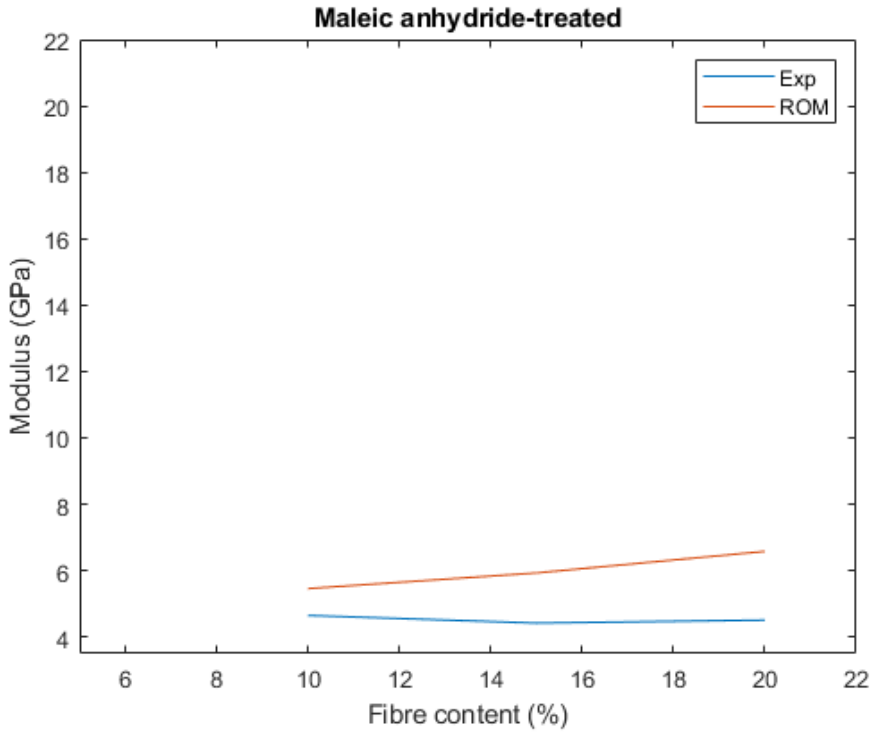

Maleic Anhydride-treated hemp yarn reinforced epoxy composite.